DRAFT:

December 2019

Author
Daniel E. Meeroff, Ph.D.
Florida Atlantic University, Department of Civil, Environmental & Geomatics Engineering

And
Co-Authors
Sharmily Rahman
Florida Atlantic University, Department of Civil, Environmental & Geomatics Engineering

David M. Binninger, Ph.D.
Florida Atlantic University, Department of Biological Sciences

Hinkley Center for Solid and Hazardous Waste Management
University of Florida
P. O. Box 116016
Gainesville, FL 32611
www.hinkleycenter.org

Report # (leave blank)

PROJECT TITLE: DEVELOPMENT OF A BIOSENSOR FOR MEASURING ODORANTS IN THE AMBIENT AIR NEAR SOLID WASTE MANAGEMENT FACILITIES

PRINCIPAL INVESTIGATOR(S):
Daniel E. Meeroff, Ph.D., Professor & Associate Chair, Dept. of Civil, Environmental & Geomatics Engineering, Florida Atlantic University, Phone: (561) 297-2658, E-Mail: dmeeroff@fau.edu

David M. Binninger, Ph.D., Associate Professor & Associate Chair, Dept. of Biological Sciences, Florida Atlantic University, Phone: 561-297-3323, E-Mail: binninge@fau.edu

PROJECT WEBSITE: labees.civil.fau.edu

PROJECT DURATION: 2017 - 2019

ABSTRACT:

The objective of the study is to investigate a novel biosensor technology that has the potential to objectively and rapidly measure odor concentrations in real-time, transforming how nuisance odors are monitored and regulated. The Bill Hinkley Center for Solid and Hazardous Waste Management funded this follow up study in 2017 to find ways to improve odor detection including development of a novel technology that uses human odor binding proteins to detect and potentially quantify odors.

Key words:
Odors, landfills, biosensor, odor detection

METRICS REPORTING:

Student Researchers:

Full Name: Sharmily Rahman
Email: rahmans2018@fau.edu
Anticipated Degree: MSCV
Department: CEGE

Full Name: Yasmeen Ampuero
Email: yalmanzaampu2014@fau.edu
Anticipated Degree: MS Biology
Department: BIO

Full Name: Cynthia Raaijmakers
Email: craaijmakers2014@fau.edu
Anticipated Degree: MS Biology
Department: Bio

Metrics:

1. List research publications resulting from **THIS** Hinkley Center project.

None yet

2. List research presentations resulting from **THIS** Hinkley Center project

Meeroff, D.E. (2019). Cutting Edge Solid/Hazardous Waste Management Research at Florida Atlantic University, 2019 FL SWANA Summer Conference, Tampa, FL.

3. List who has referenced or cited your publications from this project.

None so far

4. How have the research results from **THIS** Hinkley Center project been leveraged to secure additional research funding? What grant applications have you submitted or are planning on submitting?

Year two funding from the Hinkley Center for Solid and Hazardous Waste Management was secured. "Development of a biosensor for measuring odorants in the ambient air near solid waste management facilities (this project)," Hinkley Center, $50,487. 12/01/2017 (delayed project start to 08/01/2018) – 12/31/2019.

Additional funding was secured from the Environmental Research and Education Foundation, "*Detection of nuisance odors using odor binding protein sensor,*" Environmental Research and Education Foundation (EREF), $150,000. 12/01/2017 – 06/30/2020.

5. What new collaborations were initiated based on **THIS** Hinkley Center project?

- Deguo Du, Assistant Professor, Chemistry, FAU is allowing us to use his sophisticated fluorometry equipment for this project.
- Dr. Daniela Scheurle, Coordinator for Academic Support Services, Chemistry, FAU is allowing us to use her SpinTrap TALON column to purify the protein.

6. How have the results from **THIS** Hinkley Center funded project been used (not will be used) by the FDEP or other stakeholders?

To date, the results have not been used by stakeholders yet.

ACKNOWLEDGEMENTS

The researchers would like to acknowledge the William W. "Bill Hinkley Center for Solid and Hazardous Waste Management for funding this project. The researchers would also like to thank the Technical Advisory Group members and all the stakeholders for their invaluable advice, feedback, and support of this work.

Full Name: Sharmily Rahman
Email: rahmans2018@fau.edu
Anticipated Degree: MSCV
Department: FAU CEGE

Bio: Sharmily led the FAU team that finished first place in the 2019 SWANA Student Design Competition for Evaluating Recycling Rate Metrics to Achieve 80% Recycling Goal for Phoenix, AZ. She is the recipient of the FAU Graduate Student Leadership Prize and the FAU Presidential Fellowship to pursue her doctoral degree starting summer 2020.

Full Name: Yasmeen Ampuero
Email: yalmanzaampu2014@fau.edu
Anticipated Degree: MS Biology
Department: FAU BIO

Bio: Switched from a Biology Master's Thesis degree to Professional Science Master's degree (non-thesis) to pursue entrance to medical school.

Full Name: Cynthia Raaijmakers
Email: craaijmakers2014@fau.edu
Anticipated Degree: MS Biology
Department: FAU BIO

Bio: Switched from a Biology Master's Thesis degree to Professional Science Master's degree (non-thesis) to pursue entrance to medical school.

TAG members:
Mark Eyeington (SWA), Mark Maclean (SWA), Mark Bruner (SWA), Owrang Kashef (CDM), Craig Ash (WM), Ravi Kadambala (CDM), Ron Schultz (SWA), Jeff Roccapriore (WM), André McBarnette (Stantec), Dan Schauer (Geosyntec), Damaris Lugo (Broward County), Amanda Krupa (SWA), Richard Meyers (Broward County), Amede Dimonnay (Broward County), Art Torvela (FDEP)

TABLE OF CONTENTS

..... 1

1 INTRODUCTION 13

1.1 Background 13

1.2 Landfill Odorants and Possible Sources 13

1.3 Odor Characteristics 15

1.3.1 Odor Dimension 16

1.3.2 Odor Threshold 17

1.3.3 Odor Unit (OU) 20

1.3.4 Factors Affecting Dispersion of Odorants 21

1.4 Issues Arising from Malodors 22

1.4.1 Health Hazards 22

1.4.2 Health Effects of Specific Odorants 24

1.4.3 Decreasing Property Values and Lawsuits 25

1.5 Odor Measurement Techniques 26

1.5.1 Human Assessment 27

1.5.2 Field Olfactometry 28

1.5.3 Atmospheric Dispersion Model 29

1.5.4 Gas Chromatography (GC) and Mass Spectrometry (MS) 29

1.5.5 Electronic Nose 30

1.5.6 Chemical Sensor 31

1.5.7 Shortcomings of Stated Odor Measurement Techniques 32

1.6 Physiology of Human Olfactory Perception 33

1.7 Odorant Binding Protein (OBP) 34

1.7.1 Structures and Properties of OBP 34

1.7.2 Interaction of OBPs with Odorants 35

1.7.3 Human Odorant Binding Protein-2A (hOBPIIa) 36

1.7.4 Biosensor Development Using OBP 38

1.8 Fluorophores 39

1.8.1 1-Aminoanthracene as a Fluorophore 41

1.9 Objectives 42

2 METHODOLOGY 43
2.1 Materials 43
2.2 Purified hOBPIIa 43
2.3 Fluorescence Binding Assay 44
2.4 Reactor Chamber 46
2.5 Fluorescence Measurements 47
3 RESULTS AND DISCUSSION 49
3.1 Fluorescence Binding Assay With The Extrinsic Fluorophore (1-AMA) 49
3.2 Biosensor Sensitivity Experiments On Model Compounds 51
3.2.1 Experimentation with hydrogen sulfide (H_2S) 51
3.2.2 Experimentation with ammonia (NH_3) 56
3.2.3 Experimentation with methyl mercaptan (CH_3SH) 58
3.2.4 Experimentation with methane (CH_4) 59
3.2.5 Experimentation with landfill gas mixture 1 (NH_3 + CH_4) 60
3.2.6 Experimentation with landfill gas mixture 2 (H_2S + CH_4 + CO) 60
3.3 Results From Experiments With PID Sensor 65
3.4 Biosensor Reversibility Experiment 65
4 CONCLUSION AND RECOMMENDATIONS 67
4.1 Major Findings 67
4.2 Recommendations 68
REFERENCES 69

List of Tables

Table 1: Components of landfill gas along with their sources and possible release mechanism (Parker et al. 2002). 14
Table 2: Components of landfill gas and their concentrations (Takuwa et al. 2009). 15
Table 3: Description of odor associated with various landfill gas components (ATSDR 2016). 17
Table 4: Verbal descriptions associated with each point of the hedonic scale of odors (Li et al 2019). 17
Table 5: Odor descriptions of various gases found in landfills along with their detection limits for humans (Ruth 1986). 18
Table 6: Odor ranking plan based on detection concentration for humans (Parker et al. 2002). 19
Table 7: Ranking of odor importance in landfills based on physical and odor rankings (Parker et al. 2002). 20
Table 8: Different mood states along with the number of recorded instances and odds ratio of such cases, together with 95% CI (Heaney et al. 2011). 23
Table 9: Parameters in odor measurement and along with characteristics of odour measurement techniques. (Brattoli et al. 2011). 32
Table 10: Quantitation range of odorant gases tested at different flow rates 63
Table 11: Slope of emission intensity curves of odorant gases tested at different flow rates 63

List of Figures

Figure 1: Relationship between odor concentration and intensity according to Stevens (left). Weber-Fechner model of change in odorant concentration vs odor intensity (right). (Belgiorno et al. 2013). 16

Figure 2: Graph showing the general trend of decreasing odor threshold against increasing molecular weight (left). The odor threshold decreases for an increase in the number of carbon atoms in aliphatic alcohols (right). (Nagata and Takeuchi 2003). 18

Figure 3: Results of survey showing percentage of people identifying each meteorological factor as the most important factor in odor dispersion/concentration (Sakawi et al. 2011). 21

Figure 4: Odor concentration in a landfill at different times grouped over the four annual seasons (years 2012 and 2013) (Wenjing et al. 2015). 22

Figure 5: Percentage of respondents being impacted in each category (Sakawi et al. 2011). 24

Figure 6: Health issues arising from exposure to hydrogen sulfide at different concentration levels (ATSDR 2001). 25

Figure 7: Block diagram showing the process of lab olfactometry and the components associated with it. (Laor et al. 2014). 27

Figure 8: Instruments used in field olfactometry (Laor et al. 2014). 29

Figure 9: Block diagram showing the various components of an e-nose system (Belgiorno et al. 2013). 31

Figure 10: Block diagram representing the components in a solid state chemical sensor (Brattoli et al. 2011). 32

Figure 11: Size filtering and interaction filtering inside the nasal cavity. Size filtering allows smaller particles and odorant molecules to pass inside the cavity (left). In interaction filtering the particles (green) that interacts less with the mucus are allowed to enter inside while others (orange) are rejected due to strong binding interaction with mucus (right) (Leal et al. 2017). 33

Figure 12: Cells within nasal epithelium allowing humans to perceive odors (Jasper 2013). 34

Figure 13: Percentages showing identical amino-acid sequence between various members of lipocalin superfamily including OBPs and PBPs (Pheromone Binding Protein) (Tegoni et al. 2000). 35

Figure 14: Tertiary structure of bOBP (bovine OBP) and pOBP (porcine OBP) modeled using DeepView software (Pelosi et al. 2014). 36

Figure 15: Tertiary structure of hOBPIIa (left) and hOBPIIb (right). β sheets, α-helices and disulfide bridge are indicated in blue, green and yellow respectively (Lacazette et al. 2000). 37

Figure 16: Tertiary structure of hOBPIIa bonded with the aldehyde, undecanal (carbon atoms are indicated in grey, oxygen is in red and nitrogen is in blue), at the middle of the ligand binding pocket. (Heydel et al. 2013). 38

Figure 17: 1-AMA competetive binding assay of pOBP-m2 (pig OBP mutant) with different polycyclic aromatic hydrocarbons . 1µM 1-AMA and 1µM protein were used in an increasing concentartion of methanolic solutions of aromatic compounds starting from 1 mM (Wei et al. 2008). 39
Figure 18: Mechanism of fluorescent turn-on probe where the ligand attaches to the specific hydrophobic ligand binding site of the protein and the surrounding hydrophobic environment allows the environment-sensitive fluorophore to emit strong fluorescence. (Zhuang et al. 2013). 40
Figure 19: Titration curve of 2µM hOBPIIa against the fluorescent probes NPN (left) and DAUDA (right) at increasing concentrations (Briand et al. 2002). 41
Figure 20: Fluorescence curve of 1-AMA at 485 nm with increasing solvent concentration. 1-AMA is displaced the least by methanol, leading to relatively high fluorescence emission even though the solvent concentration is increased (Triangle: Methanol, Circle: Ethanol, Square: Dimethylsulfoxide) (Briand et al. 2000). 42
Figure 21: Bradford curve showing a clear increase in protein concentration between induced and uninduced samples. 44
Figure 22: 12.5% SDS-PAGE Gel of crude protein (left) and 12.5% SDS-PAGE Gel of purified protein (right). 44
Figure 23: Label photograph of the experimental setup. 45
Figure 24: Reactor chamber using a centrifuge tube (left). 3-way stopcock used at the lid of the exposure chamber. The different ports and other parts are labeled (right). .. 46
Figure 25: Horiba Jobin Yvon FluoroMax-4 spectrofluorometer (left) and Fluorescence software (right). 47
Figure 26: 'Z' dimension (distance from the base to the center of the sample chamber window) of the quartz cuvette (left) and a 100 µL capacity quartz cuvette containing 100 µL of sample each time (right). 48
Figure 27: Spectrofluorometric analysis for individual biosensor components 50
Figure 28: Binding curve of 1-AMA at different concentrations to hOBPIIa 51
Figure 29: (a) Spectrofluorometric emission spectra at 380 nm excitation found by Roblyer (2017) (b) Graph showing inverse relationship between peak fluorescence intensity and exposure time for the same experiment 52
Figure 30: (a) Spectrofluorometric emission spectra at 380 nm excitation for the verification experiment at 0.5 slpm hydrogen sulfide for 25 mL sample (b) Graph showing inverse relationship between peak fluorescence intensity and exposure time for the same experiment 53
Figure 31: (a) Spectrofluorometric emission spectra at 380 nm excitation at 0.5 slpm hydrogen sulfide for 10 ml sample (b) Graph showing inverse relationship between peak fluorescence intensity and exposure time for the same experiment 54
Figure 32: (a) Intensity curves obtained for collected hydrogen sulfide samples at different times for 0.7 slpm. (b) Graph showing peak emission intensity against time of gas exposure. 54

Figure 33: (a) Intensity curves obtained for collected hydrogen sulfide samples at different times for 0.9 slpm. (b) Graph showing peak emission intensity against time of gas exposure. 55
Figure 34: (a) Comparative change in fluorescence intensity at 0.5 slpm, 0.7 slpm, and 0.9 slpm for hydrogen sulfide (b) Graph showing change in fluorescence intensity with mass flow of hydrogen sulfide at all three flow rates 56
Figure 35: (a) Graph showing peak emission intensity against time for ammonia flowing at 0.5 slpm, (b) 0.7 slpm and (c) 0.9 slpm 57
Figure 36: (a) Comparative change in fluorescence intensity at 0.5 slpm, 0.7 slpm, and 0.9 slpm for ammonia (b) Graph showing change in fluorescence intensity with mass flow of ammonia at all three flow rates 58
Figure 37: (a) Graph showing peak emission intensity against time for methyl mercaptan flowing at 0.5 slpm, (b) 0.7 slpm and (c) 0.9 slpm 59
Figure 38: (a) Comparative change in fluorescence intensity at 0.5 slpm, 0.7 slpm, and 0.9 slpm for methyl mercaptan (b) Graph showing change in fluorescence intensity with mass flow of methyl mercaptan at all three flow rates 59
Figure 39: (a) Graph showing peak emission intensity against time for methane flowing at 0.5 slpm (b) Graph showing change in fluorescence intensity with mass flow of methane at 0.5 slpm 60
Figure 40: (a) Graph showing peak emission intensity against time for landfill gas mixture 1 flowing at 0.5 slpm (b) Graph showing emission intensity curves for landfill gas mixture 1 against its individual component gases at 0.5 slpm 60
Figure 41: Graph showing peak emission intensity against time for landfill gas mixture 2 flowing at (a) 0.5 slpm, (b) 0.7 slpm, and (c) 0.9 slpm 61
Figure 42: Graph showing peak emission intensity against time for landfill gas mixture 2 flowing at 0.5 slpm, 0.7 slpm, and 0.9 slpm 62
Figure 43: Graph showing emission intensity curves for landfill gas mixture 2 against its individual component gases at (a) 0.5 slpm (b) 0.7 slpm and (c) 0.9 slpm 62
Figure 44: Comparative changes in relative fluorescence intensities for the pure odorant gases at flow rates of (a) 0.5 slpm, (b) 0.7 slpm, and (c) 0.9 slpm. 65
Figure 45: Graph showing peak emission intensity against time for nitrogen gas flowing at 0.5 slpm 66
Figure 46: Graph showing peak emission intensity against time for passing hydrogen sulfide gas through the biosensor solution at 0.5 slpm (first 240 seconds) followed by nitrogen gas at the same flow rate (last 240 seconds) 66

List of Acronyms and Abbreviations

MSW	Municipal Solid Waste
LFG	Landfill Gas
HAP	Hazardous Air Pollutant
VOC	Volatile Organic Compound
USEPA	United States Environmental Protection Agency
FIDOL	Frequency (F), intensity (I), duration (D), offensiveness (O), and location (L)
OU	Odor Unit
OU_E	European Odor Unit
ppm	Parts per million
ppb	Parts per billion
ppt	Parts per trillion
OR	Odds Ratio
CI	Confidence Interval
NIOSH	National Institute for Occupational Safety and Health
ASTM	American Society of Testing and Materials
GC/MS	Gas Chromatography/Mass Spectrometry
MOSFET	Metal–Oxide–Semiconductor Field-Effect Transistor
ANN	Artificial Neural Networks
PCA	Principal Component Analysis
DFA	Discriminant Function Analysis
OBP	Odorant-Binding Protein
ORs	Odor Receptors
PBPs	Pheromone Binding Proteins
bOBP	Bovine Odorant-Binding Proteins
pOBP	Porcine Odorant-Binding Proteins
hOBP	Human Odorant-Binding Proteins
1-AMA	1-Aminoanthracine
SDS-PAGE	??
OD	Optical Density
PID	Photo-Ionization Detector

Executive Summary

Nuisance odor levels produced by solid waste management operations such as landfill facilities are subject to regulatory standards due to their impacts on the quality of life of the residents living nearby the facility. Failure to meet such standards may result in costly fines, litigation, inability to acquire permits, mitigation, and re-siting operations. Since measurement of environmental nuisance odors is currently limited to subjective techniques, monitoring odor levels to meet such standards is often problematic. This is becoming more acute as increasing residential populations begin to encroach on properties adjacent to landfills. In order to ensure that nuisance odor issues are minimized, it is necessary to provide an objective measurement. The objective of the current research is to develop a biosensor for providing an objective, standard measurement of odors. The approach is to modify the human odorant binding protein (hOBPIIa), isolated using published biomolecular techniques, by fluorescently tagging it with a chromophore functional group. When this protein is tagged with a fluorophore marker and excited in a spectrofluorometer, it emits light of a certain wavelength that can be detected and quantified. Once odorant molecules are exposed to this complex, they start replacing the fluorophore, and as a result, the emitted light intensity decreases in proportion to the number of odorant molecules. Since the protein response depends on odorant concentration, following an inverse Beer's Law relationship, the odorants can be quantified accurately and rapidly using fluorometric measurements. The results establish quantitation ranges for different pure and mixture of odorant gases as well as the amount of gas that can be quantified across various flow rates.

1 INTRODUCTION

1.1 Background

Odor is an unpleasant smell and its presence in high levels is considered as environmental pollution. As more industrialization takes place, this issue is gaining an increased focus in recent times. By degrading the environmental quality, malodors can adversely affect the ecosystem. One of the most prominent sources of malodors are municipal solid waste (MSW) landfills. Landfills have a variety of waste coming in at different quantities which is responsible for a very complex biological and physicochemical reactions (Palmiotto et al. 2014). This leads to emission of potentially toxic compounds as well as odors, results in a serious degradation of lifestyle in nearby areas. This also leads to general degradation of relationship between the landfill authority and the local population, yielding a variety of legal measures such as fines and lawsuits against the authority. The uncertainty associated with odor measurement has also added to the increased pressure on legislators to introduce more stringent regulations regarding odor control. Although in recent times, advanced technologies have been using to better understand odor science, regulations are most often based on the perception of odor rather than objective measurements (Laor et al. 2014).

Increasing population and transportation optimization are leading the solid waste management facilities to locate in populated areas though it was not intended initially. With more people now living in the vicinity of such facilities, the number of odor complaints have also increased (De Feo et al. 2013). The emissions from landfills are unavoidable because of the nature of the waste coming into the landfill and anaerobic decomposition of the biological waste (Ritzkowski et al. 2006). Moreover, such emissions can last at least three decades after the landfill ceases its operation complicating the odor control strategy (Ritzkowski et al. 2006). Considering such problems, controlling odor emissions have become a major challenge to solve for the solid waste management facility. However, a first step in achieving that goal will be to quantify the odor arising out of it. This will also help the scientific community in better exploring odor reduction techniques while enabling legislators to draft better resolutions that can curb odor emission from landfill sites and provide relief to the general public.

1.2 Landfill Odorants and Possible Sources

Landfilling has been the most common form of solid waste disposal in many countries of the world and so naturally, the most common source of odor emission (El-Fadel et al. 1997). The anerobic decomposition of waste leads to the formation of landfill gas (LFG) which is the most common cause of odor emission in landfills along with leachate (Ritzkowski et al. 2006). During vaporization from solid/liquid phase, some chemical compounds can also create a pungent smell. Of the various types of waste dumped in the landfill, there are many which have their own characteristic smell e.g. household garbage, wastewater treatment biosolids, sludge etc. Rancid odors are commonly perceived near MSW whereas sulfur odors are dominant at off-site locations (Curren et al. 2016). Table 1 shows the sources of various component gases of landfill gas along with their probable release mechanisms.

Table 1: Components of landfill gas along with their sources and possible release mechanism (Parker et al. 2002).

Trace component	Probable source	Probable release mechanism
Hydrogen	Organics acids Metals	Anaerobic Microbial respiration Corrosion
Hydrogen sulfide	Sulphate wastes	Anaerobic Microbial respiration
Vinyl chloride	Chlorinated solvents	Anaerobic Microbial respiration
Simple alkanes & alkenes	Organic wastes	Anaerobic Microbial respiration
Organic acids	Organic wastes	Anaerobic Microbial respiration
Mercaptans	Organic material	Anaerobic Microbial metabolism
Alcohols & ketones	Organic wastes Solvents	Anaerobic Microbial respiration Microbial metabolism Evaporation & gas stripping Aerosols
Aldehydes	Organic wastes	Microbial metabolism
Limonene	Plant material	Anaerobic Microbial metabolism
Ammonia	Organic wastes	Anaerobic Microbial respiration
Amines	Organic wastes	Microbial metabolism Aerosols
Esters	Organic acids & alcohols	Chemical reaction or microbial action Aerosols
Chlorinated hydrocarbons	Solvents & paints in waste	Evaporation, gas stripping
Simple aromatic hydrocarbons	Solvents & paints in waste	Evaporation, gas stripping
Chloro and chloroflurohydrocarbons	Foams & propellants in waste	Out-gassing
Mercury	Inorganic waste	Microbial methylation Evaporation Dust

Around 90% of LFG consists of a combination of methane (30%-60%) and carbon dioxide (20%-50%) whereas rest of the emission includes volatile organic compounds (VOCs), hazardous air pollutants (HAPs), water vapor and trace amount of other odorous compounds etc. (El-Fadel et al. 1997; Davoli et al. 2003; Fang et al. 2012). A considerable amount of VOC (e.g. toluene) is also found to be emitted from the exhaust of compaction vehicles and trucks operating in landfill sites (Chiriac et al. 2007). Depending on the type of waste, age, water content, temperature, pH, alkalinity etc., the characteristics of the LFG emission varies from landfill site to landfill site (Yazdani 2015). Table 2 contains the main components found in landfill gas.

Table 2: Components of landfill gas and their concentrations (Takuwa et al. 2009).

Compound	Typical concentration
Methane (CH_4)	30%–60%
Carbon dioxide (CO_2)	20%–50%
Oxygen (O_2)	<2%
Nitrogen (N_2)	<10%
Water (H_2O)	Saturated
Trace compounds	< 4000 ppmv

Since the two main components (methane and carbon dioxide) of the LFG emission are odorless, only a small percentage of trace components contributes to the malodor existing in landfills. 140 trace components have been identified in landfill gases in seven United Kingdom waste disposal sites, of which 90 were observed in all the considered landfill sites (Allen et al. 1997). The trace components were categorized into six main groups (Parker et al. 2002):

- Alkanes, 302 - 1543 mg/m^3;
- Aromatic compounds, 94 - 1905 mg/m^3;
- Cycloalkanes, 8 - 487 mg//m^3;
- Terpenes, 35 – 652 mg/m^3;
- Alcohols and ketones, 2 – 2069 mg/m^3; and
- Halogenated compounds, 327 – 1239 mg/m^3

The molecular structure of the odorant compounds largely varies though most of them are non-ionic hydrophobic organic compounds having a molecular weight of less than 300 (Schiffman et al. 2000). Reactive inorganic gases such as ammonia (NH_3) and hydrogen sulfide (H_2S), which are also responsible for contributing offensive odor in landfills, don't belong to any certain functional group like organic odorants. While conducting a study on different sources of odor in a landfill in Turkey, Dincer et al. found that aldehydes and ketones were most responsible for creating odor among the 53 compounds detected. Mostly, the odors in landfill result from sulfur compounds such as hydrogen sulfide, dimethyl sulfide, methanethiol, propanethiol, nitrogen compounds such as ammonia and amines, hydrocarbons such as benzene, phenols, terpenes, styrene, toluene, xylene, acetone, methanol, n-butanone, n-butylaldehyde, volatile fatty acids, etc. (Parker et al. 2002; Fang et al. 2012). At times the odor released from some of the VOCs may be acceptable which is rather dependent on experience and socio-economic status, but most people find the odor emitted from H_2S, mercaptans, amines, and nitrogenous heterocylic compounds quite offensive.

1.3 Odor Characteristics

Various socio-economic and cultural factors, previous experience with odor, sensitivity, social structure, surrounding environment etc. determine an individual's perception of odor annoyance in most of the cases. Scientists all over the world are putting considerable resources to discover a relationship between odor perception and the molecular structure of the odorants (Belgiorno et al. 2013). There are various dimensions in which odor can be measured since it has a highly subjective tone to it. There are also different measurement units associated with this process. The following subsections discuss various dimensions of odor perception as well as odor units used in

characterizing odor. Discussion is also included about odor threshold for humans as well as factors which may affect the odor perception of humans.

1.3.1 Odor Dimension

There are various classifications of odor dimension but the four most common dimensions of odor perception are: detectability, intensity, quality, and hedonic tone (USEPA, 2001). Descriptions of all the four dimensions are provided in the following paragraphs.

Detectability is same as that of odor threshold which refers to minimum concentration of an odorant detected by the human nose (CalRecycle 2019). It varies from individual to individual depending on the situation at a particular time (Pearce et al. 2006). Intensity refers to strength of the odor sensation at a concentration level that has already exceeded the perceptibility threshold i.e. the detection limit (Pearce et al. 2006). In case of some odorants such as H_2S, the perceived intensity may be high even at a very low concentration level and these odorants are commonly unpleasant in nature (Belgiorno et al. 2013). A 6-point scale is often used to measure the odor intensity starting from 0 to 5 with 0 being no odor and 5 being very strong odor (Lacey et al. 2004). Several mathematical functions have been established to correlate the interdependency between odor concentration and odor intensity. In case of Steven's law, the relationship follows an exponential function whereas in Weber-Fechner equation, the relationship is logarithmic (Figure 1) (Curren et al. 2013; Stuetz and Frechen 2001).

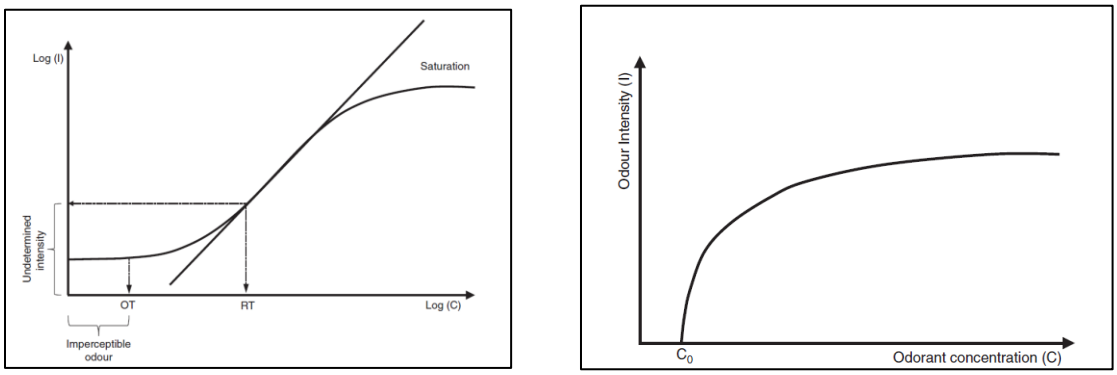

Figure 1: Relationship between odor concentration and intensity according to Stevens (left). Weber-Fechner model of change in odorant concentration vs odor intensity (right). (Belgiorno et al. 2013).

Odor quality is the adjective descriptor of an odorant i.e. how the substance smells like (e.g. fruity, pungent, rancid etc.) which helps to detect the source of the odor (Yuwono and Lammers 2004). The American Society for Testing and Materials established 146 adjective descriptors which are most commonly used in describing odors (Schiffman et al. 2000). Table 3 presents standard odor description of some common odorants typically observed in landfills.

Table 3: Description of odor associated with various landfill gas components (ATSDR 2016).

Component	Odor description
Hydrogen Sulfide	Strong rotten egg
Ammonia	Pungent acidic or suffocating
Benzene	Paint thinner-like
Dicholoethylene	Sweet, ether-like, slightly acrid
Dichloromethane	Sweet, chloroform-like
Ethylbenzene	Aromatic, benzene-like
Toluene	Aromatic, benzene-like
Tricholoroethylene	Sweet, chloroform-like
Tetrachloroethylene	Sweet, ether-like or chloroform-like
Vinyl chloride	Faintly sweet

Hedonic tone refers to relative pleasantness (like) or unpleasantness (dislike) of an odor. This is a very subjective term and depends on an individual's perception of the nature of the odor (Perace et al. 2006). A smell which is unpleasant to one person may not be agreeable to another person (CalRecycle 2019). A 9-point scale (Table 4) is used to describe hedonic tone ranging from extremely unpleasant (low negative score, "-4") to extremely pleasant odor (high positive score, "+4") (Li et al 2019).

Table 4: Verbal descriptions associated with each point of the hedonic scale of odors (Li et al 2019).

Hedonic Tone	Verbal Description
-4	Extremely unpleasant
-3	Moderate unpleasant
-2	Unpleasant
-1	Slightly unpleasant
0	Neutral
1	Slightly pleasant
2	Pleasant
3	Moderate pleasant
4	Extremely pleasant

Since human perception of odor is a highly subjective term and may largely vary among individuals, there are other dimensioning procedures as well apart from above mentioned four dimension. Five interactive components commonly known as FIDOL are widely accepted in many countries such as Australia, New Zealand etc. (Freeman and Cudmore 2002; Nicell 2009) to facilitate odor investigation. FIDOL which stands for frequency (F), intensity (I), duration (D), offensiveness (O), and location (L), are used to understand odor annoyance, its impact and adverse effect on humans (Nicell 2009). These parameters are also very much helpful in characterizing odor as they capture five essential data points of odor characterization.

1.3.2 Odor Threshold

Odorants can be detected at different concentrations based on people's perception of odor which normally varies from person to person. Odor detection threshold (ODT) is the minimum

concentration of any odorant that can be detected by the olfactory system of typically by 50% of the human test population (Yuwono and Lammers 2004). Although the relationship between the molecular weight of the odorants and the odor detection threshold is not clear, a study conducted by Nagata and Takeuchi in 2003 found that the threshold decreases with the increase in molecular weight of the odorants where the molecular weights have a range of 120-130 (Figure 2). The tendency is more apparent in the case of homologous chemical compounds such as alcohol, aldehyde, mercaptan, ketone and hydrocarbon.

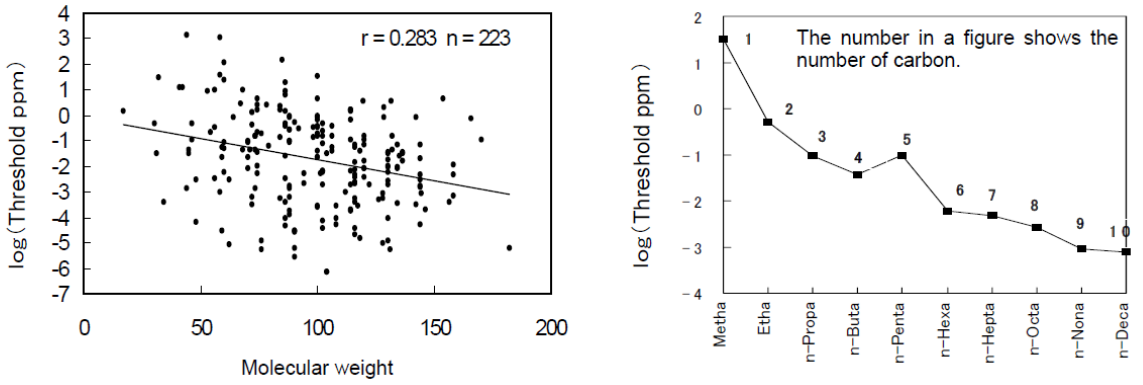

Figure 2: Graph showing the general trend of decreasing odor threshold against increasing molecular weight (left). The odor threshold decreases for an increase in the number of carbon atoms in aliphatic alcohols (right). (Nagata and Takeuchi 2003).

In 1986, Ruth reported odor threshold values for possible trace components found in landfill gas (Table 5).

Table 5: Odor descriptions of various gases found in landfills along with their detection limits for humans (Ruth 1986).

Compounds	Odor (Description)	Detection Limits µg/m^3	ppbv
Sulphur compounds			
Hydrogen sulphide	rotten eggs	0.7	0.5
Carbon disulfide	disagreeable, sweet	24.0	7.7
Dimethyl sulphide	rotten cabbage	2.5	1.0
Dimethyl disulfide	rotten cabbage	0.1	0.026
Dimethyl trisulfide	rotten cabbage	6.2	1.2
Methyl mercaptan	rotten cabbage	0.04	0.02
Ethyl mercaptan	rotten cabbage	0.032	0.01
Allyl mercaptan	garlic coffee	0.2	0.1
Propyl mercaptan	Unpleasant	0.2	0.1
Amyl mercaptan	Putrid	0.1	0.02
Benzyl mercaptan	Unpleasant	1.6	0.3
Thiophenol	Putrid garluc	1.2	0.3
Sulphur dioxide	Irritating	1175.0	449.3
Carbon oxysulfide	Pungent	NA	NA
Nitrogen Compounds			
Ammonia	Pungent, sharp	26.6	38.3
Aminomethane	Fishy, pungent	25.2	19.5

Compounds	Odor (Description)	Detection Limits µg/m^3	ppbv
Dimethylamine	Fishy, amine	84.6	46.0
Trimethylamine	Fishy, pungent	0.1	0.046
Skatole	Faeces, chocolate	0.00004	0.00001
Volatile Fatty Acids			
Formic	Biting	45.0	24.0
Acetic	Vinegar	2500.0	1019.1
Propionic	Rancid, pungent	84.0	27.8
Butyric	Rancid	1.0	0.3
Valeric	Unpleasant	2.6	0.6
Ketones			
Acetone	Sweet, minty	1100.0	463.9
Butanone	Sweet, minty	737.0	250.4
2-Pentanone	Sweet	28000.0	7967.5
Acetaldehyde	Green sweet	0.2	0.1
Methanol	Alcohol	13000	9953.1
Ethanol	Alcohol	342	342
Phenol	Medicinal	178	46

It is worth mentioning that the lower the detection limit of an odorant, the higher the potential importance of that odorant would be since odorants having lower detection limit can be perceived by human even when they are present in very small amounts relative to others (Parker et al. 2002). Due to this fact, odorants such as sulfur compounds, nitrogen compounds and oxygenated compounds often arouse more attention and interest among researchers (Wenjing et al. 2015). Additionally, what may seem to be an unpleasant odor to a person may not be unpleasant at all to another person; that's why the reported threshold values for odorous compounds in the literatures are only a widely accepted estimation (ATSDR 2016). Depending on the value of threshold detection limit, Parker et al. provided an odor ranking plan (Table 6) in 2002.

Table 6: Odor ranking plan based on detection concentration for humans (Parker et al. 2002).

Odor Ranking	1	2	3	4	5
Detection Concentration Range (µg m^{-3})	>1000	100-1000	10 - 100	10 – 1	<1

Based on the odor ranking and physical property ranking (1 if mobility is lower than benzene and 2 if mobility is higher than benzene), an odor importance ranking has been provided to twelve odorants (Table 7) having the greatest potential to cause odor in landfills (Parker et al. 2002).

Table 7: Ranking of odor importance in landfills based on physical and odor rankings (Parker et al. 2002).

	Chemical Name	Chemical Group	Physical Ranking	Odour Ranking	Odour Importance
1	Hydrogen sulphide	Organo Sulphur Compounds	2	5	10
2	Methanthiol	Organo Sulphur Compounds	2	5	10
3	Carbon disulphide	Organo Sulphur Compounds	2	3	6
4	Propanethiol	Organo Sulphur Compounds	1	5	5
5	Butyric acid	Carboxylic acids	1	5	5
6	Dimethyl disulphide	Organo Sulphur Compounds	1	5	5
7	Ethanal	Aldehyde	1	5	5
8	Ethanethiol	Organo Sulphur Compounds	1	5	5
9	Butanethiol	Organo Sulphur Compounds	1	4	4
10	Pentene	Alkenes	2	2	4
11	Dimethyl sulphide	Organo Sulphur Compounds	1	4	4
12	Ethyl butyrate	Ester	1	4	4

Among the twelve compounds listed in Table 7, the organo-sulfur compounds dominate mostly. This is especially because of older waste where the emission contains relatively low amounts of carboxylic acids, aldehydes, and esters. Odorants having a low threshold value can trigger the human sense of smell even at low concentrations. For example, if only three drops of ethyl mercaptan is added to an Olympic-sized swimming pool, its presence can be detected by humans (Sela & Sobel 2010). The odorant having the lowest detection threshold is isoamyl mercaptan, having a threshold value of 0.77 ppt (Nagata & Takeuchi 2003). When people are repeatedly exposed to an odorant, it also causes a decrease in threshold value in some cases.

1.3.3 Odor Unit (OU)

An odor unit (OU) or threshold odor number is used to express odor concentration. A European Odor Unit (OU_E) which is commonly used in European countries refers to the concentration of any odorant which when evaporated to 1 m^3 of neutral gas (odor-free air) produces the same response when 123 µg of n-butanol disperses into 1 m^3 of neutral gas (Zhang 2001). 1 OU_E is basically the concentration of any odorant equivalent to its threshold concentration (Lacey et al. 2004). It is more convenient for using in calculations than for normal purposes since ppm or ppb (volume per volume) is more common for expressing odor concentration (Yuwono & Lammers 2004). However, the strength of the odor or offensiveness cannot be perceived by means of odor unit

since the unit only conveys the meaning of how many times the concentration of the odor is greater than its threshold concentration (Laor et al. 2014). As a result, two facilities emitting same unit of odor concentration might not be perceived equally by the receptors as to the offense they create. The odorants having lower detection threshold might be perceived much more negatively than the other though both may have the same unit of concentration.

1.3.4 Factors Affecting Dispersion of Odorants

As soon as odor is released from a source, transportation of odorants around the atmosphere happens within a very short moment due to their highly fugitive nature. Various environmental factors including climate, topography, wind speed and direction, temporal variation, humidity, source strength etc. affect the dispersion and dilution of odorants along with their impact on the respondents (Sakawi et al. 2011). According to a survey conducted in Malaysia by Sakawi et al. in 2010, 92.6% of the respondents living within 2 km radius of an open landfill concluded that nuisance odor in the vicinity of the landfill is largely affected by meteorological factors of which 40.6% identified wind, rain and hot weather to be the largest factors. 30.5% of them agreed that wind has the highest influence whereas 22.6% perceived rain to be highest followed by 6.3 % who believed hot weather to be the largest factor (Figure 3).

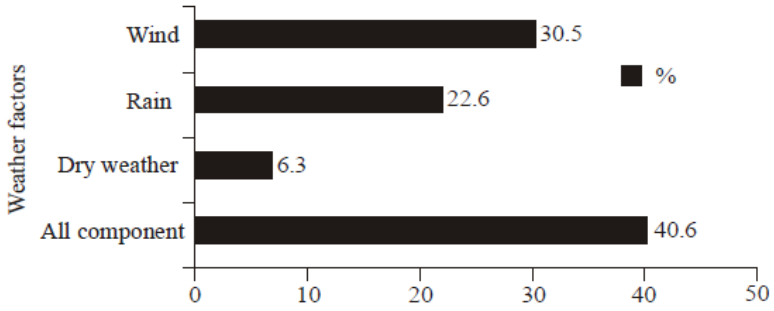

Figure 3: Results of survey showing percentage of people identifying each meteorological factor as the most important factor in odor dispersion/concentration (Sakawi et al. 2011).

High vapor pressure and low solubility of VOC compounds facilitate their emission during summer, thus causing higher strength of nuisance odor that is most commonly found in air downwind from the landfill site (Paraskaki and Lazaridis 2005; Reinhart 1993; Wood and Porter 1987). However, the unstable weather condition in hot days disperse them quickly leading to lower number of odor complaints (Energy and Environmental Affairs 2017; Epstein 2011). The opposite happens in winter when the cold weather does not promote emission, but the dispersion also remains lower, keeping the odorants nearer to the source for a longer time (Sattler and Devanathan 2012). A study conducted on odor pollution from a large sanitary landfill in China showed that the pollution is higher in spring and autumn while it remains comparatively lower during summer and winter (Wenjing et al. 2015). The study also found that different odorous compounds are triggered at different seasons around the landfill, e.g., aldehydes and ketones exist in higher concentration in spring; alcohols, esters and ethers are observed during summer and sulfur compounds are triggered in autumn and winter. Figure 4 shows the odor concentration at different time periods in a day at the above-mentioned landfill.

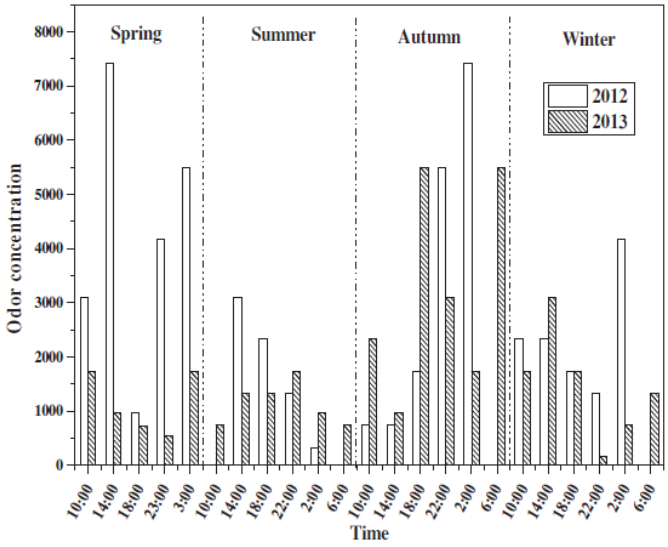

Figure 4: Odor concentration in a landfill at different times grouped over the four annual seasons (years 2012 and 2013) (Wenjing et al. 2015).

1.4 Issues Arising from Malodors

Having a landfill near to residential property is clearly not an attractive prospect for the residents. The deteriorate relationship between the landfill authority and surrounding population often leads to vandalism (Etkathimerini 2019) targeting the landfill and other retaliatory acts which is certainly not the ideal case for any party. Nevertheless, newer technologies are being used to facilitate landfill design and operation in recent times, nearby residents are found to continuously report against malodor and nuisance issues arising from landfill (Heaney et al. 2011). This problem is much more frequent in urban areas than rural due to increasing population growth leading to public encroachment in areas surrounding landfills (Ying et al. 2012). The following sections describe a few issues arising from presence and dispersion of odorants in inhabited places.

1.4.1 Health Hazards

Long-term exposure to odorous compounds has various adverse health impacts on residents living nearby (De Feo et al. 2013). Not only the odors, but also the odorants (chemicals or the mixture of chemicals which give off the smell) are equally responsible for potential health risks in human (Schiffman et al. 2000). The hazardous air pollutants and non-methanic volatile organic compounds emitted from landfill gas induce most of the health problems (Palmiotto et al. 2014). Shen at el. showed that exposure to VOC emission increases the risk of cancer among the nearby residents and is also responsible for an optimum ozone formation in the atmosphere. The most often reported symptoms due to odor exposure include eye, nose, and throat irritation, headache, nausea, hoarseness, cough, nasal congestion, palpitations, shortness of breath, stress, drowsiness, and alterations in mood (Schiffman et al. 2000). In a study conducted by Atamila et al. in 2006, several physical symptoms were found to be reported by 1142 residents living within 1.5, 3.0 and 5.0 km of waste treatment centers in Finland: unusual shortness of breath (Odds Ratio: 1.5, 95% Confidence Interval: 1.0–2.2), eye irritation (1.5, 1.1–2.1), hoarseness/dry throat (1.5, 1.1–2.0), toothache (1.4, 1.0–2.1), unusual tiredness (1.5, 1.1–2.0), fever/shivering (1.7, 1.1– 2.5), joint pain

(1.5, 1.1–2.1) and muscular pain (1.5, 1.1–2.0). Another study conducted by Heaney et al. on 23 individuals who lived within 0.75 miles of the Orange County, NC regional landfill, indicated that odor is largely responsible for the alteration of daily activities. Table 8 shows the relationship between twice-daily odor reports, mood states, irritant and physical symptoms.

Table 8: Different mood states along with the number of recorded instances and odds ratio of such cases, together with 95% CI (Heaney et al. 2011).

	No. of records	Binary odor OR[a] (95% CI)
Mood states		
Stressed	558	2.1 (1.2, 3.8)
Angry, grouchy, bad-tempered	336	3.9 (1.8, 8.5)
Weary, bushed, exhausted	469	1.8 (0.8, 4.0)
Gloomy, blue, unhappy	358	3.1 (1.6, 6.1)
Nervous or anxious	420	2.5 (1.3, 5.0)
Confused, poor concentration	262	0.3 (0.03, 2.1)
Active, energetic, peppy	415	0.6 (0.2, 1.5)
Mucous membrane irritation		
Burning eyes	368	5.3 (2.5, 11.6)
Burning nose	386	5.0 (2.5, 10.2)
Burning throat	309	3.3 (1.5, 7.1)
Upper respiratory		
Cough	334	2.0 (1.0, 3.9)
Difficulty breathing	310	1.9 (0.9, 4.2)
Runny nose	555	2.6 (1.4, 4.9)
Sore throat	359	1.9 (0.8, 4.2)
Gastrointestinal		
Diarrhea	164	2.6 (0.2, 29.5)
Nausea or vomiting	127	2.7
Loss of appetite	181	0.7
General ill feeling	310	2.7 (1.1, 6.6)
Headache	387	3.3 (1.5, 7.4)
Dizzy or lightheaded	176	4.1 (1.3, 12.5)
Skin		
Skin rash	210	1.2 (0.2, 6.3)
Skin boils	166	4.6 (0.6, 37.8)
Itchy skin	295	1.9 (0.6, 5.6)
Skin irritation	187	4.7 (1.1, 21.0)
Ringing in ears	176	2.9 (0.6, 14.2)

[a] Conditional fixed effects logistic regression models adjusted for time of day (morning/evening) of diary record. OR= odds ratio; CI= confidence interval.

Odor annoyance also induces olfaction disorders which in turn results in abnormally acute or distorted smell function in most of the cases (Murphy et al. 2003). For example, a person suffering from phantosmia, a disease for hallucinogenic smell function, can sense odors even in the absence of an odor stimulus (Hirsch 2009). People living nearby landfills are also found to complain about

nuisance flies and their associated diseases to Environmental Health Officers (Howard 2001). In a study by Sakawi et al., it had been found that a staggering 80.5% of the respondents feel their health had been adversely affected by the odor while an even greater 83.7% feel that their quality of life has been negatively affected by the presence of malodor. A very significant 60% of the respondents have moved simply to get away from the odor (Figure 5).

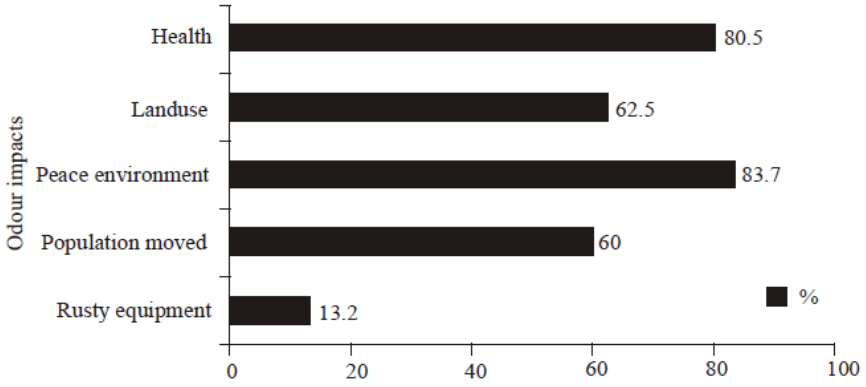

Figure 5: Percentage of respondents being impacted in each category (Sakawi et al. 2011).

1.4.2 Health Effects of Specific Odorants

Specific landfill odorants have their own health side effects. This section addresses such effects for a few such odorants, namely hydrogen sulfide, methyl mercaptan and ammonia. Methyl mercaptan, hydrogen sulfide and dimethyl sulfide are all reduced sulfur compounds which form the primary sources of malodor at various landfills. Hydrogen sulfide, an extremely hazardous, flammable gas and one of the most odorous gases contributing to landfill odor, exerts a strong 'rotten egg' smell upon its release in the environment. In fact, 90% of the mass concentration of all sulfur gases in LFG is formed of H_2S (Jin 2015; Kim et al. 2005b; Scheutz et al. 2009; Xia et al. 2015). It is also known as sewer gas, swamp gas or manure gas (OSHA 2005). A large amount of hydrogen sulfide is released in nearby landfills as organic matter, human and animal waste breakdown biologically with time. Less than 15 ppb hydrogen sulfide is often detected in landfill air (ATSDR 2016). Although no long-term health issues among the residents living nearby landfills has yet been detected due to an exposure to low-level hydrogen sulfide, a higher amount always causes considerable health hazard. Various health effects due to hydrogen sulfide exposure at different levels is presented in Figure 6.

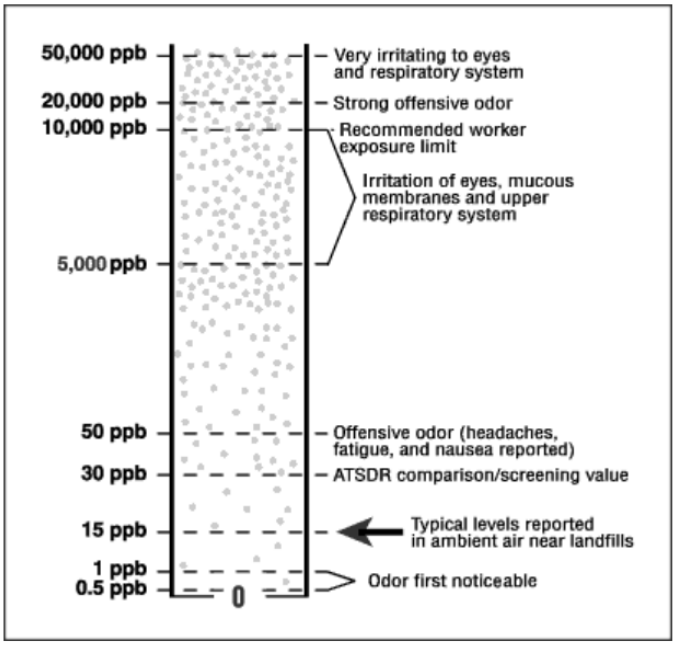

Figure 6: Health issues arising from exposure to hydrogen sulfide at different concentration levels (ATSDR 2001).

Ammonia, another highly irritating odor-causing compound, exerts a sharp and pungent odor when it is present in concentrations of more than 5 ppm in the environment (ATSDR 2015). Its smell is easily detectable by human because of its presence in smelling salt and various household cleaning products. General irritation to ammonia exposure begins at concentrations of 50,000 ppb for less than a day (ATSDR 2001). Exposure to ammonia above 500,000 ppb for 30 minutes can cause serious nose and throat soreness in humans (ATSDR 2001). Lungs, skin and eyes can also be permanently damaged due to a higher-level exposure, culminating to death in case of an exposure to 5,000,000 ppb of ammonia for less than 30 minutes. The National Institute for Occupational Safety and Health (NIOSH) recommends an exposure of no more than 5 minutes if the concentration of ammonia in air is 50 ppm (Bai et al. 2006).

Methyl mercaptan also known as methanethiol is another flammable gas with rotten cabbage smell. It can be easily perceived if its concentration is more than 1.6 ppb in the air (ATSDR 2014). Human moist tissues such as eyes, skin, and upper respiratory tract can be seriously irritated when they are exposed to a high-level of methyl mercaptan. Inhaling a significant dosage of mercaptan causes headache, dizziness, nausea, vomiting and can even lead to coma and death (ATSDR 1992). Methyl mercaptan also acts on the central nervous system, causing respiratory paralysis. The vapors originating from liquid methyl mercaptan are denser than air and so sits at the ground level, which makes it particularly dangerous (ATSDR 2014).

1.4.3 Decreasing Property Values and Lawsuits

The impact of the presence of landfills on housing prices in the locality has been reported in a number of studies. Almost all studies show that having a landfill negatively affects the property values in the vicinity. Du Preez and Lottering found that property values increase by 5~7% for

every mile between the landfill and the property. In 1982, Baker conducted a study on a landfill in Dryden, NY and found that the property values decrease by as much as 21% at 0.25 miles from the landfill while the reduction is only 0.55% at 2 miles from the landfill. A similar study in Minnesota found that property values decreased by 6.2% for each mile closer to the landfill (Nelson et al. 1992). In 2010, Ready conducted that high-volume landfills (accepting over 500 tons waste per day) impact property values more than low-volume landfills. On average, high-volume landfills lower property values nearby by 12.9% while low-volume ones lower values by 2.5% (Ready 2010).

A different line of study concentrates on the socio-economic status of the population living in the vicinity of landfills. A national level study on 9565 landfill sites uncovered that the area within a 2 km radius of a landfill is more deprived than a reference area (Elliott et al. 2009). There are also studies showing that landfill sites are disproportionately present in areas with lower housing values and where there is a higher proportion of people of color (Martuzzi et al. 2010; Norton et al. 2007). This makes low-income residents more vulnerable to the effects of landfill than their more affluent counterparts. Along with the health risk issues and devalued properties, odor deteriorates the relationship between the landfill management authorities and people living nearby landfills, ultimately leading them towards filing recurring complaints against them (ATSDR 2016).

It is evident that the landfill authorities must bear a large cost of penalties and hassle just because of the nuisance it creates. In March 2019, residents living nearby Grand Central Sanitary Landfill in Pen Argyl, Pennsylvania filed a second lawsuit against the landfill authority for creating a public nuisance due to offensive odors and their ineffectiveness even though being charged just one month prior to that (Salamone 2019). A reimbursement of at least $4.5 million had been asked from the authority by 90 complainants, each asking for $50,000. In a separate case, residents of Slate Belt asked for $100,000 in reimbursement against a landfill authority, arguing that the odors and pollutants emitted from the plant interfered with their enjoyment of property which resulted in damages exceeding $5 million. A settlement of $4.1 million had been approved after two years of filing a federal-class action lawsuit by a Moraine resident against Stony Hollow Landfill in Ohio in 2018 (Blizzard 2018). Several lawsuits had been filed against the owner of the Bridgeton Landfill by the residents of the Spanish Village subdivision neighborhood in St. Louis, MO (Bernhard 2014). The complainants rejected a settlement offer of $26,250 per household which resulted in filing an additional 14 lawsuits against the authority arguing that the money would not be enough for all the nuisance the landfill had already created and would create in the future.

1.5 Odor Measurement Techniques

The task of objectively quantifying odor emission has turned out to be quite challenging. Without proper quantification, it is not possible to design legislation to curb odor pollution since there would be no way to set legal odor emission limits. Currently, the measurement techniques vary from place to place. Such techniques range from panels of humans for detecting smells to electronic noses designed to sniff out smells to analytical models for downwind receptors (Laor et al. 2014). The sections below will address several such odor measurement techniques.

1.5.1 Human Assessment

The most common form of odor measurement technique comes in the form of a panel of humans selected to apply their olfactory senses to test the presence of odorants in ambient air. The odor assessment can be done in two ways: dynamic and static. In dynamic olfactometry, a device known as an olfactometer is used to blow a stream of air mixed with an odorant towards the human nose. The olfactometer can be used to control the concentration of the odorant using an odorless gas to control the dilution. Such a process can be used to test gaseous samples collected in Tedlar bags or other cylinders as shown in Figure 7 (Schiffman et al. 2000). In fact, this process has been standardized in the US as ASTM E679-04 (ASTM 2004), in Europe as EN13725 (CEN 2003), and in Australia and New Zealand as AS/NZS 4323.3:2001 (Laor et al. 2014). For measuring odor in this method, a human panel is formed consisting of people with a "normal" sense of odor perception. For reference, members are selected according to their sensitivity to n-butanol in the range of 20-80 ppb and a specific standard deviation (Laor et al. 2014). It is worth stating that the human perception threshold for n-butanol is 40 ppb or 123 $\mu g/m^3$-air (van Harreveld et al. 1999). The panel is then exposed to a stream of odorless air. The concentration of the odorant gas in the air is slowly increased (i.e. the dilution of the odorant is slowly decreased) until all members of the panel can distinguish the smell of odorant in the stream of air (St. Croix Sensory 2005; Baltrėnas et al. 2012). The concentration of the odorant can then be determined by various statistical and averaging methods (Laor et al. 2014). During the process, the panel may also be asked to provide other information such as rating the odor on other qualities including quality (odor character), intensity (odor strength), and irritation intensity (Schiffman et al. 2015).

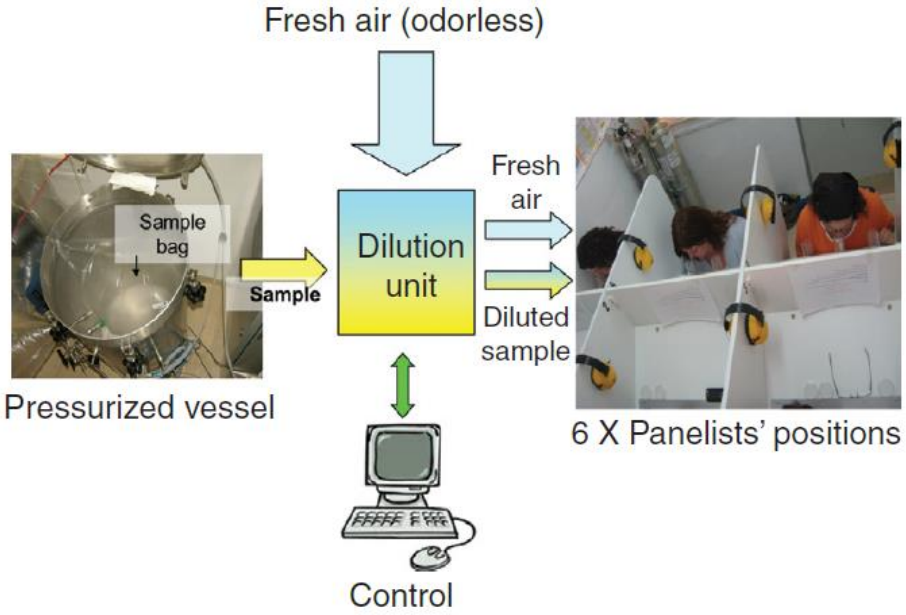

Figure 7: Block diagram showing the process of lab olfactometry and the components associated with it. (Laor et al. 2014).

In static olfactometry, the odorant is sampled from a bottle which either contains the odorant emitting substance itself or, for example, cotton pieces which contains the odorant emitting substance. Another method for measuring odor is known as the triangle odor bag method. This is the recommended odor measurement method from factories and livestock in Japan (Offensive

Odor Control Law, 1995; Iwasaki 2004). Triangular odor bag method is an air dilution process in which odor concentration and index are measured (Belgiorno et al. 2013). Odor concentration is the dilution ratio when an air with odorant in it is mixed with odorless air such that the odor cannot be detected. The odor index is the logarithm of odor concentration of air times 10.

There are some obvious problems in dynamic olfactometry. Since human panelists are used in this technique, some measure of subjectivity is introduced which is not the norm for scientific measurements (Belgiorno et al. 2013). The subjectivity comes from the physiological differences in the smelling capabilities of different people. It is also a costly procedure and is difficult to recreate (Yuwono, & Lammers 2004). Different measurements may be obtained at different times, even keeping all the factors constant and so, this is not a method which can scale well with time. With a different panel, the result varies even further. There is also the impracticality of conducting this procedure in case of poisonous gases (Yuwono, & Lammers 2004). Cases of olfactory fatigue also cannot be ruled out and is a barrier to objective results. To reduce the subjectivity, multiple panelists may be used to test the same odorant and obtain results. In practice, the team of panelists may just be two people, or even one in some cases (Nicolas et al., 2006). The approach just described here can be termed what is known as a sensorial approach since it depends on the human sensation of odors. Although it gives data on odor concentration, it does not provide information on the magnitude of disturbance experienced by the population or the effective contribution of individual components of the complete odorant mixture (Jiang 1996; Sneath 2001).

1.5.2 Field Olfactometry

While laboratory olfactometry depends mostly on human assessment, field olfactometry depends on static olfactometry and is accomplished using a device known as a scentometer or field olfactometer (Figure 8) (Laor et al. 2014). This device works by adjusting the ratio of odorous (non-filtered) and non-odorous (filtered) air. The Dilution to Threshold (D/T) ratio which is the number of dilutions to the threshold level of an odorant is determined under field conditions (Laor et al. 2014). Different types of scentometers include the Nasal Ranger® scentometer, the Barneby box scentometer, and the mask scentometer (Newby & McGinley 2004, Sheffield et al. 2004, Henry et al. 2011b).

Figure 8: Instruments used in field olfactometry (Laor et al. 2014).

Scenteometers are an economically viable option and there is also the advantage that readings are taken on field instead of in a lab (Brattoli et al. 2011). However, there are disadvantages such as odour fatigue which is caused by the difficulty of not exposing the scentometer to the odorous environment before the actual readings are taken (Henry et al. 2011b; Bokowa, 2010b). There are also no options of dilutions and the sniffers cannot be rated against their ability to detect a known reference concentration. The quantification process itself is a difficult task due to factors such as shifts in the odor plume, variation of wind speed and direction and presence of other background odors (Schiffman et al. 2000). Tracer gases such as SF_6 or objects such as helium balloons can be used to monitor the dispersion of odorants (Flyer et al. 1977; Lehning et al. 1994).

1.5.3 Atmospheric Dispersion Model

Atmospheric dispersion models are an analytical method of calculating the concentration of odorants at downwind receptors at a certain distance from the emission source. Inputs to these dispersion models include source odor concentrations which have been determined by other methods such as human assessment or electronic nose measurements in the first place. So, the accuracy of this process depends very much on the accuracy of the source concentration measurement. Dispersion models predict the number of dilutions required to reach the threshold concentration at a specific distance from the source. So, there is no way to accurately predict odor annoyance unless the relationship between odor concentration and perceived offensiveness is quantified objectively (Laor et. al, 2014). There is also the shortcoming that such models are odorant specific and non-quantitative. Community perceptions of odors are usually carried out using such models (Sarkar and Hobbs 2002; Sarkar et al. 2003; Roebuck et al. 2004; Laister et al. 2002).

1.5.4 Gas Chromatography (GC) and Mass Spectrometry (MS)

A method of identifying odorants is gas chromatography (GC) which is paired with Mass spectrometry (MS) as a detection technique. An advantage of GC is that very small concentrations

of odorants can be detected in this method. For this technique, the odor is collected beforehand and then passed through a chromatographic column where the sample travels through a carrier gas (Yuwono & Lammers 2004). The detector is sensitive to the sample and not the carrier gas. The movement of the gas is analyzed, and a graph is formed which is then compared to a reference graph for identifying the specific compound.

There are a few disadvantages to using this method. At its core, GC is a method of measuring the concentration of the compounds which are responsible for causing the odor. At times, the intensity of odors does not match with the concentration of the compound. It may be that a very small amount of the compound is present, but the odor intensity is quite high. Thus, GC is not able to give information about the actual intensity of the odor (Davoli, 2004; Zarra *et al.*, 2007b; Belgiorno et al. 2013). The sampling techniques also influence the results to some extent (Gostelow *et al.*, 2001), but the effect can be reduced by means of portable GC-MS analyzers (Zarra *et al.*, 2008b; Zarra *et al.*, 2008c). Another issue is the relative costliness of the technique as well as the higher skills required for using this method for analysis Gardner and Bartlett (1999).

1.5.5 Electronic Nose

The electronic nose (E-nose) is an instrument which can quantify odors by means of electronic and chemical sensors (Yuwono & Lammers 2004). A concise definition can be obtained from Gardner and Bartlett (1999) who stated e-nose to be an array of electronic and chemical sensors which can detect simple and complex odors using pattern recognition systems. An odor stimulus generates specific signals known as fingerprint (or smell print) for the odorant. In this way, a database of different fingerprints can be built, each corresponding to a specific odorant, which can then be used to detect an unknown odorant as shown in Figure 9 (Yuwono & Lammers 2004). There are three components to an e-nose (Schiffman et al. 2000). The principal component is a number of gas sensors which can detect the presence of VOCs. Such sensors can be in the form of metal–oxide–semiconductor field-effect transistors (MOSFETs). The second component is known as the sample handler whose purpose is to transfer the odorant from the collection device to the gas sensors. The final component is the signal processing system which acts like the “brain” of the whole device. Signal processing can be done using pattern recognition which in turn is performed using Artificial Neural Networks (ANN), principal component analysis (PCA), cluster analysis, and discriminant function analysis (DFA) (Schiffman et al. 2000). As the output, the e-nose can return the actual odorants present as well as their concentration.

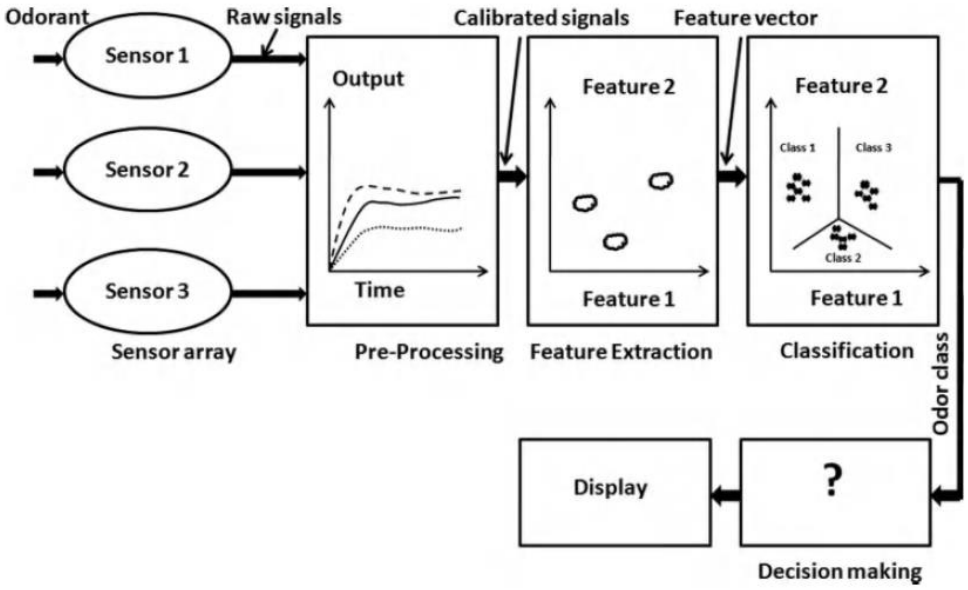

Figure 9: Block diagram showing the various components of an e-nose system (Belgiorno et al. 2013).

Recently, e-noses have been used along with real-time dispersion modeling for regulation of odor emission sources (Laor et al. 2014). An added advantage of e-noses is their portability and their usability in places where humans do not have to be present. They can also be quite economical and fast in their analysis. However, they can detect odorants having concentrations of ppm or ppb while the human nose can detect concentrations in the ppt range which is considered as a disadvantage of e-nose technology (Schiffman et al. 2000). They must also undergo a training phase before they can be used in accurately detecting odorant concentrations (Brattoli et al. 2011).

1.5.6 Chemical Sensor

A chemical sensor is a device which responds to a particular chemical in a way which can be used to confirm the presence and concentration of the chemical (Figure 10) (Yuwono & Lammers 2004). This definition also includes biosensors which are highly specific in nature and can be used to determine the presence of certain chemical species (Cattrall, 1997). Another definition is provided by Göpel and Schierbaum (1991) where it is stated that chemical and biochemical sensors are devices capable of converting chemical states (e.g. concentrations, partial pressures, or activities of particles) into electrical impulses (Yuwono & Lammers 2004). The same authors classified such sensors into categories based on the specific property which is used for the detection such as potential, voltages, conductivity and capacity, mass, heat, optical constant, etc. Generally, chemical sensors are composed of a chemically active substance with a transducer. The substance detects the presence of the chemical while the transducer converts the change induced in the chemical into an electrical impulse (Gardner et al. 1988).

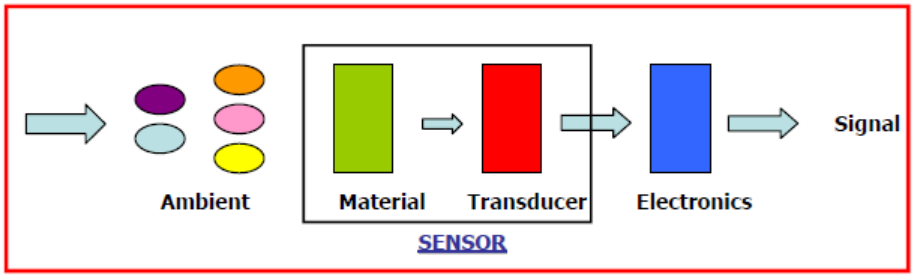

Figure 10: Block diagram representing the components in a solid state chemical sensor (Brattoli et al. 2011).

1.5.7 Shortcomings of Stated Odor Measurement Techniques

A number of odor detection techniques have been discussed in the preceding paragraphs. It is clear that each of them has shortcomings. No one technique is able to perform all forms of analysis and can be said to be the best in all parameters. To provide a summary of the discussed techniques, Table 9 shows a number of parameters and how a particular technique performs with respect to that parameter.

Table 9: Parameters in odor measurement and along with characteristics of odor measurement techniques. (Brattoli et al. 2011).

Parameters	Olfactometry	Other Sensorial Methods	Electronic Nose	GC
Objective measurement of odor concentration	+	+	-	+
Quantitative measurement of odor concentration	+	-	+	+
Measurement standardization	+	+/-	-	-
Continuous measurement	-	+/-	+	-
Single species determination	-	-	-	+
Temporal representativity of measurement	-	+/-	+	-
Time of analysis	+/-	-	+	+/-
Costs	+	+/-	-	+

(+ = high; +/- = medium; - = low)

There has been ongoing research which focuses on rapid identification of odors at low concentrations (Liu et al. 2013; Sakaran et al. 2012). However, these only work for specific odorants and are not quantitative in nature. The techniques are also irreversible which is not an ideal way of detecting odorants. An example of such odorant-specific chemical sensor is that found by Carlson et al. (2006) which can detect fluorine in concentrations of 10 ppt and is irreversible in nature. Liu et al. (2013) proposed a method for testing for the presence of different components of body odor. But their work does not include a way to quantify the odorants in any way. Similarly, other methods have shortcomings which are specific to their own characteristics and have already been described in the preceding sections.

1.6 Physiology of Human Olfactory Perception

Human's perception of odor is considered as a complex phenomenon. The air containing odorous chemicals are at first inhaled by the nose and warmed in the nasal cavity while passing through the series of small bones known as turbinates (Figure 11) (ATSDR 2016; Ruth 1986). Deep inside the cavity, there exist olfactory membranes less than 1 square inch in size, which contain a group of specialized nerve cells on small hairs (cilia). These nerve cells are known as olfactory neurons or receptor cells (chemoreceptor) that interact with the odorous chemicals and convey the sensation of smell through the olfactory bulb in the form of electric signal to the higher regions of the brain (ASTDR 2016). The human nasal cavity contains 10-20 million of olfactory receptor neurons which are the only regenerative nerve cells in the human body (Saladin 2004). However, before reaching the receptor neurons, the odorants must be conveyed through the aqueous nasal mucous and sensillar lymph that surround the olfactory membrane at the surface of the nasal epithelium (Tegoni et al. 2000). Since odorants are most commonly hydrophobic molecules and nasal mucus is hydrophilic, it acts as a barrier to the odorants from being transported further. Nasal mucus, secreted by the supporting cell in the epithelium along with Bowmans's glands of mammals and insects, consists of 95% water, 2% mucopolysaccharides, lysozyme, high-molecular-weight glycoproteins, antibodies, salts, odorant-binding proteins and other enzymes (Heydel et al. 2013). Several mechanisms such as molecular size, hydrophobic interaction as well as some other binding interactions allow the particles and odorants to cross the barrier of aqueous nasal mucus (Figure 11) (Leal et al. 2017).

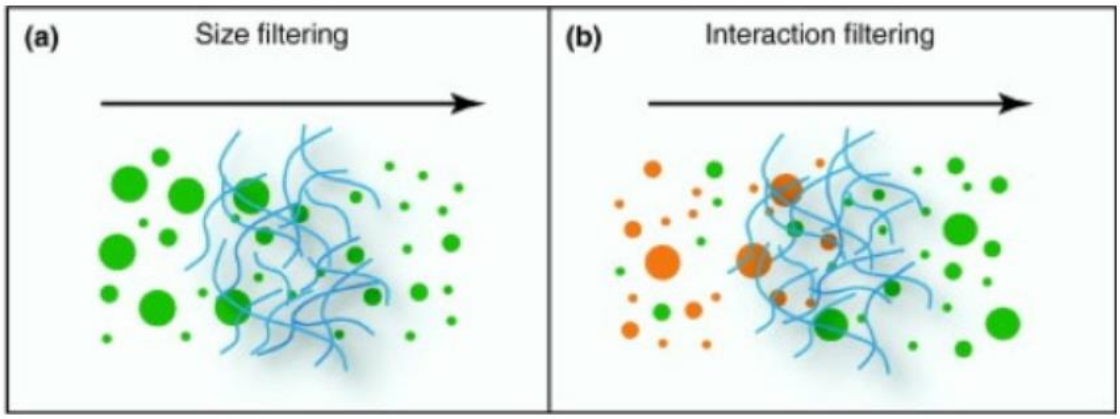

Figure 11: Size filtering and interaction filtering inside the nasal cavity. Size filtering allows smaller particles and odorant molecules to pass inside the cavity (left). In interaction filtering the particles (green) that interacts less with the mucus are allowed to enter inside while others (orange) are rejected due to strong binding interaction with mucus (right) (Leal et al. 2017).

The odorant-binding proteins (OBPs) which is secreted in the nasal mucus by the olfactory epithelium, bind with odorant molecules in the hydrophobic ligand binding pocket and thus transport them towards the olfactory receptors (ORs) (Schiefner et al. 2015). As soon as the odorants reach the receptors, it allows the brain to be able to distinguish them. Detecting the odor stimulants, converting them into signal and integrating the signal are the three main physiological processes that combinedly build an olfactory image in the brain (Heydel et al. 2013). The quality

of the olfactory signal depends on any mechanism that helps in the conveyance of the odorants or changes the ligand binding properties of the odorants during the detection process. Such mechanisms are called perireceptor events which involve an active participation of proteins that secreted in the nasal mucus to arouse an odorant stimulant (Heydel et al. 2013). Figure 12 shows the longitudinal cross section of the human nasal cavity along with the cells inside of it which help to realize the sense of smell.

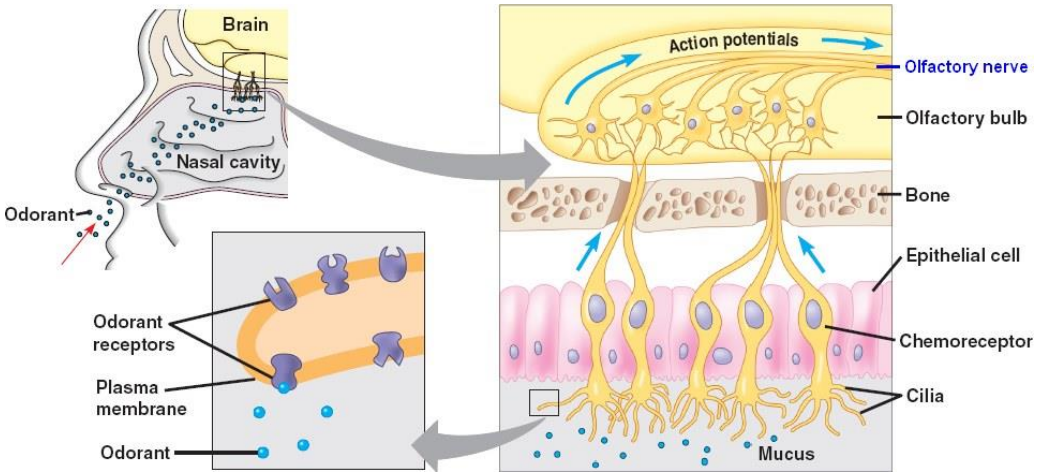

Figure 12: Cells within nasal epithelium allowing humans to perceive odors (Jasper 2013).

Humans can detect up to 10,000 odors and are able to distinguish between odorants whose difference in concentration varies by as little as 7% (ATSDR 2016; Sela & Sobel 2010). Even the slightest change in the molecular structure, for example, odorants having equal number of carbon atoms but different functional group or having same functional group but having a difference in chain length by one carbon only can be perceived by humans (Sela & Sobel 2010). A study conducted by Yale University showed that women can distinguish more odors than men though they are no better than men in detecting odors (Ruth 1986). The reason they mentioned is that women are more concerned about odors than men. Besides, when people are constantly exposed to the same odor, they eventually lose the ability to perceive it due to the fatigue of olfactory receptor neurons (Ruth 1986).

1.7 Odorant Binding Protein (OBP)

This section describes odorant binding proteins and their properties. Their structure is described in general before diving into details about the human odorant binding protein and how they can be used in biosensor development.

1.7.1 Structures and Properties of OBP

Odorant binding proteins (OBPs) are small, extracellular proteins which are soluble in nature and found in the nasal mucus of a large variety of vertebrates including porcine, bovine, mouse, rat, elephant, human etc. and even in insects (Briand et al. 2002; Tegoni et al. 2000; Pelosi, 2001). However, the only OBPs isolated from non-mammalian species are those from frogs and xenopus (Millery et al. 2005). OBPs belong to lipocalin superfamily and are secreted at a high concentration

(10mM) in the nasal epithelium (Heydel et al. 2013). They are known to reversibly bind volatile chemicals i.e. airborne odorants with micromolar affinities and have dissociation constants in the micromolar range (Briand et al. 2002). They are thought to be a good carrier of inhaled odorants towards the olfactory neurons and participate in the selection or deactivation of odorant molecules as well (Brind et al. 2002). Since most of the proteins that belong to lipocalin superfamily can bind with hydrophobic molecules, a clear distinction between OBPs and other proteins is most essential. Besides, odorants have diverse physical and chemical structures and functional groups. So, the question remains as to whether it is only a single lipocalin group that binds with these wide variety of odorants, which is rather impossible (Tegoni et al. 2000). Hence, various types of OBPs with broad binding affinity towards ligands are supposed to be more appropriate to accomplish this role.

Although the structural pattern of vertebrate and insect OBP is quite dissimilar, their role in olfaction has been proved to be similar (Wei et al. 2008). Commonly, less than 20% amino-acid sequence is identical among the members of lipocalin superfamily as shown in Figure 13 (Briand et al. 2002). The vertebrate OBP follow a generic structural pattern comprising of 8 stranded antiparallel β-barrel bounded on both sides with an α-helix (Briand et al. 2002). A central apolar cavity named "calix" exists within the barrel inside of which odorant binding takes place in the ligand binding site. The broad binding activity of OBPs having dissimilar amino acid sequence in the same animal species allows them to bind with odorants of different chemical structure. Such OBPs have been observed in a number of mammals including cow, rat, mouse, pig, porcupine and human etc. (Schiefner et al. 2015). To date, 9 different OBP subtypes have been reported in porcupine which is the highest among all the mammals (Ganni et al. 1997). Additionally, three OBP subtypes have been reported in pig, four in mouse, three in rabbit and three in rat (Briand et al. 2002). OBPs can be monomer, dimer or heterodimer depending on the species it is present in and their molecular weights vary between 18~20 kDa (Heydel et al. 2013; Briand et al. 2002). Most of these subtypes are acidic (pH 4~5) but a few of them exhibit basic or neutral state (Heydel et al. 2013).

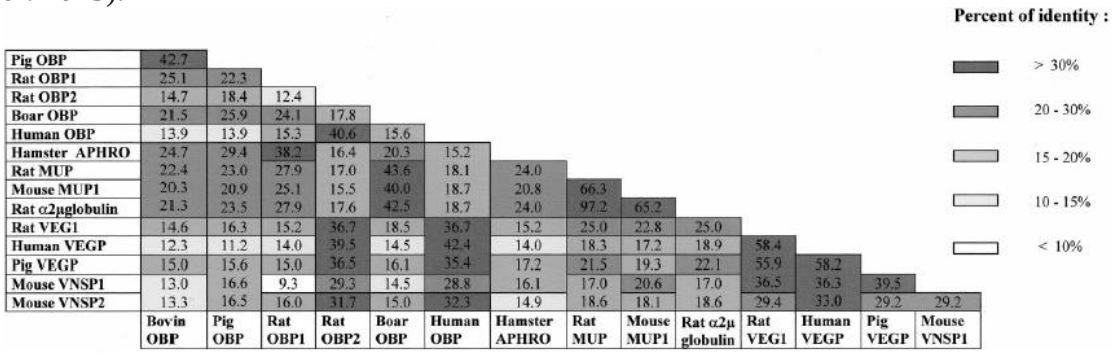

Figure 13: Percentages showing identical amino-acid sequence between various members of lipocalin superfamily including OBPs and PBPs (Pheromone Binding Protein) (Tegoni et al. 2000).

1.7.2 Interaction of OBPs with Odorants

The concept of OBP acting as an odorant-carrier was hypothesized when Pelosi et al. first discovered that bovine OBP is able to bind with pyrazine (2-isobutyl-3-metoxypyrazine), an odorant of bell-pepper with low detection threshold. Eventually a broad binding affinity towards medium sized hydrophobic odorants has been specified for bOBP and pOBPs (Tegoni et al. 2000).

In case of the dimer bovine OBP which was considered as the prototypic OBP for quite a while, two odor molecules replace the naturally occurring endogenous ligands existing inside the inter dimer open cavity (Spinelliet al. 1998; Paolini et al. 1999). Unlike bOBP, the monomeric porcine OBPs does not hold any natural ligand inside of its β barrel cavity and one binding site per monomer has been reported by Paolini et al. The cysteine residue, that is commonly observed in most of the OBPs, is in the form of a disulfide bridge in case of pOBPs whereas it is completely missing in bOBP (Paolini et al. 1999). A 3D structure of bOBP and pOBP is shown in Figure 14.

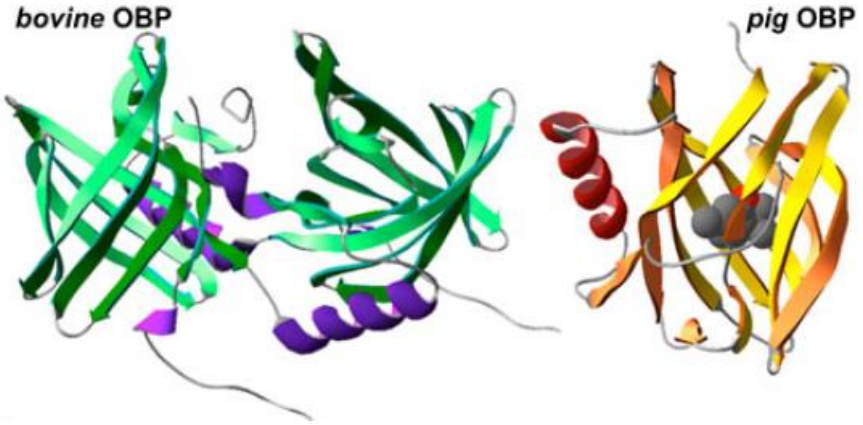

Figure 14: Tertiary structure of bOBP (bovine OBP) and pOBP (porcine OBP) modeled using DeepView software (Pelosi et al. 2014).

Researchers have established that heterocyclic derivates have the highest affinity towards OBPs whereas fatty acid with short chain, spherically shaped terpinoids e.g camphor and its analogues have less affinity (Tegoni et al. 2000). Thiazoles, pyrazine, terpenoids, menthol, thymol, aliphatic alcohols and aldehydes were found to exhibit good affinity for OBPs with dissociation constant within range of 0.1^1 μM (Tegoni et al. 2000). In case of rat OBPs, the relative fluorescence intensity in displacement assays has proved that each type of the OBPs binds with a distinct class of odorants. For example, rOBP-1 tends to interact with heterocyclic compounds (e.g. pyrazine and its derivatives), rOBP-2 specifically prefers long-chain aliphatic aldehydes as well as carboxylic acids and rOBP-3 normally binds with odorants having a ring structure (Briand et al. 2002).

In 2013, Silva et al. first used pOBP for odor control strategy where a cationized cotton surface coated with pOBP was used to mask the smell of cigarettes by delaying the release of citrenellol, a fragrance often uses in perfumes. This idea introduced the possibility that OBPs can be efficiently used to trap unpleasant odors from fabrics and can be more effective than cyclodextrins in this regard (Silva et al. 2014). Increasing the temperature was also observed to increase the affinity of OBP towards a particular fragrance which demonstrated that textiles treated with OBP can be a good option for making perfumes last longer than usual as the temperature rises from ambient to human body temperature.

1.7.3 Human Odorant Binding Protein-2A (hOBPIIa)

Two possible odor binding protein genes, hOBPIIa and hOBPIIb being 95% identical, have recently been discovered in humans (Briand et al. 2002; Tegoni et al. 2000). The hOBPIIa gene,

which codes for the protein hOBPIIa, has been transcribed in nasal mucus, lung, lachrymal and salivary gland. This is contrary to the hOBPIIb gene, which has been found mainly in the genital sphere organs (e.g. prostate and mammary glands) (Tegoni et al. 2000; Lacazette et al. 2000). The amino acid sequence of hOBPIIa is 45.5% homologous to rat OBP-2 whereas hOBPIIb is 43% identical to that of human tear lipocalin-1 (Heydel et al. 2013). A central eight-stranded antiparallel β-barrel (strands A–H) with a C-terminal α-helix, which is a traditional lipocalin fold for all other OBPs, has also been observed in case of the monomeric hOBPIIa (Schiefner et al. 2015). Additionally, another short β-barrel (strand I), running slightly antiparallel to strand A, at the downstream of the α-helix (Figure 15) and a disulfide bridge located between cys59 and cys151 have been detected in hOBPIIa. A positive charge exists in the entire cavity inside the β-barrel, more specifically at the entrance of the loop region, which is another common feature for all amino acid side chains pointing towards the cavity (Schiefner et al. 2015). Most of the OBPs are acidic but the measured isoelectric point (PI) of a recombinant hOBPIIa manufactured by Briand et al. to characterize its odorant binding activity was found to be 7.8 (neutral) (Briand et al. 2002).

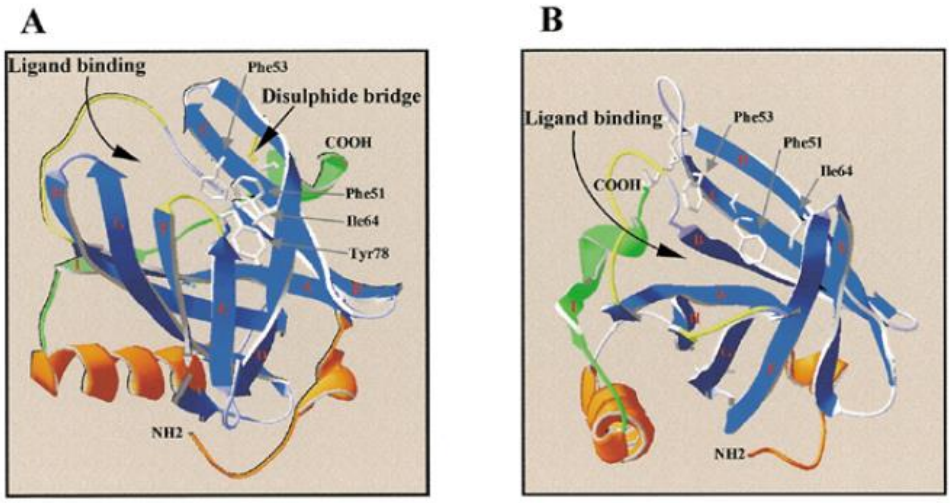

Figure 15: Tertiary structure of hOBPIIa (left) and hOBPIIb (right). β sheets, α-helices and disulfide bridge are indicated in blue, green and yellow respectively (Lacazette et al. 2000).

The remarkably large ligand binding cavity inside the β-barrel of hOBPIIa allows it to bind a large variety of hydrophobic odorants having different structures and sizes with affinities in the micromolar range though comparatively low affinity has been seen for some very strong odorants such as 2-isobutyl-3-methoxy pyrazine and eugenol (K_{diss} > 10 μM) (Schiefner et al. 2015; Briand et al. 2002; Heydel et al. 2013) . In case of hOBPIIa, a more restricted binding specificity than porcine OBP and rOBP-1 or rOBP-3 has been reported due to the fact that it shows very strong affinity for aldehydes (e.g. undecanal: K_{diss} ~ 0.3 μM, lilial, the odor of the lily of the valley: K_{diss} ~ 0.5 μM, and vanillin: K_{diss} ~ 1 μM) and large chain fatty acids (K_{diss} ~ 0.3 μM) (Heydel et al. 2013; Briand et al. 2002). Moreover, the affinity is even stronger for aldehyde compounds with respect to acids, since the lysine residue located at the edge of the pocket binds strongly with aldehydes by forming a hydrogen bond than with acids (Figure 16) (Heydel et al. 2013).

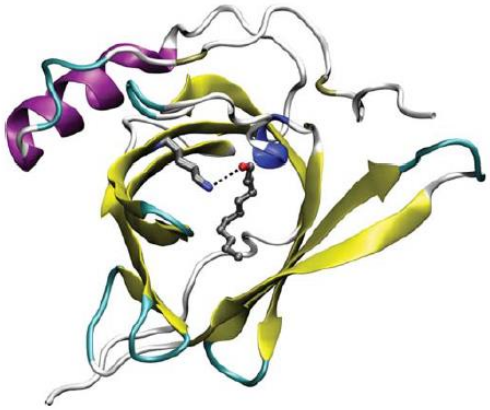

Figure 16: Tertiary structure of hOBPIIa bonded with the aldehyde, undecanal (carbon atoms are indicated in grey, oxygen is in red and nitrogen is in blue), at the middle of the ligand binding pocket. (Heydel et al. 2013).

The affinity of hOBPIIa for aldehyde compounds (either aliphatic or aromatic) increases as the molecular size of the odorants increases when compared with their chemical series (Tcatchoff et al. 2006). As the cavity opens to transfer the odorants towards olfactory receptors (ORs), water enters the cavity and recovers the chemical integrity of lysine and aldehydes (Charlier et al. 2009).

1.7.4 Biosensor Development Using OBP

There have been previous cases of OBP being used as a biosensor. There are certain properties of OBPs which make them viable candidates in such usage (Ko et al. 2010). They have high thermal stability, which is ideal for environmental monitoring. They are also not affected by presence of an increased concentration of organic solvents (Wei et al. 2008). OBPs can easily accommodate site-directed mutagenesis which can make them bind specifically with certain compounds (Wei et al. 2008). For any solution to work commercially, cost is an important consideration and this is alleviated in case of using OBPs as biosensors since they can be easily synthesized from recombinant DNA in bacteria. Re-engineered porcine OBP has been used to monitor polycyclic aromatic hydrocarbons in the environment (Figure 17) (Wei et al. 2008). The reasons behind the selection of pig OBP as a biosensor are those that have been stated in the preceding paragraph.

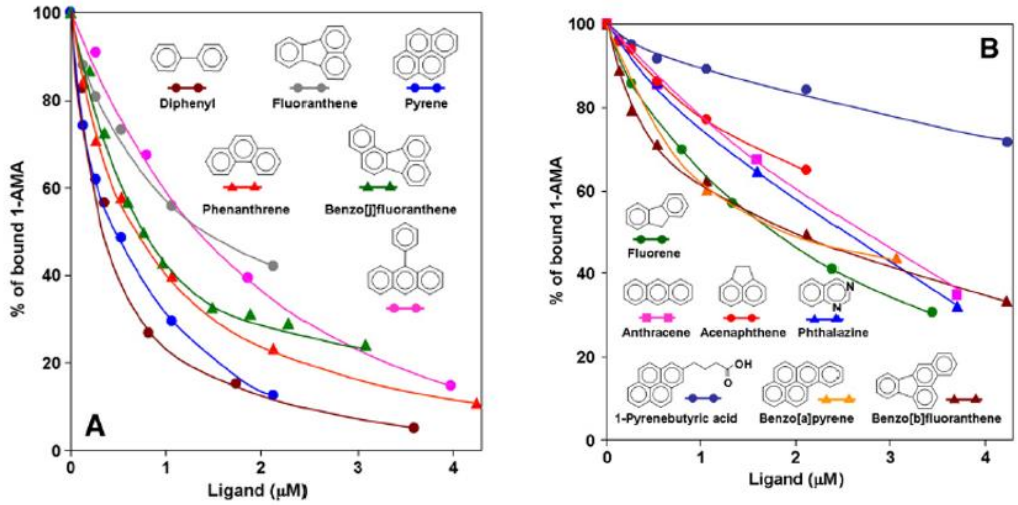

Figure 17: 1-AMA competetive binding assay of pOBP-m2 (pig OBP mutant) with different polycyclic aromatic hydrocarbons . 1μM 1-AMA and 1μM protein were used in an increasing concentartion of methanolic solutions of aromatic compounds starting from 1 mM (Wei et al. 2008).

An effective biosensor needs to be sensitive enough to detect different compounds (Kim et al. 2008; Song et al. 2008; Mirmohseni et al. 2008) and there have been efforts to improve the sensitivity of systems relying on biosensors [Choi et al. 2004; Kang et al. 2006; Lee et al. 2009; Kim et al. 2009; Yoon et al. 2009). In case of olfactory receptor-based biosensors, OBPs can be used to boost the sensitivity (Ko & Park 2008). This enhancement for OBP through interacting with the receptor has been described for a Drosophila OBP (Xu 2005). OBPs have also been used for detecting important ligands in complex environments. This is displayed by Lu et al. in 2014 where honeybee OBPs was designed to detect ligands found in floral odors and pheromones. Ramoni et al. investigated the use of advanced nano-biosensors derived from bovine OBP (bOBP) and immobilized into carbon nanotubes to detect the presence of hazardous compounds in luggage storage facilities, airports and other public places. The same author also investigated the detection of explosive compounds using the protein scaffold of the lipocalin OBP (Ramoni et al. 2007).

1.8 Fluorophores

Fluorophores are used to study the interaction of different ligands with proteins, among proteins themselves as well as in the study of protein properties and structures (Mikhailopulo et al. 2008; Abdurachim et al. 2006; Sreejith et al. 2009; Kazakov et al. 2009). Addition of an extrinsic fluorophore such as fluorescein to a protein does not modify the structure of the protein in any way and this property makes such fluorescent compounds effective probes for the purpose of study (Kmiecik & Albani 2010).

In biology and medical science, small-molecule fluorescent turn-on probes are used to detect specific proteins. Such probes are especially capable of detecting and monitoring enzyme activities such as glycosidases, proteases, lactamases, and kinases (Kobayashi et al. 2009, Sakabe et al. 2012, Xing et al. 2005, Shults & Imperiali 2003). Generally, such fluorescence mechanism works by

reacting with the enzyme and converting itself from a non-fluorescent product to a fluorescent one. However, there are also some environment sensitive fluorophores with emission properties depending on the environment. Such fluorophores display weak fluorescence in polar environments but show strong fluorescence in hydrophobic environments (Figure 18) (Zhuang et al. 2013). Most of the ligand binding sites of proteins are hydrophobic in nature. So, binding of ligands to the hydrophobic ligand-binding domain will cause the environment-sensitive fluorophore to be closer to the hydrophobic region of the protein and emit high fluorescence. However, not all ligands bind with all proteins. Differences exist in the nature of hydrophobic molecules bound to the proteins. This difference arises because of the amino acid residue surrounding the hydrophobic pocket in proteins (Flower 1995). An example of this case will be progesterone binding to α1-acid glycoprotein but not to β-lactoglobulin (Kmiecik & Albani 2010).

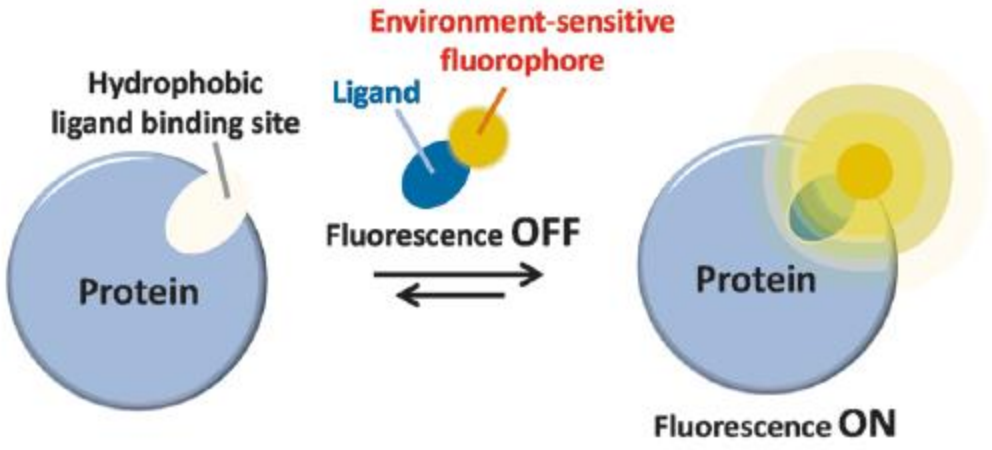

Figure 18: Mechanism of fluorescent turn-on probe where the ligand attaches to the specific hydrophobic ligand binding site of the protein and the surrounding hydrophobic environment allows the environment-sensitive fluorophore to emit strong fluorescence. (Zhuang et al. 2013).

To date, the interaction of several fluorophores have been investigated with hOBPIIa. The binding capability of a recombinant hOBPIIa has been tested with a number of extrinsic fluorescent probes such as DAUDA, DACA and ASA (Figure 19) (Mei et al. 1997; Lechner et al. 2001). The results showed that DAUDA shows a weak emission spectrum with a peak at 545 nm while DACA and ASA had their maxima at 475 nm and 425 nm respectively (Briand et al. 2002). The spectral properties of probe fluorescence emission confirm that the binding site of the recombinant hOBPIIa is present in the hydrophobic pocket within the β-barrel.

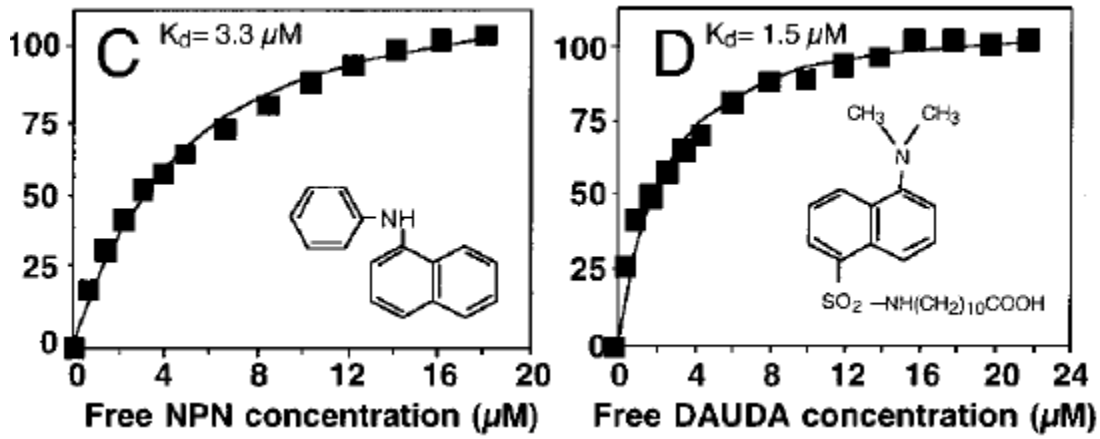

Figure 19: Titration curve of 2μM hOBPIIa against the fluorescent probes NPN (left) and DAUDA (right) at increasing concentrations (Briand et al. 2002).

1.8.1 1-Aminoanthracene as a Fluorophore

1-Aminoanthracene (1-AMA) is a widely used fluorophore to study the interaction among lipocalin family proteins. Aminoanthracene is a cytotoxic compound (Boudreau et al. 2016) and introduces mutation in DNA, altering the protein structure (Daniel Kmiecik, Albani et al. 2015). 1-AMA is a hydrophobic ligand. So, it follows that it will only show fluorescence when bound to a hydrophobic site in a protein. A free 1-AMA solution shows a peak fluorescence intensity at 600 nm. However, while forming complex with OBPs, the peak intensity occurs at 481 nm (Gonçalves et al. 2018; Silva et al. 2014; Paolini et al. 1999; Briand et al. 2003). The dissociation constant of 1-AMA while interacting with a purified recombinant rat OBP (rOBP-1F) has been found to be 0.6 $\pm$ 0.3 mm (Briand et al. 2000).

Since 1-AMA is a hydrophobic fluorophore, various experiments have been performed with different alcohols as solvents to find out the displacement of 1-AMA by a particular solvent. Experiments with ethanol, methanol and dimethylsulfoxide (Figure 20) revealed that methanol has a relatively low rate of displacement of the fluorophore, leads to it being an attractive solvent for using 1-AMA as a marker in OBP experiments (Briand et al. 2000).

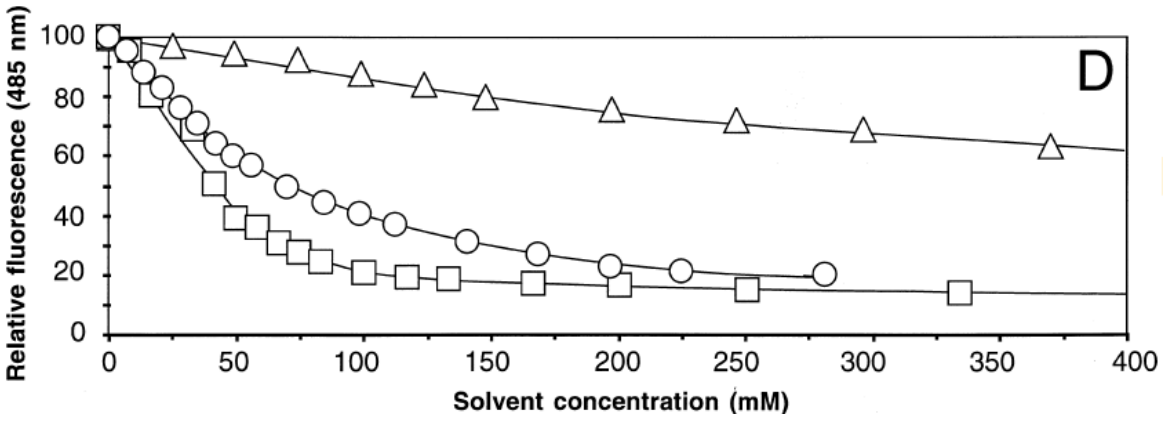

Figure 20: Fluorescence curve of 1-AMA at 485 nm with increasing solvent concentration. 1-AMA is displaced the least by methanol, leading to relatively high fluorescence emission even though the solvent concentration is increased (Triangle: Methanol, Circle: Ethanol, Square: Dimethylsulfoxide) (Briand et al. 2000).

Since 1-AMA has attractive properties as a fluorophore, its mixture with methanol has the potential to be used as a fluorescent probe to study the interaction of hOBPIIa and various odorants in more detail as used in the cases of rat and porcine OBPs.

1.9 Objectives

??????????????

2 METHODOLOGY

This chapter details lists the materials used as well as discusses the procedures followed in conducting the experiments. Details have been included regarding the procurement of purified hOBPIIa protein. In discussing the procedure, the fluorescence binding assay used in the experiments and the measurement techniques have been described. The experiments have been conducted using a prototype reactor chamber. The construction as well as the design considerations of that chamber have been laid out. The chapter concludes with a description of the fluorescence measurement techniques using the spectrofluorometer.

2.1 Materials

The fluorophore, 1-AMA (technical grade, 90%) was obtained from Sigma Aldrich in powdered form. Gas cylinders (29 L gas cylinder containing H_2S, 25 ppm (+/- 5%) gas balanced with N_2; 34 L gas cylinder containing NH_3, 25 ppm (+/- 5%) gas balanced with N_2; 34 L gas cylinder containing CH_4, 25 ppm (+/- 5%) gas balanced with Air; 34 L gas cylinder containing a mixture of H_2S, 25 ppm (+/- 5%), CO, 50 ppm (+/- 5%) and CH_4, 2.5% (+/- 2%)) were procured from Geotech Environmental Equipment, Inc. (Colorado, USA). Another, 34 L gas cylinder containing Methyl Mercaptan, 50 ppm gas balanced with N_2 was obtained from ShopCross (North Carolina, USA).

2.2 Purified hOBPIIa

The purified human odorant binding protein (hOBPIIa) was produced under the supervision of Dr. David Binninger, an Associate Professor in the Department of Biological Science at FAU, by his research team following the protocol described by Roblyer in 2017. Earlier in 2015, the bacterial expression plasmid was obtained from Dr. Artur Ribeiro, a Professor in Biological Engineering Department at the University of Minho, Portugal that contained the coding sequence for the recombinant protein variant hOBPIIa. Later, Dr. Binninger's research team had cultured and induced *E. coli* containing the human odor binding protein gene. The protein was then isolated from the batch, following a Bradford assay analysis which was conducted to determine the concentration of the induced, purified protein samples (Figure 21).

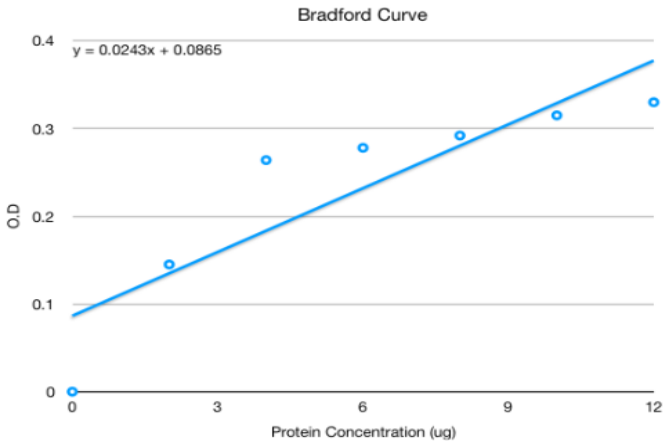

Sample	O.D
Induced Sample (2uL)	0.278
Un-induced Sample	0

Figure 21: Bradford curve showing a clear increase in protein concentration between induced and uninduced samples.

After obtaining a positive result from the Bradford assay, an SDS-PAGE electrophoresis was conducted to verify the base-pair size of the purified protein (Figure 22).

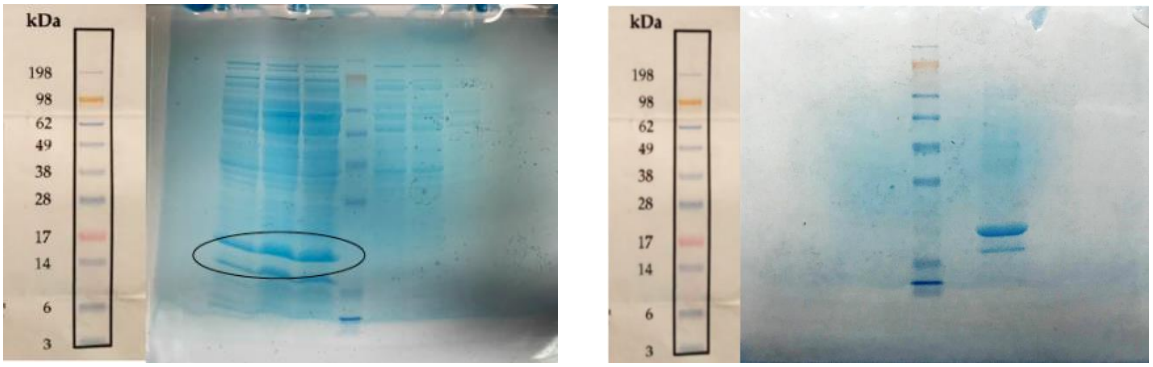

Figure 22: 12.5% SDS-PAGE Gel of crude protein (left) and 12.5% SDS-PAGE Gel of purified protein (right).

The measured OD and linear equation were used to calculate the amount of isolated protein to be 3.94 µg/µl in 50 mM Tris–HCl, p^H7.4 solution, with a molecular weight of around 17 kDa.

2.3 Fluorescence Binding Assay

For analyzing the competitive binding assay of the biosensor complex to the odorants, 1-AMA was used as the fluorescent probe and pure gases such as H_2S, NH_3, CH_4 and Methyl Mercaptan were selected as model compounds/odorants. Also, a gas mixture of H_2S, CH_4 and CO were used as "standard landfill gas" mixture. Since 1-AMA is hydrophobic, it was first dissolved in 100% methanol and then D.I. water was added to it for a final methanol concentration of 10%. Since 1-AMA is very sensitive to light, it was always stored in a brown colored glass bottle. Previously, in

an experiment conducted by Roblyer in 2017, it was evaluated that the optimal ratio of hOPBIIa to 1-AMA is approximately 1:1. Following up from that experiment, to prepare the biosensor complex, 1μM hOBP2A was mixed with 1μM 1-AMA (protein to fluorophore 1:1 ratio as before) solution in 50mM Potassium Phosphate-KOH, pH 7.5 buffer solution. The solution was then poured into an enclosed reactor chamber. For a conservative use of the protein, the total volume of the aqueous protein- 1-AMA solution in each experiment was limited to 10 ml. The rest of the headspace of the reactor chamber after pouring the solution in it was utilized for the gas which was exposed to the chamber later on. The gas was allowed to escape from the chamber through a one-way valve easily so that it would not exert any undue pressure on the chamber wall. The buffer solution helps to keep the p^H of the system at a constant level of 7.5, so that the properties of the solution remains unchanged while combining with acidic or basic gases.

The reactor chamber containing the buffered protein – 1-AMA solution was then exposed to pressurized gas for a certain amount of time. Since the gas is dissolving in the solution placed in the reaction chamber, the concentration of the odorant in the solution increases with time. Three different flow rates (0.5 standard liters per minute or slpm, 0.7 slpm and 0.9 slpm) were used for each of the gases (i.e. three separate experiments for each gas) to examine the competitive binding assay of the biosensor complex. In each experiment, 100 μL sample solutions were drawn separately from the reactor chamber by means of disposable syringes attached at the top of the chamber at successive intervals of time. The samples were then transferred to a quartz cuvette separately from the syringes for spectrofluorometry. The experimental setup is illustrated in Figure 23.

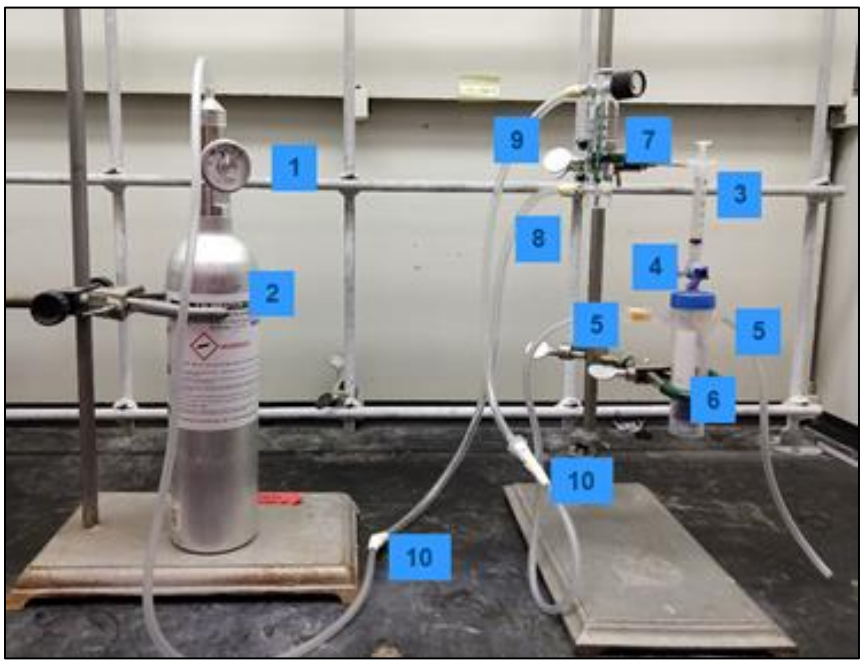

KEY

1 Regulator
2 34 L H_2S Tank
3 Syringe
4 3-way stopcock
5 One-way check valve
6 Reactor chamber
7 Flowmeter
8 Tube connected to cylinder
9 Tube connected to chamber
10 Tube connector

Figure 23: Label photograph of the experimental setup.

2.4 Reactor Chamber

The reactor chamber was built using a modified 50 ml centrifuge tube. The centrifuge tube has two one-way check valves attached to the top of it. A flowmeter (0.1-1 L/Min capacity) connects a gaseous cylinder and the reactor chamber with one of the check valves through quarter-inch flexible pipe lining. Another pipe leads from that valve into the chamber and ends in an aquarium-grade, pumice stone bubbler, which is mainly used to increase the surface area of solution exposed to the dispersed influent gas. By means of the second one-way valve, the gas escapes through the top of the reactor chamber. The biosensor complex exists in the buffered solution at the bottom of the chamber. The use of a narrow centrifuge tube as the reactor chamber instead of a wide one increases the efficiency of the process by exposing a lesser surface area of the protein - 1-AMA complex to the space above. Due to this fact, the amount of odorant escaping to the space above is reduced. Another benefit comes from the tube being elongated, which improves the likelihood of successful binding of the target odorant with the protein complex as it travels a greater distance to reach the surface.

To collect sample for fluorometry, a 3-way stopcock is attached to the cap of the centrifuge tube. One of the ports (shown as #4 in Figure 24 right) of the stopcock was only opened to draw a sample of the solution from the chamber using a syringe, which could be screwed on using a Luer-lok mechanism. Each time after collecting sample, an empty new syringe was substituted for the old one with the sample in it. The other port was kept closed for the whole time. This kind of setup ensures that the inside of the reaction chamber is never exposed to the external environment, thus eliminating the introduction of any external contaminants. Moreover, this also eliminated the issue arising from collecting samples by opening the cap of the centrifuge tube that might have introduced external contaminants. The experimental apparatus was set-up under a fume hood as a precautionary step and to keep in line with the safety protocols.

KEY

1 Syringe

2 Syringe opening

3 Support knob

4 Port 1 to reactor chamber

Figure 24: Reactor chamber using a centrifuge tube (left). 3-way stopcock used at the lid of the exposure chamber. The different ports and other parts are labeled (right).

2.5 Fluorescence Measurements

Fluorescence spectroscopy (i.e. spectrofluorimetry) was done using the machine Horiba Jobin Yvon FluoroMax-4 spectrofluorometer (Horiba-Jobin Yvon, Longjumeau, France) which is configured at right angle (Figure 25). Two hours prior to starting the experiments, the spectrofluorometer was powered up so that ample time was provided to keep the instrument warmed up. The fluorescence emission spectra were recorded using FluorEssence software at room temperature using an excitation wavelength of 380 nm. The emission spectrum was recorded between 410 and 700 nm at 1 nm interval.

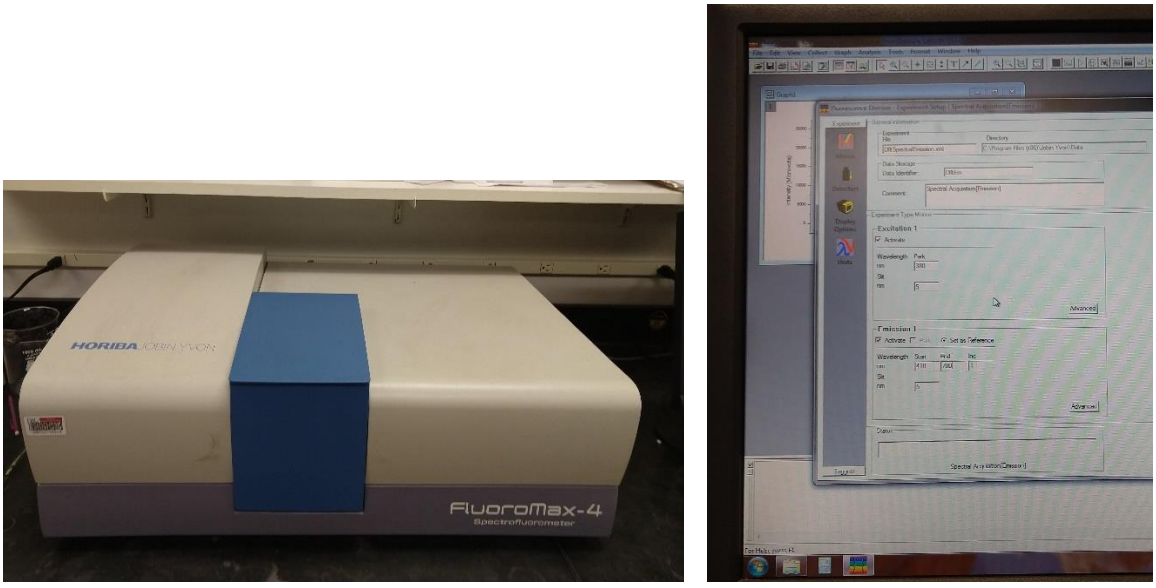

Figure 25: Horiba Jobin Yvon FluoroMax-4 spectrofluorometer (left) and Fluorescence software (right).

Samples were collected using 100 µl capacity (nominal volume) fluorometric quartz cuvette ("Z" Dim 15 mm) with 10 mm path length (Figure 26). Slit widths were set to 5nm in both excitation and emission stage. Between sample collection in the cuvette, care was taken to wash the cuvette properly using diluted ethanol and D.I. water so that no residue remains in the cuvette and causes cross-contamination.

Figure 26: 'Z' dimension (distance from the base to the center of the sample chamber window) of the quartz cuvette (left) and a 100 µL capacity quartz cuvette containing 100 µL of sample each time (right).

3 RESULTS AND DISCUSSION

3.1 Fluorescence Binding Assay With The Extrinsic Fluorophore (1-AMA)

Spectrofluorometry is used to assess the binding assay between hOBPIIa and different odorant gases where 1-AMA, which forms a complex with OBPs, has an effective role in understanding the interaction between the protein and odorants. 1- AMA is a fluorophore whose quantum yield increases when it remains in a hydrophobic environment. OBPs contains a hydrophobic cavity inside their β-barrel (Briand 2002) and this explains the increased quantum yield when 1-AMA forms a complex with these proteins. 1-AMA by itself in an aqueous solution does not have the same high quantum yield (Briand 2000).

Figure 27(a) shows the spectrofluorometric emission spectra of four different solutions excited at 380 nm: 1) 50 mM Potassium Phosphate-KOH, pH 7.5 buffer solution, 2) 1 µM 1-AMA in buffer, 3) 1 µM hOBPIIa in buffer, and 4) 1:1 hOBPIIa:1-AMA () in buffer. The mixture of hOBPIIa and 1-AMA (solution #4), a sharp spike is observed near 485 nm. This is a 96-fold increase in fluorescence intensity over that obtained for 1-AMA solution alone in the buffer, with peak at 565 nm. So, a blue shift emission spectrum was observed in this case along with the increased fluorescence intensity. Figure 27(b) shows only the curves for solutions 1, 2 and 3 since with solution 4 these curves were not clearly understandable in figure 1(a). This result is similar to previous results reported in Briand et al. (2000) for other OBPs e.g. there was a 15-fold increase in intensity in case of rat OBP-1F whereas this measure is 80-fold for porcine OBP-1. All other combinations in the fluorescence intensity curves show small spikes in the 400-450 nm range. These peak emissions are likely due to light scattering effects. There is no other peak near 485 nm for any of the other three curves, which provided evidence that the protein-fluorophore complex (hOBPIIa:1-AMA) is responsible for the high emission intensity at that wavelength. These results also verify the findings obtained by Roblyer (2017).

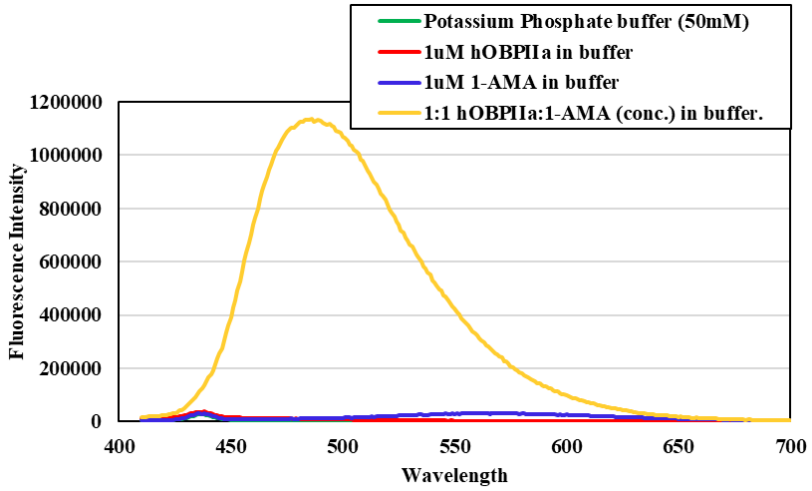

(a)

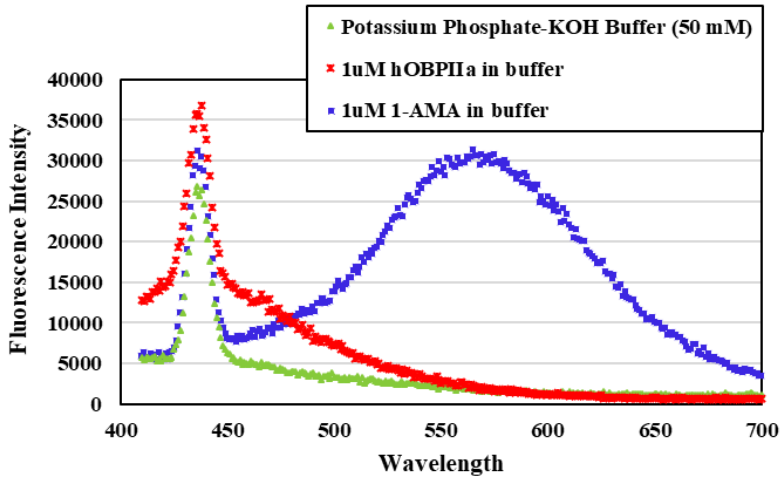

(b)

Figure 27: Spectrofluorometric analysis for individual biosensor components

Now that it is established that the protein-fluorophore complex causes an increased intensity in the spectrofluoroscopic experiments, it is important to establish the optimum concentration ratio between 1-AMA and hOBPIIa. This was accomplished by conducting a saturation binding experiment of the protein and fluorophore complex. Keeping the concentration of hOBPIIa fixed at 1 μM, the concentration of 1-AMA was increased in increments of 0.1 μM, starting from 0.1 μM up to 1.5 μM. Figure 28 shows the binding curve of hOBPIIa to 1-AMA. The relative fluorescence of the complex increases as the concentration of 1-AMA is increased gradually. The binding experiment reaches the saturation point at around 1 μM of 1-AMA. With further increase in the concentration of 1-AMA, the fluorescence intensity increase is negligible. The concentration ratio of 1-AMA to hOBPIIa found here confirms the same ratio obtained by Roblyer (2017).

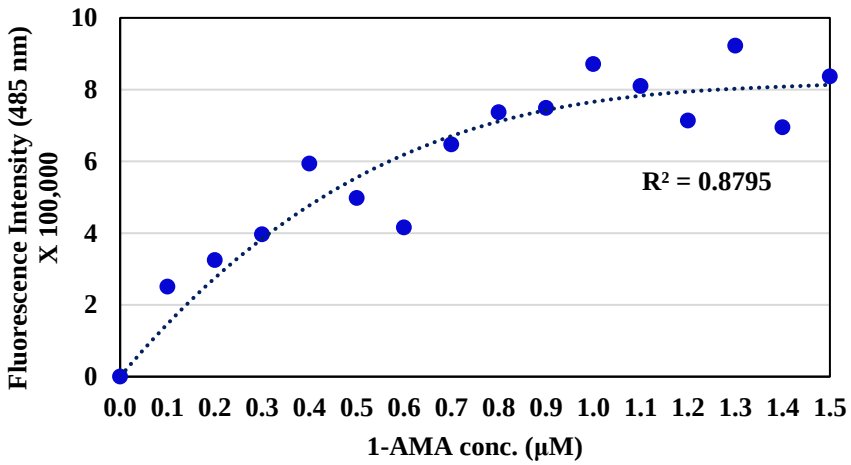

Figure 28: Binding curve of 1-AMA at different concentrations to hOBPIIa

3.2 Biosensor Sensitivity Experiments On Model Compounds

For selecting the model odorants for the experiments, some of the more commonly found gases in landfills were considered. Hydrogen sulfide is considered for its pungent smell and also due to its acidic nature. Ammonia is another common landfill gas and is alkaline. In landfills, mixtures of gases are usually present, and this has been replicated using a mixture of methane, hydrogen sulfide and carbon monoxide. Methane has been tested by itself as well so that its response can be better understood. Methyl mercaptan has been selected since it has a very low detection threshold and a powerful smell.

3.2.1 Experimentation with hydrogen sulfide (H_2S)

The first odorant to be tested with the biosensor is hydrogen sulfide (25 ppm +/- 5% balanced with N_2), identifiable by its rotten-egg smell. It also has a very low odor threshold concentration, which makes it detectable even at very low amounts. One of the objectives of this research was to replicate and verify previous experimentation carried out in 2017 by Roblyer, where an inverse relationship had been established between peak fluorescence intensity occurring at 485 nm and the amount of hydrogen sulfide passed in the biosensor complex (Roblyer 2017). In that experiment, a total of 100 mL protein-fluorophore complex was used for a protein to fluorophore ratio 1:1 (i.e. 1 µM hOBPIIa and 1µM 1-AMA) which was then exposed to 0.5 standard liters per minute (slpm) of hydrogen sulfide gas in a prototype reactor chamber. Samples of 1 mL were extracted at a constant time interval of 30 seconds for a total range of 450 seconds for spectrofluorometric analysis. The fluorescence intensity decreases with time as shown in Figure 29(a). The results established an inverse fluorescence relationship with time below 200 seconds and showed increased scatter above that time limit in Figure 29(b). The decrease in intensity is due to the fact that as more gas is passed into the biosensor complex solution, more of the 1-AMA bound to the protein is substituted by the odorant gas.

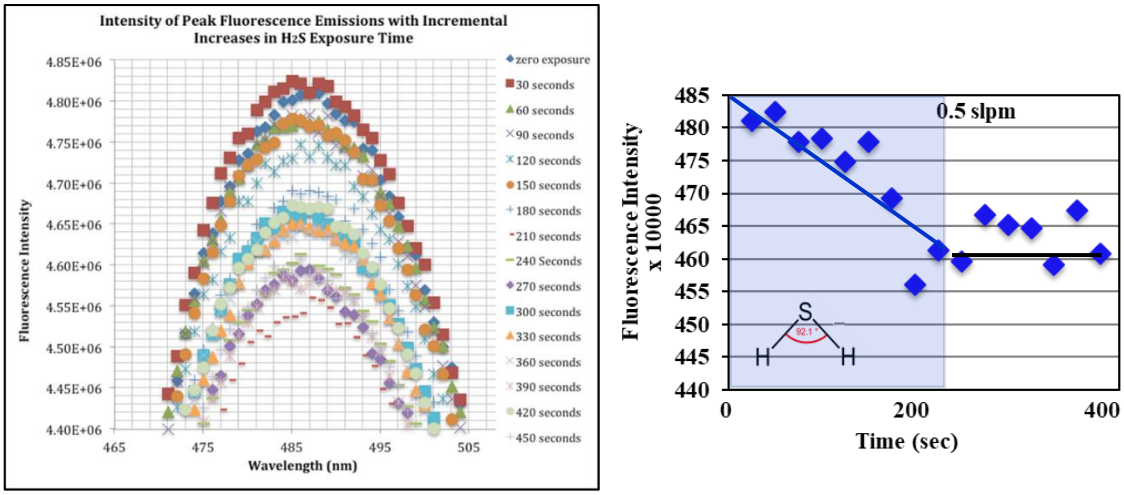

(a) **(b)**

Figure 29: (a) Spectrofluorometric emission spectra at 380 nm excitation found by Roblyer (2017) (b) Graph showing inverse relationship between peak fluorescence intensity and exposure time for the same experiment

To verify those results for hydrogen sulfide, an experiment was conducted using the revised reactor chamber as explained in the previous section. The concentration of the protein and 1-AMA were kept the same as the previous ratio, but due to limited protein availability, the total volume of the biosensor complex was 25 mL as compared to 100 mL. Another reason for keeping the volume to 25 mL was the capacity of the reactor chamber was 50 mL. Keeping the surface area of the interface low was expected to reduce potential mass loss due to stripping. Since the total volume of the biosensor complex was reduced, the amount of protein needed was also reduced. Therefore, it was necessary to adjust the sampling time interval to analyze the fluorescence intensity trend correctly. The overall experiment runtime was also kept shorter since it will take a shorter time for the hydrogen sulfide gas to bind with the protein present in the smaller reactor chamber. Figure 30(a) shows the measured emission spectra where the emission peaks occurred at ~485 nm as expected for each 1 mL of sample for the biosensor complex. As expected, an inverse relationship between fluorescence intensity and the amount of time the biosensor was exposed to hydrogen sulfide gas as shown in Figure 30(b) has been revealed when plotting the peak emission obtained at each time. The intensity decreases initially in a linear fashion with increasing exposure to hydrogen sulfide, as in the previous experiments reported by Roblyer (2017). One of the objectives of this research is to find out the quantitation range, i.e. the time up to which the biosensor complex shows an inverse relationship between emission intensity and time of odorant gas exposure. This has been derived by plotting linear trendlines, y-intercepted at the initial value and up to the point of any substantial decrease in fluorescence intensity. Therefore, the estimated quantitation range maximum is the point in which the initial linear trendline and the zero-slope portion of the curve intersect. However, in this verification experiment, the point up to which the biosensor complex remained effective was not clearly observed, although it is approximately around 180 seconds.

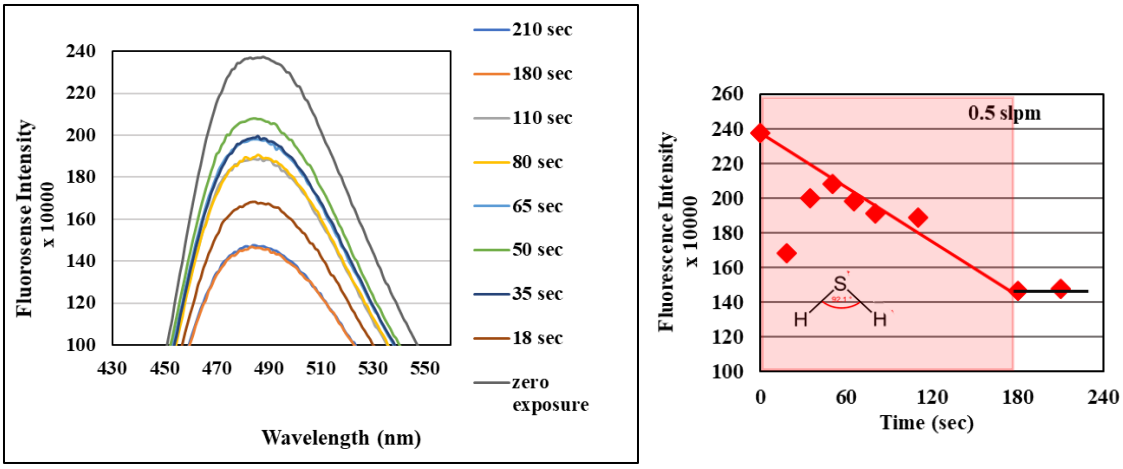

(a) **(b)**

Figure 30: (a) Spectrofluorometric emission spectra at 380 nm excitation for the verification experiment at 0.5 slpm hydrogen sulfide for 25 mL sample (b) Graph showing inverse relationship between peak fluorescence intensity and exposure time for the same experiment

The previous experiment was repeated using 10 mL solution of biosensor complex and keeping the same gas flow rate (0.5 slpm). This was done to check whether the biosensor complex is able to function at even lower volumes. Also, the overall goal was to conserve as much protein as possible during the research. Instead of collecting 1 mL sample each time, a reduced sample volume of 100 µL was drawn at 10 second interval for the first 30 seconds followed by a 15 second interval up to 90 seconds and then a 30 second interval for the remainder of the experiment. Figure 31(a) shows the intensity curves obtained at different times. The intensities are shown in relative terms, which allows for better comparison of the results. As time passes, the intensity decreases gradually as before. Figure 31(b) shows the graph plotted for peak emission intensity against time of gas exposure. The graph also shows the quantitation range of the biosensor solution and has been derived by plotting linear trendlines in a similar way as mentioned above, but y-intercepted at 100 (since the relative intensity of all samples at the beginning is 100). In this case, the quantitation range is around 120 seconds after which the intensity does not show a considerable change with time. A probable reason for this is the biosensor complex becomes saturated by the hydrogen sulfide gas passed through it within the first 120 seconds, thus establishing a possible quantitation range for a gas flowrate of 0.5 slpm.

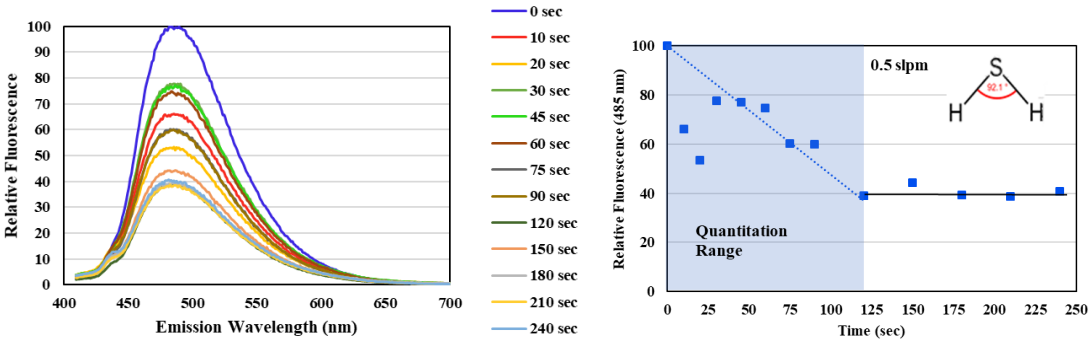

(a) **(b)**

Figure 31: (a) Spectrofluorometric emission spectra at 380 nm excitation at 0.5 slpm hydrogen sulfide for 10 ml sample (b) Graph showing inverse relationship between peak fluorescence intensity and exposure time for the same experiment

For the next experiment, a flow rate of 0.7 slpm was used for hydrogen sulfide gas to check the change in the quantitation range with an increased flow rate. The intensity curves obtained at different times is shown in Figure 32(a). As shown in Figure 32(b), the biosensor complex becomes saturated in a shorter time than before (approximately around 110 seconds), giving an even lower quantitation range at this higher flow rate. This is logical since the higher gas flow rate causes more of the odorant gas to bind with the biosensor complex more quickly, so the saturation occurs faster than before.

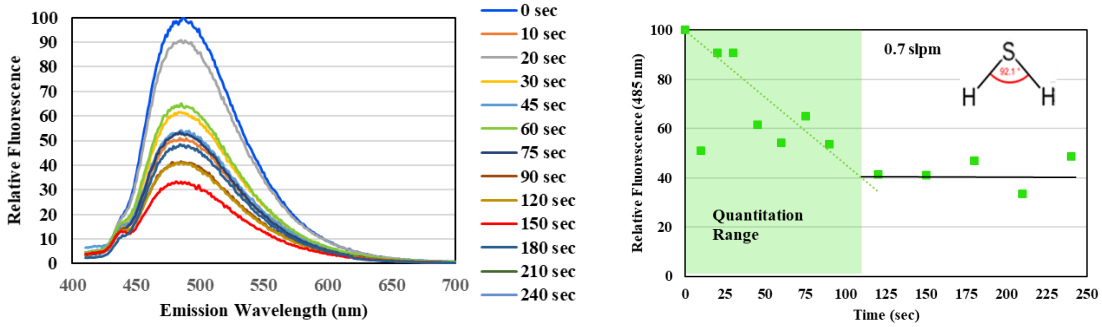

(a) **(b)**

Figure 32: (a) Intensity curves obtained for collected hydrogen sulfide samples at different times for 0.7 slpm. (b) Graph showing peak emission intensity against time of gas exposure.

Next, a higher flow rate of 0.9 slpm was used to check whether the quantitation range falls even further. Figure 33 shows the intensity curves obtained at different times for 0.9 slpm flowrate. Here, the biosensor complex becomes saturated in an even shorter time than the previous two times (approximately around 90 seconds).

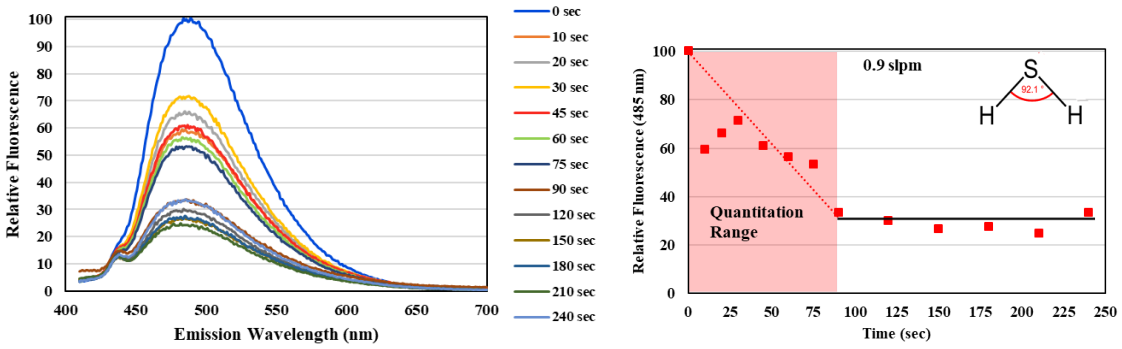

(a) **(b)**

Figure 33: (a) Intensity curves obtained for collected hydrogen sulfide samples at different times for 0.9 slpm. (b) Graph showing peak emission intensity against time of gas exposure.

In Figure 34(a) comparison has been made between the effect of the three different flow rates for hydrogen sulfide gas. The quantitation range is highest for the lowest flow rate and lowest for the highest flow rate. The curve for 0.7 slpm is expectedly between those of 0.5 slpm and 0.9 slpm although it is very close to the 0.5 slpm one. Also, the decrease in intensity is faster for the higher flow rate as evident by a steeper slope. This is likely due to increased mass flux of hydrogen sulfide at higher flow rates, which results in increased binding with the biosensor complex in a given time. Although it was expected that a lower gas flow rate would facilitate the mixing of the odorant gas in the biosensor solution possibly resulting in a shorter quantitation range, this has not been observed in this case as shown by the longer quantitation range found for lower flow rates. Since the research goal is quantifying odorants, the flow rate of hydrogen sulfide has been converted to mass flow using the modified form of ideal gas equation. Figure 34(b) shows the mass flow in µg of hydrogen sulfide against decreasing intensity up to the quantitation range in each case. For all three flow rates, the change in intensity with mass is found to be relatively close to each other, signifying that a certain mass of hydrogen sulfide binds with the protein for a certain decrease in intensity. Overall, the 10 mL biosensor solution (around 180 µg of protein) had an upper limit of measuring hydrogen sulfide in the range of around 35-45 µg depending on the flow rate.

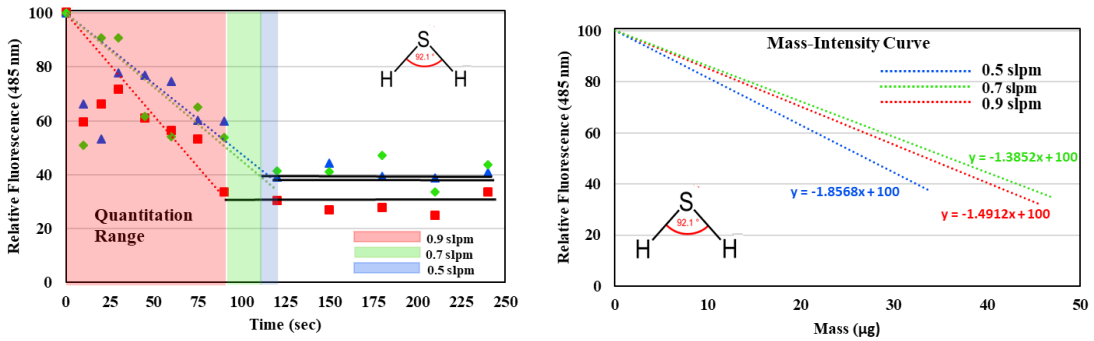

(a) **(b)**

Figure 34: (a) Comparative change in fluorescence intensity at 0.5 slpm, 0.7 slpm, and 0.9 slpm for hydrogen sulfide (b) Graph showing change in fluorescence intensity with mass flow of hydrogen sulfide at all three flow rates

Hydrogen sulfide is an acidic gas and therefore it is important to know whether there is any change in the pH of the solution due to its addition since even small changes in pH are known to denature proteins (O'Brien 2012). Since the reactor chamber is closed, it was not possible to measure pH in realtime using a pH meter. However, in all the experiments, pH strips have been used to measure the pH of the samples collected at each time interval and no pH change was observed visually during testing. As expected, the buffer solution was effective in keeping the pH of the biosensor solution constant.

3.2.2 Experimentation with ammonia (NH_3)

Following the experiments using hydrogen sulfide, which is an acidic gas, experiments had been conducted using ammonia (25 ppm +/- 5% gas balanced with N_2) in order to observe the interaction of the biosensor complex with an alkaline gas. Ammonia is another common odorant in landfills, having a strong chemical-like smell. Experiments using flow rates of 0.5 slpm, 0.7 slpm and 0.9 slpm were conducted. The peak emission curves are shown in Figure 35. For the lower flow rate of 0.5 slpm, the intensity seems to decrease up to around 90 seconds before becoming stable. For 0.7 slpm the quantitation range was around 75 seconds whereas, in case of the higher flow rate, no considerable change is observed after 50 seconds. Though ammonia is a basic odorant, the pH strips in all experiments did not indicate the solution to become basic in nature.

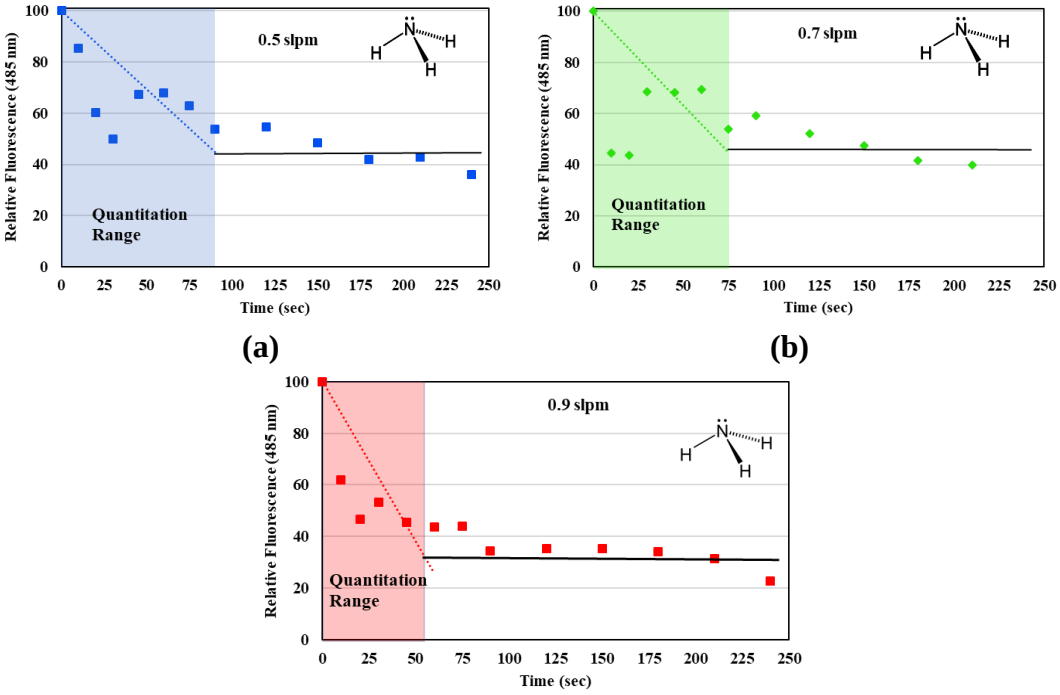

Figure 35: (a) Graph showing peak emission intensity against time for ammonia flowing at 0.5 slpm, (b) 0.7 slpm and (c) 0.9 slpm

Figure 36(a) shows the comparison of the three different flow rates for ammonia. The results generally follow the same trend as that obtained for hydrogen sulfide gas. Here again, the quantitation range is highest for the lowest flow rate and lowest for the highest flow rate. Similarly, the higher flow rate curves have a steeper slope, indicating a faster decrease in intensity. Also, the curve for 0.7 slpm lies between the other two curves. Figure 36(b) shows the mass flow of ammonia against decreasing intensity. Yet again, the curves show that a certain mass of ammonia binds with the protein for a certain decrease in intensity, just like in the case of hydrogen sulfide gas. The same amount of protein is able to measure ammonia up to around 12-18 µg dependent on the flow rate.

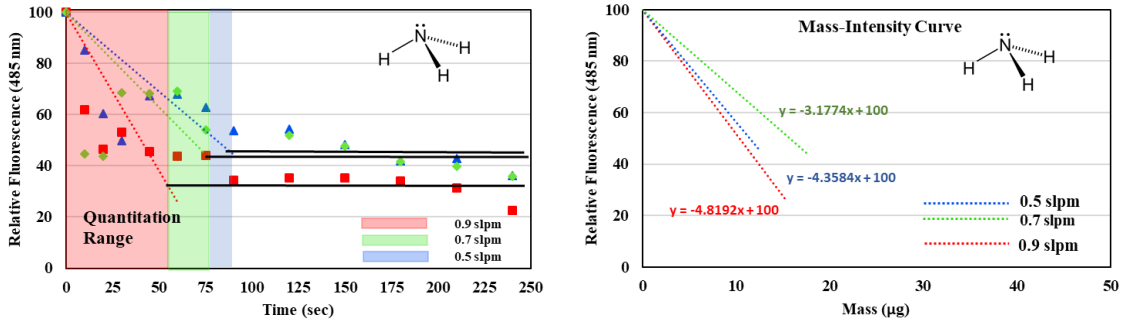

(a) **(b)**

Figure 36: (a) Comparative change in fluorescence intensity at 0.5 slpm, 0.7 slpm, and 0.9 slpm for ammonia (b) Graph showing change in fluorescence intensity with mass flow of ammonia at all three flow rates

3.2.3 Experimentation with methyl mercaptan (CH_3SH)

Organo-sulfur compounds play a significant role when it comes to odorants in landfills. Methyl mercaptan, known for its rotten cabbage-like smell, is one such compound which also has been tested in this research. The odor threshold value for methyl mercaptan is around 25 times lower than that of hydrogen sulfide (Ruth 1986). In case of 0.5 slpm flow rate, the intensity seems to be decreasing up to around 95 seconds. For 0.7 slpm, the quantitation range is around 75 seconds while for the higher flow rate of 0.9 slpm, the range became even shorter than the other two (around 60 seconds). The peak emission curves for methyl mercaptan are shown in Figure 37.

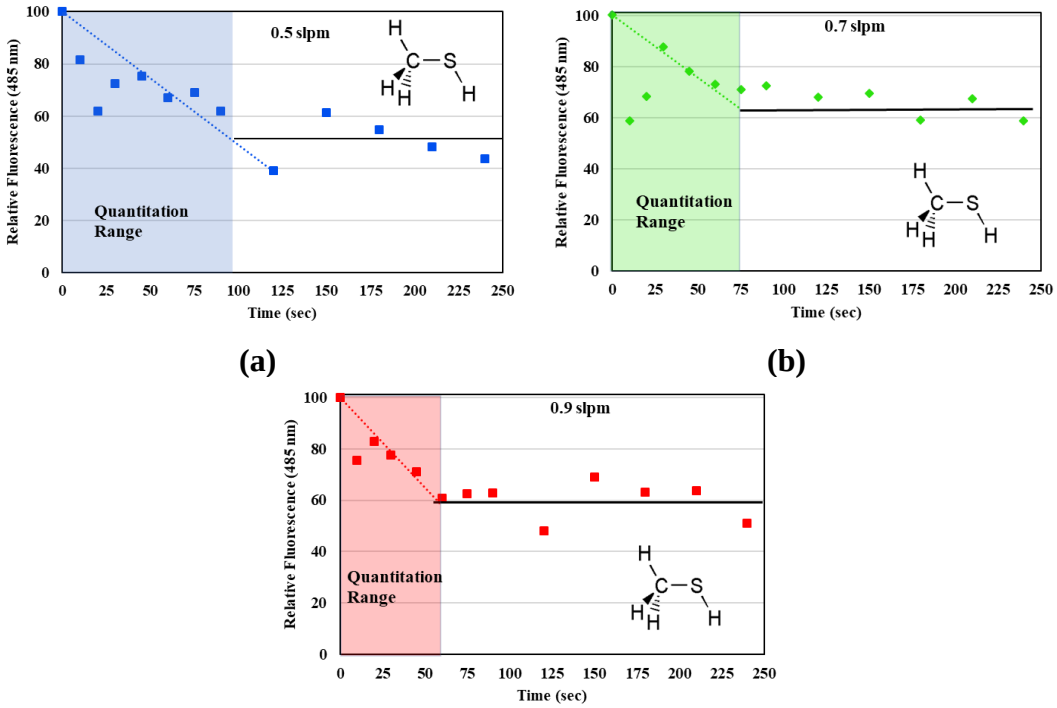

(a) **(b)**

(c)

Figure 37: (a) Graph showing peak emission intensity against time for methyl mercaptan flowing at 0.5 slpm, (b) 0.7 slpm and (c) 0.9 slpm

The comparative fluorescence intensity curves of methyl mercaptan are shown in Figure 38(a). The graph is different than the previously tested gases. While in case of the other gases the intensity decreased more in case of the higher flow rates, this is not completely true in this case as the intensity for 0.5 slpm decreases the most. As a higher flow rate of methyl mercaptan is passed into the solution, it seems that the gas is escaping faster from the solution in the form of droplets due to its highly volatile nature and was unable to lower the fluorescence intensity by a larger amount than the lower flow rate. However, the change in quantitation range follows the usual rule, i.e. increases with an increase in flow rate. Figure 38(b) shows the mass flow curve for all flow rates for methyl mercaptan. Using 180 µg of protein in 10 mL solution, around 83-95 µg of methyl mercaptan can be measured dependent on the flow rate.

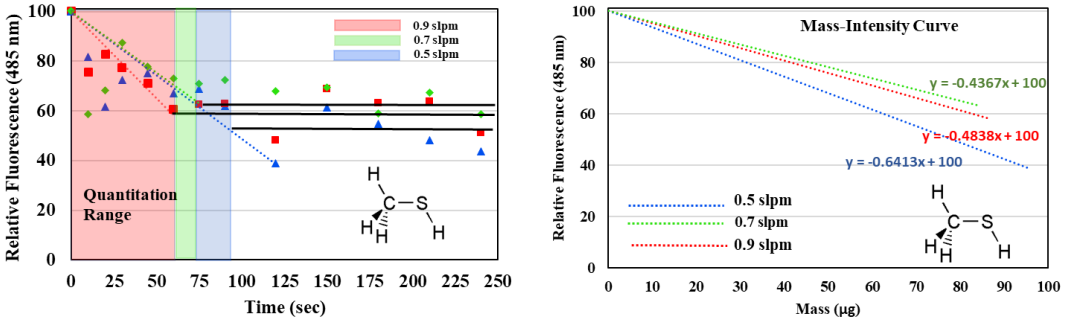

(a) **(b)**

Figure 38: (a) Comparative change in fluorescence intensity at 0.5 slpm, 0.7 slpm, and 0.9 slpm for methyl mercaptan (b) Graph showing change in fluorescence intensity with mass flow of methyl mercaptan at all three flow rates

3.2.4 Experimentation with methane (CH_4)

One of the main focuses of this research is to determine how the biosensor reacts to landfill gas mixtures. For this purpose, two different mixtures have been used, both of which contain methane. Therefore, before testing the mixtures, the reaction of methane (25 ppm +/- 5%) gas balanced with air) with the biosensor was tested. Methane is an odorless compound that is typically found in relatively large concentrations in air near landfills. Following the same procedure as in the previous cases, methane interference was examined at a flow rate of 0.5 slpm since a lower flow rate seemed to delay the saturation of the biosensor by hydrogen sulfide. Figure 39(a) shows the peak emission intensities obtained at different times for this particular experiment. An inverse relationship between time and intensity is maintained for approximately 100 seconds. In Figure 39(b), the mass flow of methane against decreasing intensity is shown. Here, up to 15 µg of methane has been measured within the quantitation range.

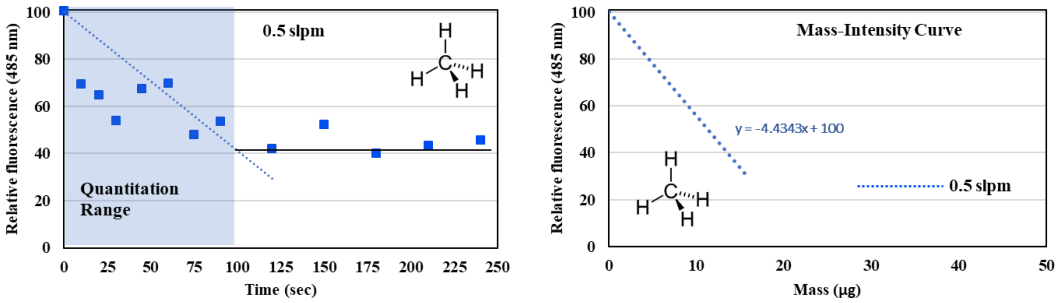

(a) **(b)**

Figure 39: (a) Graph showing peak emission intensity against time for methane flowing at 0.5 slpm (b) Graph showing change in fluorescence intensity with mass flow of methane at 0.5 slpm

3.2.5 Experimentation with landfill gas mixture 1 (NH_3 + CH_4)

Since the research is focused on landfill odorants, the reaction of the biosensor in presence of a landfill gas mixture has been tested. The first such gas consists of a mixture of NH_3 (25 ppm +/- 5%), and CH_4 (25 ppm +/- 5%). They are passed at 0.5 slpm into the reaction chamber by means of a Y-connector as mentioned in the Methodology (Chapter 2) of this thesis. Figure 40(a) shows the emission intensity against time curve while the gas is passed. The quantitation range of this mixture is around 90 seconds which is the same as that obtained for 0.5 slpm of ammonia, but a little lower than that obtained for methane at the same flow rate (100 seconds). Also, no change in pH is observed throughout the time for this experiment. Figure 40(b) shows the emission intensity curves of the mixture as well as the individual components obtained from previous experiments. As it can be seen, the gas mixture has a less steep slope (-0.38) than either of its component gases (-0.59 and -0.62).

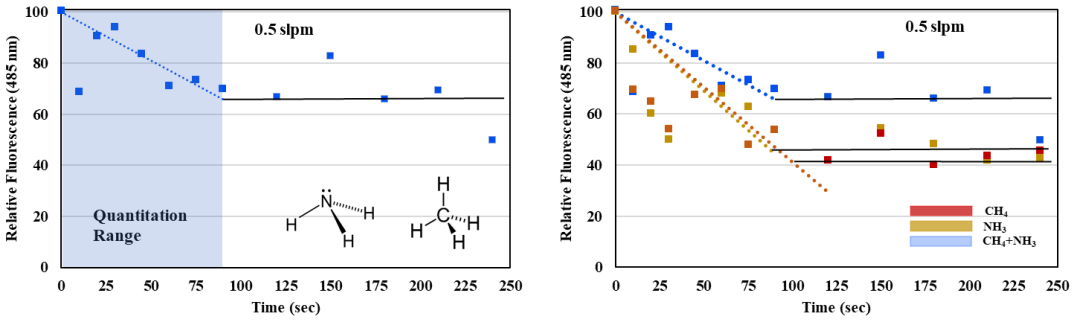

(a) **(b)**

Figure 40: (a) Graph showing peak emission intensity against time for landfill gas mixture 1 flowing at 0.5 slpm (b) Graph showing emission intensity curves for landfill gas mixture 1 against its individual component gases at 0.5 slpm

3.2.6 Experimentation with landfill gas mixture 2 (H_2S + CH_4 + CO)

The final set of experiments was conducted using a gas consisting of a mixture of H_2S (25 ppm +/- 5%), CO (50 ppm +/- 5%) and CH_4 (2.5% +/- 2%) balanced with air, all components being mixed in the same gas cylinder. For the lower flow rate, i.e. 0.5 slpm, the intensity decreases slowly with time and the possible quantitation limit is longer

(approximately 115 seconds) because of that. This limit is shorter for 0.7 slpm (around 90 seconds) and even shorter in case of a higher flow rate of 0.9 slpm, where the intensity becomes stable at around 70 seconds. The peak emission intensities obtained for all three cases are shown in Figure 41. Again, no change in pH is observed throughout the time for experiments with any of the flow rates.

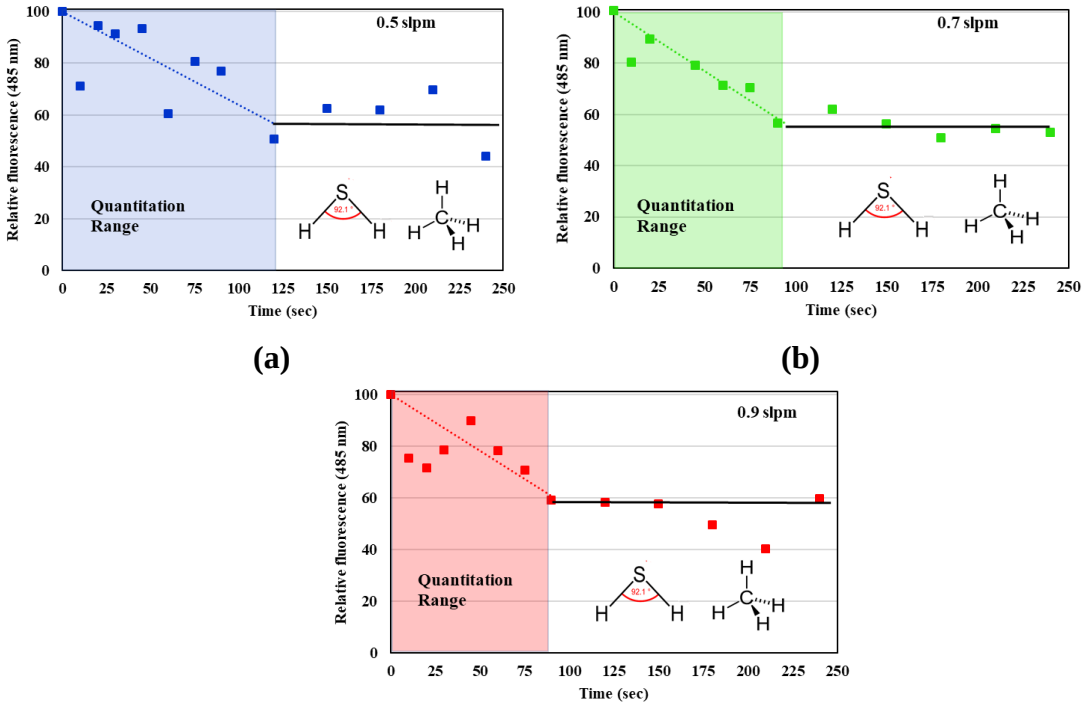

Figure 41: Graph showing peak emission intensity against time for landfill gas mixture 2 flowing at (a) 0.5 slpm, (b) 0.7 slpm, and (c) 0.9 slpm

Figure 42 shows the emission intensity curves for all three flow rates for the landfill gas mixture 2. There is little difference observed in the quantitation ranges for the higher flow rates of 0.7 slpm and 0.9 slpm. In all three cases, the decrease in intensity is almost the same.

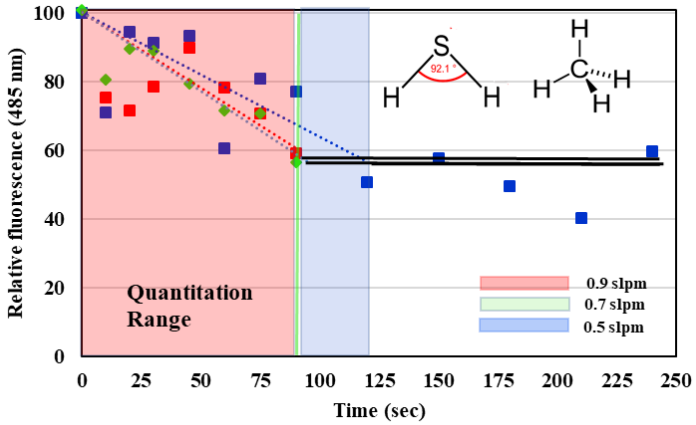

Figure 42: Graph showing peak emission intensity against time for landfill gas mixture 2 flowing at 0.5 slpm, 0.7 slpm, and 0.9 slpm

Figure 43 shows the emission intensity curves of the landfill gas mixture 2 as well as the constituent gases for all the flow rates. Experiment with methane has only been conducted for 0.5 slpm and so it is absent from the other curves. As it can be seen, the gas mixture decreases the intensity by a lower amount for all three flow rates than its constituents, just like the case previously with landfill gas mixture 1.

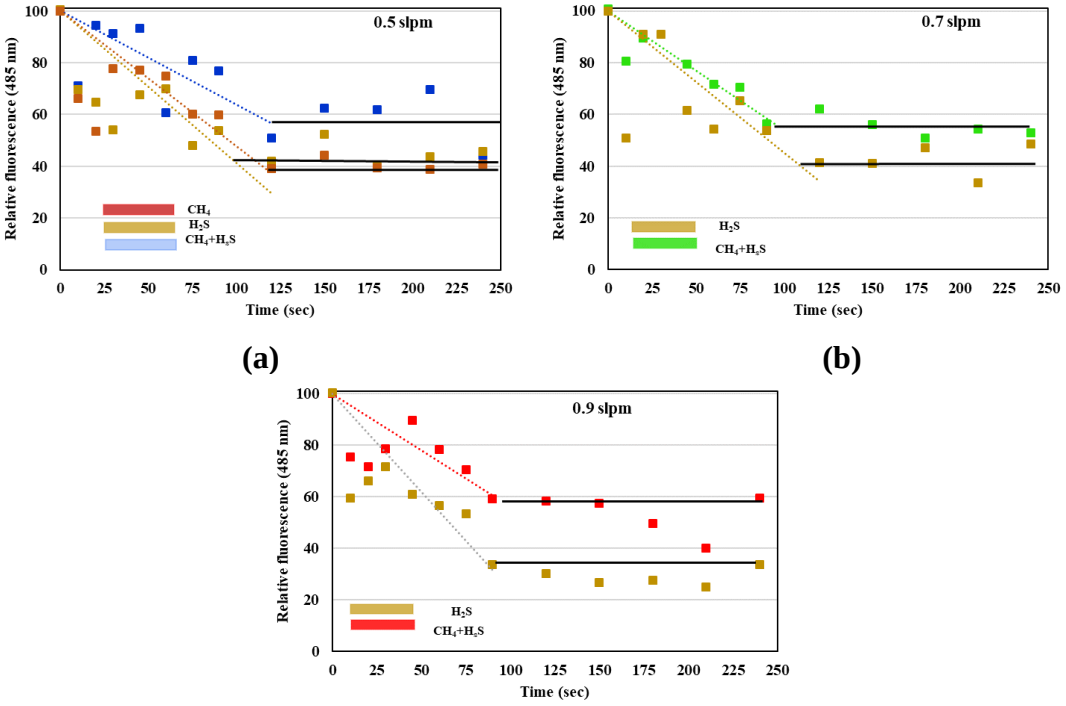

Figure 43: Graph showing emission intensity curves for landfill gas mixture 2 against its individual component gases at (a) 0.5 slpm (b) 0.7 slpm and (c) 0.9 slpm

The quantitation ranges (Table 10) and slope of emission intensity curves (Table 11) of different odorant gases tested for different flow rates were summarized. Generally, for all gases, the quantitation range decreases with an increase in flow rate. The general trend for slopes is also the same, i.e. a steeper slope is obtained when the flow rate is comparatively higher. In case of the mixtures, it can be seen that the slopes obtained have a lower magnitude than that of its component gases in all cases. This indicates that gas mixtures are generally less capable of decreasing the fluorescence intensity than their constituents.

Table 10: Quantitation range of odorant gases tested at different flow rates

Odorant gas	Quantitation Range (seconds)		
	0.5 slpm	0.7 slpm	0.9 slpm
Hydrogen Sulfide	120	110	90
Ammonia	90	75	50
Methyl Mercaptan	95	75	60
Methane	100	-	-
Landfill gas mixture 1 (ammonia + methane)	90	-	-
Landfill gas mixture 2 (hydrogen sulfide + methane + carbon monoxide)	120	90	90

Table 11: Slope of emission intensity curves of odorant gases tested at different flow rates

Odorant gas	Slope		
	0.5 slpm	0.7 slpm	0.9 slpm
Hydrogen Sulfide	-0.52	-0.55	-0.76
Ammonia	-0.62	-0.74	-1.23
Methyl Mercaptan	-0.51	-0.49	-0.70
Methane	-0.59	-	-
Landfill gas mixture 1 (ammonia + methane)	-0.38	-	-
Landfill gas mixture 2 (hydrogen sulfide + methane + carbon monoxide)	-0.36	-0.46	-0.44

At all flow rates, the quantitation range for hydrogen sulfide is the highest followed by methyl mercaptan and ammonia (refer to Figure 44). A possible reason might be the high solubility of ammonia leading to faster saturation than the other gases. The higher volatility keeps the saturation time lower for methyl mercaptan, which is a little higher than ammonia. Though the solubility of methane is lower, the saturation did not seem to be delayed for 0.5 slpm by that much. Methane is a purely hydrophobic compound and since odorant binding protein has affinity for hydrophobic ligands, the effect of solubility was not significant enough in this case. In all cases, ammonia has the steepest slope, followed by hydrogen sulfide and methyl mercaptan among the pure gases. This indicates that ammonia has the highest affinity for protein among the gases, resulting in the largest decrease in fluorescence intensity compared to other gases.

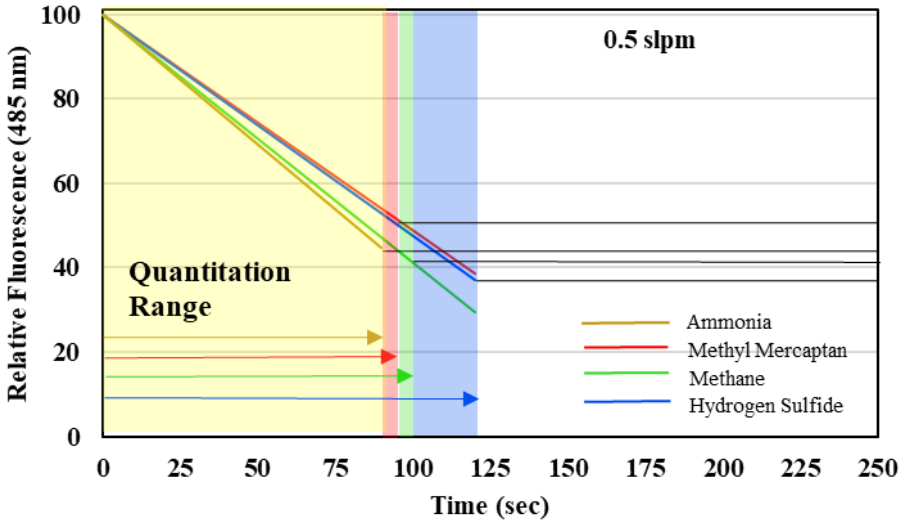
0.5 slpm
Relative Fluorescence (485 nm)
Time (sec)
Quantitation Range
Ammonia
Methyl Mercaptan
Methane
Hydrogen Sulfide
0
20
40
60
80
100
0
25
50
75
100
125
150
175
200
225
250

(a)

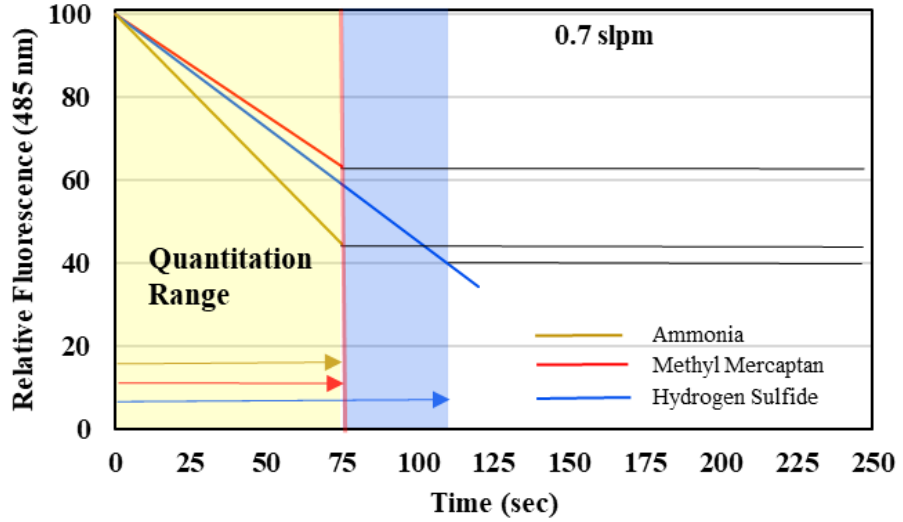
0.7 slpm
Relative Fluorescence (485 nm)
Time (sec)
Quantitation Range
Ammonia
Methyl Mercaptan
Hydrogen Sulfide
0
20
40
60
80
100
0
25
50
75
100
125
150
175
200
225
250

(b)

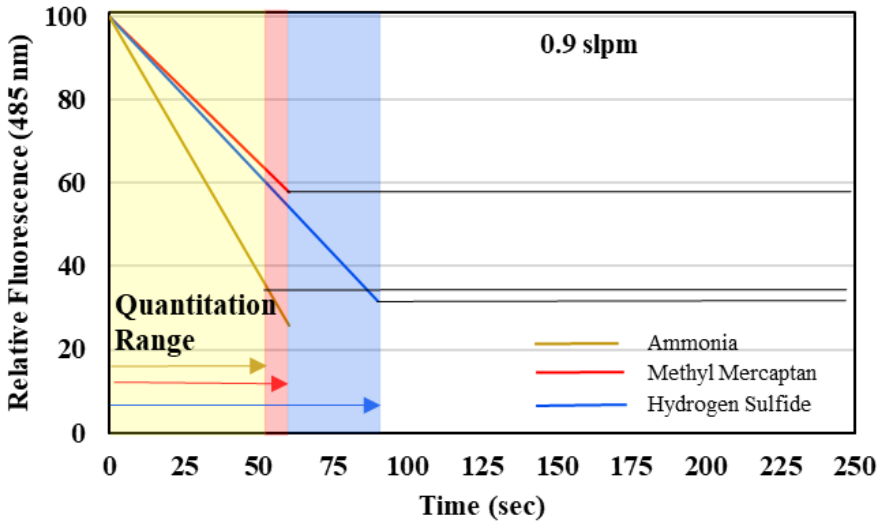

(c)

Figure 44: Comparative changes in relative fluorescence intensities for the pure odorant gases at flow rates of (a) 0.5 slpm, (b) 0.7 slpm, and (c) 0.9 slpm.

3.3 Results From Experiments With PID Sensor

For verification experiments regarding the outlet gas concentration with the PID analyzer, hydrogen sulfide gas was passed through the biosensor solution at 0.5 slpm both with and without the filter. Without the filter, the outlet concentration showed a constant value of 0 ppm for all 4 minutes of the experiment whereas with the filter, the concentration reading showed a non-zero value, indicating that a little amount of gas might be escaping in the form of droplets. This shows the importance of fitting a filter at the outlet to prevent the escaping of odorant gas from the reaction chamber.

3.4 Biosensor Reversibility Experiment

An objective of this research is to test the reversibility of the odorant-protein binding. If the protein can be obtained back after it binds with the odorant, this will make any future device constructed using this principle much cheaper to produce. The idea is to pass an odorant gas through the biosensor solution for some time followed by passing air or pure nitrogen through the solution to see if the intensity curve shows an upward trend, meaning that the protein - 1-AMA bonding has been regenerated. Air had been considered since this can be easily used in landfill for any possible regeneration. However, the presence of carbon dioxide may affect the pH of the solution and thus nitrogen has been selected for this experiment instead and hydrogen sulfide has been selected as an odorant gas. Before checking the reversibility of the reaction, the experiment was conducted only with pure nitrogen gas (99.998% N_2) to check whether it has any effect on the biosensor solution. The results obtained shows that nitrogen has a very negligible effect on the biosensor solution and is unable to lower the fluorescence intensity of the solution (Figure 45).

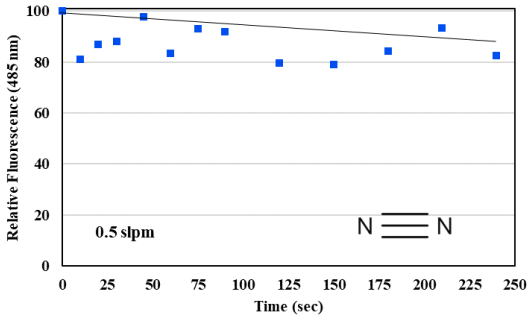

Figure 45: Graph showing peak emission intensity against time for nitrogen gas flowing at 0.5 slpm

For the reversibility test, hydrogen sulfide has been passed through the biosensor solution for 4 minutes at 0.5 slpm and right after that, nitrogen gas has been passed through the solution for another 4 more minutes at the same flow rate. The intensity curve obtained is shown in Figure 46. As it can be seen, the intensity curve is not changed due to the passage of nitrogen. However, at the very end, there is a slight upward trend of the curve. This is promising to some extent as there is the possibility of a reversible reaction if nitrogen is passed for a much longer period time.

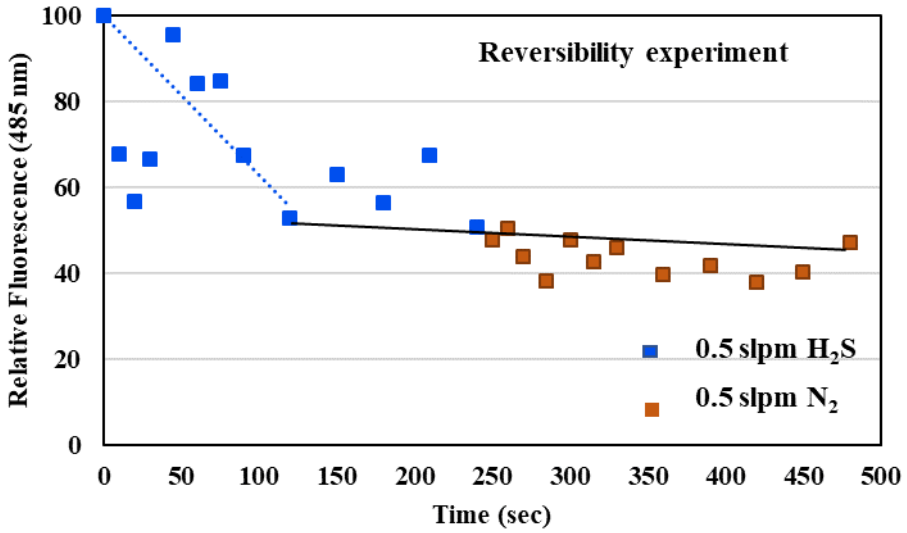

Figure 46: Graph showing peak emission intensity against time for passing hydrogen sulfide gas through the biosensor solution at 0.5 slpm (first 240 seconds) followed by nitrogen gas at the same flow rate (last 240 seconds)

4 CONCLUSION AND RECOMMENDATIONS

4.1 Major Findings

This research has made several important findings regarding human odorant binding protein and its response when binding with odorant gases. There were experiments using hydrogen sulfide, ammonia, methyl mercaptan, methane, and two different landfill gas mixtures. This helped in obtaining fluorescence response curves for a diverse range of gases including acidic and basic gases found in landfills. The usage of different flow rates for the gases has helped establish trends in quantitation range based on the flow rates. Generally, it was found that the biosensor complex saturates faster with an increased gas flow rate. This has been shown in the form of shorter quantitation ranges for the higher flow rates for all the gases, indicating that the biosensor complex can keep working for a longer time with lower flow rates. Also, the higher flow rates led to more decrease in fluorescence intensity in most cases, which was found in the form of steeper slopes of the fluorescence intensity curves. The likely cause might be that a higher flow rate causes more of the gas to dissolve in the aqueous solution and interrupt the fluorescence emission.

The trends across various gases have also been found through the experiments. It has been seen that ammonia has a shorter quantitation range due to its high solubility and methyl mercaptan has a shorter one as well because of its volatility. Around 180 μg of protein in 10 mL solution was able to detect approximately 35-45 μg of hydrogen sulfide, 12-18 μg of ammonia, 83-95 μg of methyl mercaptan, and 15 μg of methane. An important aspect of this research has been the verification of the optimum concentration ratio of hOBPIIa and 1-AMA. This has been verified to be 1:1 at which point, an optimum level of fluorescence was observed. Increasing the concentration of 1-AMA in the mixture above that ratio increases the fluorescence intensity only very slightly.

Experiments were conducted to check for reaction reversibility of the protein-odorant gas binding so that the protein binds with 1-AMA just like before by releasing the odorant gas and can be reused. This was carried out by passing nitrogen gas through the biosensor solution right after passing an odorant gas through it. Although the intensity shows no change during most of the time the nitrogen gas was passed, there was a slight upward trend at the very end which makes this idea promising to explore with a larger time range.

A PID analyzer was used to verify that the odorant gases passed into the reaction chamber did not leak out into the environment through the outlet and affect the assumptions that all of the odorant gas is combining with the biosensor solution during the experiment. Experiments without the filter has shown no presence of gas at the outlet of the chamber. Using the filter, it was seen that a small amount of gas is present in the form of droplet which can be overcome by placing a suitable filter at the outlet.

In all experiments, pH readings were taken for each sample collected by means of pH strips. It had been seen that no change in pH occurs with time as the odorant gas is passed into the biosensor complex. This is an important finding since any such change may influence the binding capacity of hOBPIIa and may have hugely impacted the findings of this work.

A revised experimental chamber had been developed and used in this research. The new chamber has allowed the effective mixing of the odorant gases with the biosensor complex, leading to more accurate results. The chamber also minimizes error in obtained results by not allowing contaminants to be introduced while drawing samples and allows the samples to be drawn more effectively.

4.2 Recommendations

For future research, more experiments should be conducted at different flow rates for the odorant gases so that the change of the fluorescence response curves for different flow rates may be better understood. This will also allow a deeper understanding of the relationship between flow rates and the time it takes for the biosensor complex to be saturated.

More odorant samples need to be included as part of the experiments. Although this research has used a diverse array of gases, these are bottled gases and has a uniform concentration throughout. Experiments need to be conducted using field samples collected from landfills. Observing the reaction with such gas is the ultimate objective of using the biosensor and will help understand the response of the complex in real-world scenarios.

One of the problems of using a small amount of protein for each experiment is that the sample sizes themselves need to be reduced. Although it has benefits such as requiring a smaller reactor chamber and conservation of protein, small samples required quartz cuvettes for testing the fluorescence intensity using the spectrofluorometer since plastic disposable cuvettes need larger sample size. Also, quartz cuvettes need to be washed and dried repeatedly between samples, making the process of obtaining accurate results difficult since even a small amount of residue causes large distortions in the output graph. Using a higher protein volume will allow a larger sample size for spectrofluorometry and disposable cuvettes can be used for that purpose, thus making the whole experimental process more convenient. Another way to overcome this problem is to use a higher concentration of protein, which will enable a small sample to be used easily in a flow-through cuvette which can itself be used as a reaction chamber. There are other advantages to using a flow-through cuvette as a reaction chamber such as eliminating the need of sampling the solution using a syringe. This will ensure a constant sample in the reaction chamber at all times. Also, in the current process, no matter which type of cuvette is used (quartz or disposable), if bubbles form during pouring the sample into the cuvette, the fluorescence intensity obtained varies wildly.

The protein-odorant reaction reversibility has to be explored further. There had been some encouraging results in the reversibility experiment. Further experiments need to be carried to check whether increasing the time range of passing nitrogen gas in the biosensor solution makes the reaction reversible. Obtaining back the protein will make the concept of odorant gas quantification to be used in any future constructed device easier.

REFERENCES

Aatamila, M., Verkasalo, P. K., Korhonen, M. J., Suominen, A. L., Hirvonen, M. R., Viluksela, M. K., & Nevalainen, A. (2011). Odour annoyance and physical symptoms among residents living near waste treatment centres. *Environmental Research*, *111*(1), 164-170. https://doi.org/10.1016/j.envres.2010.11.008

Abdurachim, K., & Ellis, H. R. (2006). Detection of protein-protein interactions in the alkanesulfonate monooxygenase system from Escherichia coli. *Journal of bacteriology*, *188*(23), 8153-8159.

Albani, J. R., Bretesche, L., Vogelaer, J., & Kmiecik, D. (2015). Energy Transfer Studies between Trp Residues of Three Lipocalin Proteins Family, α 1-Acid Glycoprotein,(Orosomucoid), β-Lactoglobulin and Porcine Odorant Binding Protein and the Fluorescent Probe, 1-Aminoanthracene (1-AMA). *Journal of fluorescence*, *25*(1), 167-172.

Allen, M. R., Braithwaite, A., & Hills, C. C. (1997). Trace organic compounds in landfill gas at seven UK waste disposal sites. *Environmental Science & Technology*, *31*(4), 1054-1061. https://doi.org/10.1021/es9605634

Agency for Toxic Substances and Disease Registry (ATSDR). (1992). TOXICOLOGICAL PROFILE FOR METHYL MERCAPTAN. Retrieved from https://www.atsdr.cdc.gov/toxprofiles/tp139.pdf

Agency for Toxic Substances and Disease Registry (ATSDR). (2001). Landfill Gas Primer - An Overview for Environmental Health Professionals. Retrieved from https://www.atsdr.cdc.gov/HAC/landfill/html/ch3a.html

Agency for Toxic Substances and Disease Registry (ATSDR). (2014). Toxic Substances Portal – Methyl Mercaptan. Retrieved from https://www.atsdr.cdc.gov/MMG/MMG.asp?id=221&tid=40

Agency for Toxic Substances and Disease Registry (ATSDR). (2015). Toxic Substances Portal - Ammonia. Retrieved from https://www.atsdr.cdc.gov/PHS/PHS.asp?id=9&tid=2

Agency for Toxic Substances and Disease Registry (ATSDR). (2016). Landfill Gas Safety and Health Issues. Retrieved from Agency for Toxic Substances & Disease Registry: https://www.atsdr.cdc.gov/hac/landfill/html/ch3.html

Bai, Z., Dong, Y., Wang, Z., & Zhu, T. (2006). Emission of ammonia from indoor concrete wall and assessment of human exposure. *Environment international*, *32*(3), 303-311.

Baker, B. P. (1982). *Land Values Surrounding Waste Disposal Factilities* (No. 639-2016-42174).

Baltrėnas, P., Andrulevičius, L., & Zuokaitė, E. (2013). Application of Dynamic Olfactometry to Determine Odor Concentrations in Ambient Air. *Polish Journal of Environmental Studies*, *22*(2).

Belgiorno, V., Naddeo, V. & Zarra, T. (2013). *Odour Impact Assessment Handbook.* A John Wiley & Sons, Ltd., Publication

Bernhard, B. (2014, August 12). *More odor lawsuits filed against Bridgeton Landfill owner.* Retrieved from https://www.stltoday.com/lifestyles/health-med-fit/health/more-odor-lawsuits-filed-against-bridgeton-landfill-owner/article_c059212f-0385-5124-a3bf-fc67e9aa6c99.html

Blizzard, N. (2018, December 3). *NEW DETAILS: $4.1 million settlement approved in Dayton landfill odor lawsuit.* Retrieved from https://www.daytondailynews.com/news/new-details-million-settlement-approved-dayton-landfill-odor-lawsuit/r4HZKBL7rGD9M4ctJkaD7M/

Bokowa, A. H. (2011). The effect of sampling on the measured odour concentration. *Chemical Engineering Transactions*, *23*, 43-48. https://doi.org/10.3303/CET1123008

Boudreau, M. D., Taylor, H. W., Baker, D. G., & Means, J. C. (2006). Dietary exposure to 2-aminoanthracene induces morphological and immunocytochemical changes in pancreatic tissues of Fisher-344 rats. *Toxicological Sciences*, *93*(1), 50-61. https://doi.org/10.1093/toxsci/kfl033

Brattoli, M., De Gennaro, G., De Pinto, V., Demarinis Loiotile, A., Lovascio, S., & Penza, M. (2011). Odour detection methods: Olfactometry and chemical sensors. *Sensors*, *11*(5), 5290-5322. https://doi.org/10.3390/s110505290

Briand, L., Eloit, C., Nespoulous, C., Bézirard, V., Huet, J. C., Henry, C., ... & Pernollet, J. C. (2002). Evidence of an odorant-binding protein in the human olfactory mucus: location, structural characterization, and odorant-binding properties. *Biochemistry*, *41*(23), 7241-7252. https://doi.org/10.1021/bi015916c

Briand, L., Nespoulous, C., Perez, V., Rémy, J. J., Huet, J. C., & Pernollet, J. C. (2000). Ligand-binding properties and structural characterization of a novel rat odorant-binding protein variant. *European journal of biochemistry*, *267*(10), 3079-3089. https://doi.org/10.1046/j.1432-1033.2000.01340.x

CalRecycle. (2019). Odor Characteristics of Compostable Materials. Retrieved from https://www.calrecycle.ca.gov/swfacilities/compostables/odor/characteris

Carannante I., Marasco A. (2018) Olfactory Sensory Neurons to Odor Stimuli: Mathematical Modeling of the Response.

Charlier, L., Cabrol-Bass, D., & Golebiowski, J. (2009). How does human odorant binding protein bind odorants? The case of aldehydes studied by molecular dynamics. *Comptes Rendus Chimie*, *12*(8), 905-910. https://doi.org/10.1016/j.crci.2008.09.022

Chen, S. J., Hsieh, L. T., Hwang, W. I., Xu, H. C., & Kao, J. H. (2003). Abatement of odor emissions from landfills using natural effective microorganism enzyme. *Aerosol Air Qual. Res*, *3*(1), 87-99.

Chiriac, R., Carre, J., Perrodin, Y., Fine, L., & Letoffe, J. M. (2007). Characterisation of VOCs emitted by open cells receiving municipal solid waste. *Journal of hazardous materials*, *149*(2), 249-263. https://doi.org/10.1016/j.jhazmat.2007.07.094

Choi, S. H., Lee, J. W., & Sim, S. J. (2004). Enhancement of the sensitivity of surface plasmon resonance (SPR) immunosensor for the detection of anti-GAD antibody by changing the pH for streptavidin immobilization. *Enzyme and microbial technology*, *35*(6-7), 683-687.

Curren, J., Hallis, S. A., Snyder, C. C. L., & Suffet, I. M. H. (2016). Identification and quantification of nuisance odors at a trash transfer station. *Waste management*, *58*, 52-61. https://doi.org/10.1016/j.wasman.2016.09.021

Davoli, E. (2004). I recenti sviluppi nella caratterizzazione dell'inquinamento olfattivo. *Tutto sugli odori, Rapporti GSISR*.

Davoli, E., Gangai, M. L., Morselli, L., & Tonelli, D. (2003). Characterisation of odorants emissions from landfills by SPME and GC/MS. *Chemosphere*, *51*(5), 357-368. https://doi.org/10.1016/S0045-6535(02)00845-7

De Feo, G., De Gisi, S., & Williams, I. D. (2013). Public perception of odour and environmental pollution attributed to MSW treatment and disposal facilities: A case study. *Waste management*, *33*(4), 974-987. https://doi.org/10.1016/j.wasman.2012.12.016

Dincer, F., Odabasi, M., & Muezzinoglu, A. (2006). Chemical characterization of odorous gases at a landfill site by gas chromatography–mass spectrometry. *Journal of chromatography A*, *1122*(1-2), 222-229. https://doi.org/10.1016/j.chroma.2006.04.075

Du Preez, M., & Lottering, T. (2009). Determining the negative effect on house values of

proximity to a landfill site by means of an application of the hedonic pricing method. *South African Journal of Economic and Management Sciences*, *12*(2), 256-262.El-Fadel, M., Findikakis, A. N., & Leckie, J. O. (1997). Environmental impacts of solid waste landfilling. *Journal of environmental management*, *50*(1), 1-25.

Ekathimerini. (2019, December 19). *Corfu police arrest four over landfill vandalism.* Retrieved from http://www.ekathimerini.com/238193/article/ekathimerini/news/corfu-police-arrest-four-over-landfill-vandalism

El-Fadel, M., Findikakis, A. N., & Leckie, J. O. (1997). Environmental impacts of solid waste landfilling. *Journal of environmental management*, *50*(1), 1-25. https://doi.org/10.1006/jema.1995.0131

Elliott, P., Richardson, S., Abellan, J. J., Thomson, A., De Hoogh, C., Jarup, L., & Briggs, D. J. (2009). Geographic density of landfill sites and risk of congenital anomalies in England: authors' response. *Occupational and environmental medicine*, *66*(2), 140-140.

"Energy and Environmental Affairs." (2016). *Mass.gov*. Retrieved from http://www.mass.gov/eea/docs/dep/recycle/laws/lfgasapp.pdf.

Environmental Protection Agency. (2001). Odour Impacts and Odour Emission Control Measures for Intensive Agriculture. Final Report. Retrieved from https://www.epa.ie/pubs/reports/research/air/Odour%20Impacts%20Final.pdf

Epstein, E. (2011). *Industrial composting: environmental engineering and facilities management*. CRC Press.

Fang, J. J., Yang, N., Cen, D. Y., Shao, L. M., & He, P. J. (2012). Odor compounds from different sources of landfill: characterization and source identification. *Waste Management*, *32*(7), 1401-1410. https://doi.org/10.1016/j.wasman.2012.02.013

Flower, D. R. (1995). Multiple molecular recognition properties of the lipocalin protein family. *Journal of Molecular Recognition*, *8*(3), 185-195. https://doi.org/10.1002/jmr.300080304

Flyger, H., Lewin, E., Thomsen, E. L., Fenger, J., Lyck, E., & Gryning, S. E. (1977). Physical and chemical processes of sulphur dioxide in the plume from an oil-fired power station.

Freeman, T., & Cudmore, R. (2002). Review of odour management in New Zealand. *New Zeal. Minist. Environ. Air Qual. Tech. Rep*, *24*.

Ganni, M., Garibotti, M., Scaloni, A., Pucci, P., & Pelosi, P. (1997). Microheterogeneity of odorant-binding proteins in the porcupine revealed by N-terminal sequencing and mass spectrometry. *Comparative Biochemistry and Physiology Part B: Biochemistry and Molecular Biology*, *117*(2), 287-291.

Gardner, J. W. BARTLETT. PN 1999. "Electronic Noses: Principles and Applications".

Gardner, J. W., Bartlett, P. N., Dodd, G. H., & Shurmer, H. V. (1988). Pattern recognition in the Warwick electronic nose.

Gonçalves, F., Silva, C., Ribeiro, A., & Cavaco-Paulo, A. (2018). 1-Aminoanthracene Transduction into Liposomes Driven by Odorant-Binding Protein Proximity. *ACS applied materials & interfaces*, *10*(32), 27531-27539. Gonçalves, F., Silva, C., Ribeiro, A., & Cavaco-Paulo, A. (2018). 1-Aminoanthracene Transduction into Liposomes Driven by Odorant-Binding Protein Proximity. *ACS applied materials & interfaces*, *10*(32), 27531-27539.

Gostelow, P., Parsons, S. A., & Stuetz, R. M. (2001). Odour measurements for sewage treatment works. *Water Research*, *35*(3), 579-597. https://doi.org/10.1016/S0043-1354(00)00313-4

Heaney, C. D., Wing, S., Campbell, R. L., Caldwell, D., Hopkins, B., Richardson, D., & Yeatts,

K. (2011). Relation between malodor, ambient hydrogen sulfide, and health in a community bordering a landfill. *Environmental research*, *111*(6), 847-852. https://doi.org/10.1016/j.envres.2011.05.021

Henry, C. G., Meyer, G. E., Schulte, D. D., Stowell, R. R., Parkhurst, A. M., & Sheffield, R. E. (2011). Mask scentom eter for assessing ambient odors. *Transactions of the ASABE*, *54*(2), 609-615.

Heydel, J. M., Coelho, A., Thiebaud, N., Legendre, A., Bon, A. M. L., Faure, P., ... & Briand, L. (2013). Odorant-binding proteins and xenobiotic metabolizing enzymes: implications in olfactory perireceptor events. *The Anatomical Record*, *296*(9), 1333-1345. https://doi.org/10.1002/ar.22735

Hirsch, A. R. (2009). Parkinsonism: the hyposmia and phantosmia connection. *Archives of neurology*, *66*(4), 538-542. doi:10.1001/archneurol.2009.38

Howard, J. (2001). Nuisance flies around a landfill: patterns of abundance and distribution. *Waste management & research*, *19*(4), 308-313. https://doi.org/10.1177%2F0734242X0101900407

Iwasaki, Y. (2004). Oltactory measurement of odor (new version). *Japan: Japan Association on Odor Environment*, 145-152.

Jasper, S. (2013). *The Nervous System.* Retrieved from http://www.zo.utexas.edu/faculty/sjasper/bio301L/nervous.html

Jiang, J. K. (1996). Concentration measurement by dynamic olfactometer. *Water environment & technology*, *8*(6), 55-59.

Jin, P. C. (2015). "Characteristics of Gas Emissions in Landfill Site in Recent Years." *International Journal of Environmental Science and Development*, 6(5).

Kang, C. D., Lee, S. W., Park, T. H., & Sim, S. J. (2006). Performance enhancement of real-time detection of protozoan parasite, Cryptosporidium oocyst by a modified surface plasmon resonance (SPR) biosensor. *Enzyme and microbial technology*, *39*(3), 387-390. https://doi.org/10.1016/j.enzmictec.2005.11.039

Kazakov, A. S., Markov, D. I., Gusev, N. B., & Levitsky, D. I. (2009). Thermally induced structural changes of intrinsically disordered small heat shock protein Hsp22. *Biophysical chemistry*, *145*(2-3), 79-85. https://doi.org/10.1016/j.bpc.2009.09.003

Kim, K.-H. H., Choi, Y., Jeon, E., and Sunwoo, Y. (2005b). "Characterization of malodorous sulfur compounds in landfill gas." *Atmospheric Environment*, Pergamon, 39(6), 1103–1112.

Kim, S. U., Kim, Y. J., Yea, C. H., Min, J., & Choi, J. W. (2008). Fabrication of functional biomolecular layer using recombinant technique for the bioelectronic device. *Korean Journal of Chemical Engineering*, *25*(5), 1115-1119.

Kim, T. H., Lee, S. H., Lee, J., Song, H. S., Oh, E. H., Park, T. H., & Hong, S. (2009). Single-carbon-atomic-resolution detection of odorant molecules using a human olfactory receptor-based bioelectronic nose. *Advanced Materials*, *21*(1), 91-94. https://doi.org/10.1002/adma.200801435

Kmiecik, D., & Albani, J. R. (2010). Effect of 1-aminoanthracene (1-AMA) binding on the structure of three lipocalin proteins, the dimeric β lactoglobulin, the dimeric odorant binding protein and the monomeric α 1-acid glycoprotein. Fluorescence spectra and lifetimes studies. *Journal of fluorescence*, *20*(5), 973-983.

Kobayashi, H., Ogawa, M., Alford, R., Choyke, P. L., & Urano, Y. (2009). New strategies for fluorescent probe design in medical diagnostic imaging. *Chemical reviews*, *110*(5), 2620-2640.

Ko, H. J., Lee, S. H., Oh, E. H., & Park, T. H. (2010). Specificity of odorant-binding proteins: a

factor influencing the sensitivity of olfactory receptor-based biosensors. *Bioprocess and biosystems engineering*, *33*(1), 55.

Ko, H. J., & Park, T. H. (2008). Enhancement of odorant detection sensitivity by the expression of odorant-binding protein. *Biosensors and Bioelectronics*, *23*(7), 1017-1023. https://doi.org/10.1016/j.bios.2007.10.008

Lacazette, E., Gachon, A. M., & Pitiot, G. (2000). A novel human odorant-binding protein gene family resulting from genomic duplicons at 9q34: differential expression in the oral and genital spheres. *Human Molecular Genetics*, *9*(2), 289-301. https://doi.org/10.1093/hmg/9.2.289, R. E., Mukhtar, S., Carey, J. B., & Ullman, J. L. (2004). A review of literature concerning odors, ammonia, and dust from broiler production facilities: 1. Odor concentrations and emissions. *Journal of Applied Poultry Research*, *13*(3), 500-508. https://doi.org/10.1093/japr/13.3.500

Laister, G., Stretch, D. D., & Strachan, L. (2002). Managing landfill odour using dispersion modelling and community feedback. *Proc. of Wastecon 2002*.

Laor, Y., Parker, D., & Pagé, T. (2014). Measurement, prediction, and monitoring of odors in the environment: a critical review. *Reviews in Chemical Engineering*, *30*(2), 139-166. https://doi.org/10.1515/revce-2013-0026

Leal, J., Smyth, H. D., & Ghosh, D. (2017). Physicochemical properties of mucus and their impact on transmucosal drug delivery. *International journal of pharmaceutics*, *532*(1), 555-572. https://doi.org/10.1016/j.ijpharm.2017.09.018

LECHNER, M., WOJNAR, P., & Bernhard, R. E. D. L. (2001). Human tear lipocalin acts as an oxidative-stress-induced scavenger of potentially harmful lipid peroxidation products in a cell culture system. *Biochemical Journal*, *356*(1), 129-135.

Lee, S. H., Jun, S. B., Ko, H. J., Kim, S. J., & Park, T. H. (2009). Cell-based olfactory biosensor using microfabricated planar electrode. *Biosensors and Bioelectronics*, *24*(8), 2659-2664. https://doi.org/10.1016/j.bios.2009.01.035

Lehning, M., Shonnard, D. R., Chang, D. P., & Bell, R. L. (1994). An inversion algorithm for determining area-source emissions from downwind concentration measurements. *Air & waste*, *44*(10), 1204-1213. https://doi.org/10.1080/10473289.1994.10467315

Li, J., Zou, K., Li, W., Wang, G., & Yang, W. (2019). Olfactory Characterization of Typical Odorous Pollutants Part I: Relationship Between the Hedonic Tone and Odor Concentration. *Atmosphere*, *10*(9), 524. https://doi.org/10.3390/atmos10090524

Lu, Y., Li, H., Zhuang, S., Zhang, D., Zhang, Q., Zhou, J., ... & Wang, P. (2014). Olfactory biosensor using odorant-binding proteins from honeybee: Ligands of floral odors and pheromones detection by electrochemical impedance. *Sensors and Actuators B: Chemical*, *193*, 420-427. https://doi.org/10.1016/j.snb.2013.11.045

Martuzzi, M., Mitis, F., & Forastiere, F. (2010). Inequalities, inequities, environmental justice in waste management and health. *European Journal of Public Health*, *20*(1), 21-26. https://doi.org/10.1093/eurpub/ckp216

Mei, B., Kennedy, M. W., Beauchamp, J., Komuniecki, P. R., & Komuniecki, R. (1997). Secretion of a novel developmentally regulated fatty acid-binding protein into the perivitelline fluid of the parasitic nematode, Ascaris suum. *Journal of Biological Chemistry*, *272*(15), 9933-9941.

Mikhailopulo, K. I., Serchenya, T. S., Kiseleva, E. P., Chernov, Y. G., Tsvetkova, T. M., Kovganko, N. V., & Sviridov, O. V. (2008). Interaction of molecules of the neonicotinoid imidacloprid and its structural analogs with human serum albumin. *Journal of Applied Spectroscopy*, *75*(6), 857.

Millery, J., Briand, L., Bézirard, V., Blon, F., Fenech, C., Richard-Parpaillon, L., ... & Gascuel, J. (2005). Specific expression of olfactory binding protein in the aerial olfactory cavity of adult and developing Xenopus. *European Journal of Neuroscience*, *22*(6), 1389-1399. https://doi.org/10.1111/j.1460-9568.2005.04337.x

Ministry of the Environment. (1995). *Offensive Odor Control Law*. Retrieved from https://www.env.go.jp/en/laws/air/odor/index.html

Mirmohseni, A., Shojaei, M., & Farbodi, M. (2008). Application of a quartz crystal nanobalance to the molecularly imprinted recognition of phenylalanine in solution. Biotechnology and Bioprocess Engineering, 13(5), 592-597.

Murphy, C., Doty, R. L., & Duncan, H. J. (2003). Clinical disorders of olfaction. In *Handbook of olfaction and gustation* (pp. 822-849). CRC Press.

Nagata, Y., & Takeuchi, N. (2003). Measurement of odor threshold by triangle odor bag method. *Odor measurement review*, *118*, 118-127.

Nicell, J. A. (2009). Assessment and regulation of odour impacts. *Atmospheric Environment*, *43*(1), 196-206. https://doi.org/10.1016/j.atmosenv.2008.09.033

Nicolas, J., Craffe, F., & Romain, A. C. (2006). Estimation of odor emission rate from landfill areas using the sniffing team method. *Waste Management*, *26*(11), 1259-1269. https://doi.org/10.1016/j.wasman.2005.10.013

Nelson, A. C., Genereux, J., & Genereux, M. (1992). Price effects of landfills on house values. *Land economics*, 359-365. DOI: 10.2307/3146693

Norton, J. M., Wing, S., Lipscomb, H. J., Kaufman, J. S., Marshall, S. W., & Cravey, A. J. (2007). Race, wealth, and solid waste facilities in North Carolina. *Environmental Health Perspectives*, *115*(9), 1344-1350. https://doi.org/10.1289/ehp.10161

Occupational Safety and Health Administration (OSHA). (2005). "OSHA Fact Sheet". Retrieved from https://www.osha.gov/OshDoc/data_Hurricane_Facts/hydrogen_sulfide_fact.pdf

Palmiotto, M., Fattore, E., Paiano, V., Celeste, G., Colombo, A., & Davoli, E. (2014). Influence of a municipal solid waste landfill in the surrounding environment: Toxicological risk and odor nuisance effects. *Environment international*, *68*, 16-24. https://doi.org/10.1016/j.envint.2014.03.004

Paolini, S., Tanfani, F., Fini, C., Bertoli, E., & Pelosi, P. (1999). Porcine odorant-binding protein: structural stability and ligand affinities measured by Fourier-transform infrared spectroscopy and fluorescence spectroscopy. *Biochimica et Biophysica Acta (BBA)-Protein Structure and Molecular Enzymology*, *1431*(1), 179-188. https://doi.org/10.1016/S0167-4838(99)00037-0

Paraskaki, I., & Lazaridis, M. (2005). Quantification of landfill emissions to air: a case study of the Ano Liosia landfill site in the greater Athens area. *Waste management & research*, *23*(3), 199-208. https://doi.org/10.1177%2F0734242X05054756

Parker, T., Dottridge, J., & Kelly, S. (2002). Investigation of the composition and emissions of trace components in landfill gas. *Environment Agency, R&D Technical Report P1-438/TR*.

Pearce, T. C., Schiffman, S. S., Nagle, H. T., & Gardner, J. W. (Eds.). (2006). *Handbook of machine olfaction: electronic nose technology*. John Wiley & Sons.

Pelosi, P. (2001). The role of perireceptor events in vertebrate olfaction. *Cellular and Molecular Life Sciences CMLS*, *58*(4), 503-509. https://doi.org/10.1007/PL00000875

Pelosi, P., Baldaccini, N. E., & Pisanelli, A. M. (1982). Identification of a specific olfactory receptor for 2-isobutyl-3-methoxypyrazine. *Biochemical Journal*, *201*(1), 245-248. https://doi.org/10.1042/bj2010245

Pelosi, P., Mastrogiacomo, R., Iovinella, I., Tuccori, E., & Persaud, K. C. (2014). Structure and

biotechnological applications of odorant-binding proteins. *Applied microbiology and biotechnology*, *98*(1), 61-70.

Ramoni, R., Bellucci, S., Grycznyski, I., Grycznyski, Z., Grolli, S., Staiano, M., ... & Conti, V. (2007). The protein scaffold of the lipocalin odorant-binding protein is suitable for the design of new biosensors for the detection of explosive components. *Journal of Physics: Condensed Matter*, *19*(39), 395012.

Ready, R. (2010). Do landfills always depress nearby property values?. *Journal of Real Estate Research*, *32*(3), 321-339.

Reinhart, D. R. (1993). A review of recent studies on the sources of hazardous compounds emitted from solid waste landfills: a US experience. *Waste Management & Research*, *11*(3), 257-268. https://doi.org/10.1006/wmre.1993.1025

Ritzkowski, M., Heyer, K. U., & Stegmann, R. (2006). Fundamental processes and implications during in situ aeration of old landfills. *Waste Management*, *26*(4), 356-372. https://doi.org/10.1016/j.wasman.2005.11.009

Roblyer, J. G. (2017). *Development of a Biosensor to Detect Landfill Odors Using Human Odorant Binding Protein* (Doctoral dissertation, Florida Atlantic University).

Roebuck, D. U. N. C. A. N., Strecht, D., & Strachan, L. I. N. D. S. A. Y. (2004). Investigating odour sources and odour emission rates from landfills through direct communication with residents. *Proc. of Wastecon 2004*.

Ruth, J. H. (1986). Odor thresholds and irritation levels of several chemical substances: a review. *American Industrial Hygiene Association Journal*, *47*(3), A-142. https://doi.org/10.1080/15298668691389595

Sakabe, M., Asanuma, D., Kamiya, M., Iwatate, R. J., Hanaoka, K., Terai, T., ... & Urano, Y. (2012). Rational design of highly sensitive fluorescence probes for protease and glycosidase based on precisely controlled spirocyclization. *Journal of the American Chemical Society*, *135*(1), 409-414.

Sakawi, Z., Sharifah, S. A., Jaafar, O., & Mahmud, M. (2011). Community perception of odor pollution from the landfill. *Research Journal of Environmental and Earth Sciences*, *3*(2), 142-145.

Saladin, K. S. (2004). Anatomy & physiology: the unity of form and function.

Salamone, A. (2019, March 11). *Second lawsuit alleges 'offensive odors' at Plainfield Township landfill*. Retrieved from https://www.mcall.com/business/mc-biz-grand-central-second-lawsuit-20190311-story.html

Sarkar, U., & Hobbs, S. E. (2002). Odour from municipal solid waste (MSW) landfills: A study on the analysis of perception. *Environment International*, *27*(8), 655-662. https://doi.org/10.1016/S0160-4120(01)00125-8

Sarkar, U., Longhurst, P. J., & Hobbs, S. E. (2003). Community modelling: a tool for correlating estimates of exposure with perception of odour from municipal solid waste (MSW) landfills. *Journal of environmental management*, *68*(2), 133-140. https://doi.org/10.1016/S0301-4797(03)00027-6

Sattler, M., & Devanathan, S. (2007). Which meteorological conditions produce worst-case odors from area sources?. *Journal of the Air & Waste Management Association*, *57*(11), 1296-1306. https://doi.org/10.3155/1047-3289.57.11.1296

Scheutz, C., Kjeldsen, P., Bogner, J. E., De Visscher, A., Gebert, J., Hilger, H. A., Huber-Humer, M., and Spokas, K. (2009). "Microbial methane oxidation processes and technologies for mitigation of landfill gas emissions." *ISSN 0734–242X Waste Management*

& Research, 27, 409–455.
Schiefner, A., Freier, R., Eichinger, A., & Skerra, A. (2015). Crystal structure of the human odorant binding protein, OBP IIa. *Proteins: Structure, Function, and Bioinformatics*, *83*(6), 1180-1184. https://doi.org/10.1002/prot.24797
Schiffman, S. S., Walker, J. M., Dalton, P., Lorig, T. S., Raymer, J. H., Shusterman, D., & Williams, C. M. (2000). Potential health effects of odor from animal operations, wastewater treatment, and recycling of byproducts. *Journal of Agromedicine*, *7*(1), 7-81. https://doi.org/10.1300/J096v07n01_02
Sela, L., & Sobel, N. (2010). Human olfaction: a constant state of change-blindness. *Experimental Brain Research*, *205*(1), 13-29.
Sheffield, R., Thompson, M., Dye, B., & Parker, D. (2004). Evaluation of field-based odor assessment methods. *Proceedings of the Water Environment Federation*, *2004*(3), 870-879.
Shen, T. T., Nelson, T. P., & Schmidt, C. E. (1990). Assessment and control of VOC emissions from waste disposal facilities. *Critical Reviews in Environmental Science and Technology*, *20*(1), 43-76.
Shults, M. D., & Imperiali, B. (2003). Versatile fluorescence probes of protein kinase activity. *Journal of the American Chemical Society*, *125*(47), 14248-14249. https://doi.org/10.1021/ja0380502
Silva, C., Matamá, T., Azoia, N. G., Mansilha, C., Casal, M., & Cavaco-Paulo, A. (2014). Odorant binding proteins: a biotechnological tool for odour control. *Applied microbiology and biotechnology*, *98*(8), 3629-3638.
Sneath, R. W. (2001). Olfactometry and the CEN Standard EN13725. *Odours in Wastewater Treatment: Measurement, Modelling and Control. Eds Stuetz R. and Frechen BF, IWA Publishing*.
Song, H. M., & Lee, C. S. (2008). Simple fabrication of functionalized surface with polyethylene glycol microstructure and glycidyl methacrylate moiety for the selective immobilization of proteins and cells. *Korean Journal of Chemical Engineering*, *25*(6), 1467-1472.
Spinelli, S., Ramoni, R., Grolli, S., Bonicel, J., Cambillau, C., & Tegoni, M. (1998). The structure of the monomeric porcine odorant binding protein sheds light on the domain swapping mechanism. *Biochemistry*, *37*(22), 7913-7918.
Sreejith, R. K., Yadav, V. N., Varshney, N. K., Berwal, S. K., Suresh, C. G., Gaikwad, S. M., & Pal, J. K. (2009). Conformational characterization of human eukaryotic initiation factor 2α: A single tryptophan protein. *Biochemical and biophysical research communications*, *390*(2), 273-279. https://doi.org/10.1016/j.bbrc.2009.09.106
St Croix Sensory, I. (2005). A review of the Science and Technology of Odor Measurement.
Stuetz, R. M., & Frechen, F. B. (Eds.). (2001). *Odours in wastewater treatment*. IWA publishing.
Takuwa, Y., Matsumoto, T., Oshita, K., Takaoka, M., Morisawa, S., & Takeda, N. (2009). Characterization of trace constituents in landfill gas and a comparison of sites in Asia. *Journal of Material Cycles and Waste Management*, *11*(4), 305.
Tcatchoff, L., Nespoulous, C., Pernollet, J. C., & Briand, L. (2006). A single lysyl residue defines the binding specificity of a human odorant-binding protein for aldehydes. *FEBS letters*, *580*(8), 2102-2108. https://doi.org/10.1016/j.febslet.2006.03.017
Tegoni, M., Pelosi, P., Vincent, F., Spinelli, S., Campanacci, V., Grolli, S., ... & Cambillau, C. (2000). Mammalian odorant binding proteins. *Biochimica et Biophysica Acta (BBA)-Protein Structure and Molecular Enzymology*, *1482*(1-2), 229-240. https://doi.org/10.1016/S0167-4838(00)00167-9

Van Harreveld, A. P., Heeres, P., & Harssema, H. (1999). A review of 20 years of standardization of odor concentration measurement by dynamic olfactometry in Europe. *Journal of the Air & Waste Management Association*, *49*(6), 705-715. https://doi.org/10.1080/10473289.1999.11499900

Wei, Y., Brandazza, A., & Pelosi, P. (2008). Binding of polycyclic aromatic hydrocarbons to mutants of odorant-binding protein: a first step towards biosensors for environmental monitoring. *Biochimica et Biophysica Acta (BBA)-Proteins and Proteomics*, *1784*(4), 666-671. https://doi.org/10.1016/j.bbapap.2008.01.012

Wenjing, L., Zhenhan, D., Dong, L., Jimenez, L. M. C., Yanjun, L., Hanwen, G., & Hongtao, W. (2015). Characterization of odor emission on the working face of landfill and establishing of odorous compounds index. *Waste Management*, *42*, 74-81. https://doi.org/10.1016/j.wasman.2015.04.030

Wood, J. A., & Porter, M. L. (1987). Hazardous pollutants in class II landfills. *Japca*, *37*(5), 609-615. https://doi.org/10.1080/08940630.1987.10466250

Xia, F. F., Zhang, H. T., Wei, X. M., Su, Y., and He, R. (2015). "Characterization of H2S removal and microbial community in landfill cover soils." *Environmental Science and Pollution Research*, 22(23), 18906–18917.

Xing, B., Khanamiryan, A., & Rao, J. (2005). Cell-permeable near-infrared fluorogenic substrates for imaging β-lactamase activity. *Journal of the American Chemical Society*, *127*(12), 4158-4159.

Xu, P. (2005). A Drosophila OBP required for pheromone signaling. *Science*, *310*(5749), 798-799.

Yazdani, R. (2015). Evaluation of the Landfill Odor Problem at the Sunshine Canyon Landfill.

Ying, D., Chuanyu, C., Bin, H., Yueen, X., Xuejuan, Z., Yingxu, C., & Weixiang, W. (2012). Characterization and control of odorous gases at a landfill site: A case study in Hangzhou, China. *Waste management*, *32*(2), 317-326. https://doi.org/10.1016/j.wasman.2011.07.016

Yoon, H., Lee, S. H., Kwon, O. S., Song, H. S., Oh, E. H., Park, T. H., & Jang, J. (2009). Polypyrrole nanotubes conjugated with human olfactory receptors: high-performance transducers for FET-type bioelectronic noses. *Angewandte Chemie International Edition*, *48*(15), 2755-2758. https://doi.org/10.1002/anie.200805171

Yuwono, A. S., & Lammers, P. S. (2004). Odor pollution in the environment and the detection instrumentation. *Agricultural Engineering International: CIGR Journal*.

Zarra, T. (2007). *Procedures for detection and modelling of odours impact from sanitary environmental engineering plants* (Doctoral dissertation, PhD Thesis, University of Salerno, Salerno, Italy).

Zarra, T., Naddeo, V., & Belgiorno, V. (2009). A novel tool for estimating the odour emissions of composting plants in air pollution management. *Global Nest Journal*, *11*(4), 477-486.

Zhang, Q. (2001). Odour emissions from confined swine production facilities. In *Proc. National Conference "Livestock Options for the Future* (pp. 25-27).

Zhuang, Y. D., Chiang, P. Y., Wang, C. W., & Tan, K. T. (2013). Environment-sensitive fluorescent turn-on probes targeting hydrophobic ligand-binding domains for selective protein detection. *Angewandte Chemie International Edition*, *52*(31), 8124-8128.